



UNIVERSITÉ
PARIS
DESCARTES

U^SPC

Université Sorbonne
Paris Cité

UNIVERSITÉ PARIS DESCARTES

ED 474 Frontières du vivant

*Institut Curie, PSL Research University, Mines Paris Tech, Inserm U900
Paris, France*

**COMPUTATIONAL DECONVOLUTION OF CELL
AND ENVIRONMENT SPECIFIC SIGNALS AND
THEIR INTERACTIONS FROM COMPLEX
MIXTURES IN BIOLOGICAL SAMPLES**

Par Urszula Czerwińska

Theèse de doctorat de Biostatistique

Thèse dirigée par Andrei Zinovyev et Vassili Soumelis

Présentée et soutenue publiquement le [date de soutenance]

Devant un jury composé de :

Andrei Zinovyev directeur de thèse - PSL
Vassili Soumelis directeur de thèse - PSL
Denis Thieffry advisor - ENS
Frank Pagès advisor - Université Paris Descartes
Prénom NOM [fonction] - université



Except where otherwise noted, this work is licensed under
<http://creativecommons.org/licenses/by-nc-nd/3.0/>

Résumé (français) :

Title: Computational deconvolution of cell and environment specific signals and their interactions from complex mixtures in biological samples

Abstract: In many fields of science (biology, technology, sociology) observations on a studied system represent complex mixtures of signals of various origin. Tumors are engulfed in a complex microenvironment (TME) that critically impacts progression and response to therapy. It includes tumor cells, fibroblasts, and a diversity of immune cells. Most studies have focused on individual cell types in model tumor systems, and/or on individual molecules mediating a crosstalk between two cells. Unraveling the complexity, organization, and mutual interactions of TME cellular components represents a major challenge. Methods for deconvolution of complex mixtures of signals have been developed in signal processing field. It is known that under some assumptions, it is possible to separate complex signal mixtures, using classical and advanced methods of source separation and dimension reduction. Our recent large-scale analysis of more than 6500 tumor transcriptomes, applying classical blind source separation methods showed that we can reliably separate signals coming from tumor microenvironment from the tumor-specific signals and various technical artifacts. However, the precise composition of the immune-related signals in a tumor sample remains to be deciphered.

In this project, we develop and apply the advanced methodology of signal deconvolution to decipher sources of signals shaping transcriptomes of tumor samples, with a particular focus on immune-related signals. So far, we managed to deconvolute successfully immune-related signal into groups related to immune cell-types in six breast cancer datasets. However, the precise composition of the immune-related signals and their interactions in a tumor sample remains to be deciphered and our method needs to be calibrated.

We are going to release our processing pipeline in a form of an R package. This will allow the scientific community profit from our analytical pipeline and easily reproduce our results.

In the case of success of this project, the results will be helpful in the determining diagnosis and treatment of cancer, especially for immunotherapies.

Mots-clés (français) :

Keywords: tumor microenvironment, cancer systems biology, transcriptome data analysis, single cell data analysis, bioinformatics, heterogeneity, blind deconvolution, unsupervised learning, cancer, immunology

Dédicace

And now, let's repeat the Non-Conformist Oath!

I promise to be different!

I promise to be unique!

I promise not to repeat things other people say!

— Steve Martin, *A Wild and Crazy Guy* (1978)

Avertissement

Cette thèse de doctorat est le fruit d'un travail approuvé par le jury de soutenance et réalisé dans le but d'obtenir le diplôme d'Etat de docteur de philosophie. Ce document est mis à disposition de l'ensemble de la communauté universitaire élargie. Il est soumis à la propriété intellectuelle de l'auteur. Ceci implique une obligation de citation et de référencement lors de l'utilisation de ce document. D'autre part, toute contrefaçon, plagiat, reproduction illicite encourt toute poursuite pénale.

Code de la Propriété Intellectuelle. Articles L 122.4

Code de la Propriété Intellectuelle. Articles L 335.2-L 335.10

Remerciements

Merci tout le monde

Contents

Preface	xv
Preamble about Interdisciplinary Research	13
0.1 What does interdisciplinarity in science mean in XXI century?	13
0.2 Strengths, Weaknesses Opportunities, Threats (SWOT) of an interdisciplinary PhD	13
0.3 Organisation of the dissertation	13
1 Immuno-biology of cancer	15
1.1 Cancer seen as complex environment	15
1.1.1 Our understanding of cancer over time	15
1.1.2 Tumor micro environment: friend or foe?	16
1.1.2.1 What is Tumor Microenvironment (TME)	16
1.1.2.2 TME as a tumor ally	17
1.1.2.3 Two-faced nature of immune cells	18
1.1.2.4 Immune cell (sub)types in TME	19
1.1.3 Cancer immune phenotypes	19
1.1.3.1 Immunoscore	20
1.1.3.2 Immunophenoscore	22
1.1.3.3 Immune maps	23
1.1.3.4 Summary	23
1.1.4 Immune signatures - biological perspective	23
1.2 Immunotherapies	23
1.2.1 Cancer therapies	24
1.2.2 Recent progress in immuno-therapies	24
1.3 Quantifying immune infiltration (data)	26
1.3.1 Cell sorting	27
1.3.1.1 Flow cytometry	27
1.3.1.2 Mass cytometry	27
1.3.2 Microscope Staining	27
1.3.3 omics	28

1.3.3.1	Transcriptome	28
1.3.3.2	Epigenome	30
1.3.3.3	Single cell RNA-seq	30
1.4	Biological dimension of the thesis	31
2	Mathematical foundation of cell-type deconvolution of biological data	33
2.1	Introduction to supervised and unsupervised learning	33
2.2	Blind source separation	33
2.3	Finding optimal number of components and over-decomposition of transcriptomes	35
2.4	Cell-type deconvolution models	49
2.4.1	basis matrix	49
2.4.2	regression algorithm	49
2.4.3	Others	49
2.5	Short review of most popular cell-type deconvolution tools	49
2.6	Methodological dimension of the thesis	49
3	Study of sensitivity and reproducibility of known methods	51
3.1	Reproducibility of NMF versus ICA (vs CAM?)	51
3.1.1	Comparing metagenes obtained with NMF vs ICA.	51
3.2	Impact of modification of signatures list on result for signature-based deconvolution methods	54
4	Deconvolution of transcriptomes and methylomes	55
4.1	From blind deconvolution to cell-type quantification: general overview	55
4.1.1	The ICA-based deconvolution of Transcriptomes	55
4.1.2	Interpretation of Independent components	56
4.1.2.1	Correlation based identification of confounding factors	56
4.1.2.2	Identification of immune cell types with enrichment test / other	56
4.1.3	Transforming metagenes into signature matrix	56
4.1.4	Regression-based estimation of cell-type proportions : solving system of equations	56
4.2	<i>DeconICA</i> R package for ICA-based deconvolution	56
4.2.1	Demo	56
5	Comparative analysis of cancer immune infiltration	73
6	Heterogeneity of immune cell types	75
7	Conclusions and perspectives	81
Annexes		83

PhD timeline for defence before the end of October 2018	83
Thesis writing	83
Activity Report 2017	85

List of Tables

List of Figures

- 1.1 **Percentage of publications containing phrase “tumor immunotherapy” is growing, numbers retrieved on 17.01.2018 from Medline Trends [14]** 17
- 1.2 **The microenvironment supports metastatic dissemination and colonization at secondary sites.** Different tumor sites can communicate through exosomes realized by tumor cells and also immune and stromal cells such as NK cells, CAFs and DCs. Reprinted by permission from Springer Nature [46] © 2013 Nature America, Inc. All rights reserved. 18
- 1.3 **Cancer-immune phenotypes: the immune-desert phenotype (brown), the immune-excluded phenotype (blue) and the inflamed phenotype (red).** The immune–desert phenotype is characterised by paucity of immune cells and cytokines. In the immune-excluded phenotypes the T cells are often present but trapped in stroma, enabled to migrate to the tumor site. The immune-inflamed phenotype is rich in immune cells and the most responsive to the immune check point therapies. Reprinted by permission from Springer Nature [10] © 2017 Macmillan Publishers Limited, part of Springer Nature. All rights reserved. 21
- 1.4 **This timeline describes short history of FDA approval of checkpoint blocking immunotherapies up to 2017.** Reprinted by permission from Springer Nature [56] Macmillan Publishers Limited, part of Springer Nature. All Rights Reserved. 26
- 1.5 **From Data to Wisdom.** Illustration of different steps that it takes to go from *Data* to generating *Wisdom*. It highlights that generating data is not equal to understanding it and additional efforts are needed to generate value. Image authored by Clifford Stoll and Gary Schubert published by Portland Press Limited on behalf of the Biochemical Society and the Royal Society of Biology and distributed under the Creative Commons Attribution License 4.0 (CC-BY) in [43]. 27

- 1.6 **Five categories of RNA-seq data analysis.** Differential analyses: comparing two (or more) conditions, Relative analyses: comparing to an internal reference (average, base level), Compositional analyses: inferring cell types or groups of cell types (i.e. tumor purity), Global analyses: pan-tissue and pan-cancer analyses and Integrative analyses: compiling heterogeneous data types. Reprinted by permission from Springer Nature [12] © 2018 Macmillan Publishers Limited, part of Springer Nature. All rights reserved. 29
- 2.1 **Principle of the deconvolution applied to transcriptome** Graphical illustration of the deconvolution of mixed samples. Starting from the left, gene expression of genes A B C is a sum of expression of cell types 1, 2, 3, 4. After deconvolution, cell types are separated and gene expression of each cell type is estimated taking into account cell type proportions. 34
- 3.1 **Correlation graph of ICA and NMF multiple decompositions.** In the upper part of the figure (A,B) we observe the correlation graph of all metagenes (ICA or NMF-based) disposed using edge-weighted bio layout. In the lower part of the figure (C,D) we applied >0.4 threshold in order to filter the edges. In the case of ICA (C), remaining nodes form pseudo-cliques, immune-related pseudo-clique is highlighted. In the case of NMF (D), components cluster by dataset. Edges' width corresponds to Pearson correlation coefficient. Node colors correspond to dataset from which a metagene was obtained (see legend). 53
- 4.1 **State of the deconICA package in January 2018.** The flow chart illustrates existing functions in the R package *DeconICA*. Squares represent functions, red are user-provided inputs, brown are inputs we provide but that can be replaced easily by user and in blue we marked outputs. 58
- 7.1 Timeline provided by University Paris Descartes for 2017 84

Preface

This is the index

Preamble about Interdisciplinary Research

0.1 What does interdisciplinarity in science mean in XXI century?

This will be an interdisciplinary thesis about using different disciplines, opportunities, challenges and methods.

0.2 Strengths, Weaknesses Opportunities, Threats (SWOT) of an interdisciplinary PhD

0.3 Organisation of the dissertation

Chapter 1

Immuno-biology of cancer

This chapter will introduce a basic topic of cancer and participation of stroma in cancer development, progression and response to treatment. It will also describe most important types of data used to study cancer microenvironment.

1.1 Cancer seen as complex environment

According to [GLOBOCAN study](#) [17], 14.1 million cancer cases was estimated to happen around the world in 2012. It touched 7.4 million men and 6.7 million women. It is estimated that the cancer cases will increase almost two-fold to 24 million by 2035.

In France only, in 2012 there were 194552 cases of cancer, of which leading is Prostate cancer (29,2%) followed by Lung (14,4%) and Colorectal cancers (11,1%).

For a long time studying tumor was focused on tumor cells, their reprogramming, mutations. Cancer was seen as disease of uncontrolled cells. Recent discoveries moved research focus from tumor cells to tumor cells in their context: tumor microenvironment. We will describe here what is the composition and role of the TME in tumor progression, diagnosis and response to treatment.

1.1.1 Our understanding of cancer over time

Cancer was historically described by a physician Hippocrates (460–370 B.C) [54]. Even though there exist even earlier evidence of the disease. Hippocrates stated that the body contained 4 humors (body fluids) : blood, phlegm, yellow bile and black bile. Any imbalance of these fluids will result in disease. Particularly the excess of black bile in an organ

was meant to provoke cancer. For years, it was not known what factors cause cancer and it was easily confounded with other diseases. In the middle ages in the Renaissance Period it was believed cancer is a punishment for the sins they committed against their god, that they deserved it to some extend

Until 18th century it was believed that cancer is contagious and is spread by parasites.

In the 1850s, tumor cells started to be analysed by pathologists. They were strike with their ability to proliferate uncontrollably, ability to spread and destroy the original tissue [31]. Around the same time leukocytes from the blood was first described by Gabriel Andra and William Addison. Just a few years later, in 1845 Bennett and Virchow described blood cells in leukaemia. Virchow is also a father of Chronic irritation theory (which we would call chronic inflammation) that says that cancer cells spread resulting in metastasis.

In the 20th century, molecular causes started to be investigated. It was discovered that cancer could be caused by environmental factors, i.e. chemicals (carcinogens), radiation, viruses and also inherited from ancestors. Those factors would damage but contrary to a healthy condition they would not die.

During the 1970s, oncogenes and tumor suppressor genes were discovered. Oncogenes are genes that allow a cell to become cancer cell, while the tumor suppressor genes would repair DNA or execute cell death of a damaged cell.

Since the end of the 20th century, cancer screens are developed along with multiple strategies to fight tumor. Most classical ones are based on the idea of removing tumor cells (surgery), killing tumor cells with DNA-blocking drugs (chemotherapy), radiation, inhibit cancer growth (hormonal therapy, adjuvant therapy and immunotherapy). As none of those methods is fully efficient, often a combination of treatments is proposed. Nowadays, science is aiming in the direction of targeted therapies and personalized treatment.

The recent success of immunotherapies (discussed in Immunotherapies section made realise the scientific community how important is the context in which tumor cells are found. This context called Tumor Microenvironment, as well as the communication that happens within it between different agents, become a popular scientific topics of 21st century (Fig. 1.1).

1.1.2 Tumor micro environment: fiend or foe?

1.1.2.1 What is Tumor Microenvironment (TME)

Tumor Microenvironment is a complex tissue that surrounds tumor cells. It is composed of blood and lymphatics vessels, epithelial cells, mesenchymal stem cells, fibroblast,

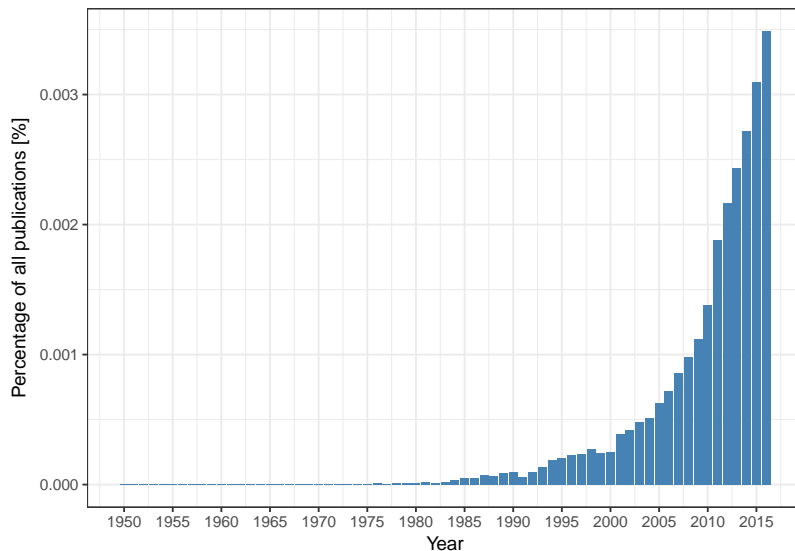


Figure 1.1: Percentage of publications containing phrase “tumor immunotherapy” is growing, numbers retrieved on 17.01.2018 from Medline Trends [14]

adipocytes and a wide variety of immune cells. Their proportion and specific roles vary significantly with tumor type and stage. Communication between the environmental cells and the tumor is critical for tumor development and its impact on patient's response to treatment.

1.1.2.2 TME as a tumor ally

In 1863 Rudolf Virchow observed a link between chronic inflammation and tumorigenesis. According to Virchov theory genetic damage would be the “match that lights the fire” of cancer, and the inflammation or cytokines produced by immune cells should be the “fuel that feeds the flames” [2]. Therefore lymphocyte infiltration was confirmed by subsequent studies as a hallmark of cancer. The question one may ask is why our immune system does not defend the organism from tumor cells as it does in a range of bacterial and viral infections? It is mainly because of the ability of tumor cells to inhibit immune response through activation of negative regulatory pathways (so called immune checkpoints).

Many examples can be cited on how TME facilitates tumor development (Fig. 1.2). For instance, in the early stages of tumorigenesis some macrophage phenotypes support tumor growth and mobility through TGF-beta signaling. Also, it was shown that NK cells and myeloid-derived suppressor cells (MDSCs) have an ability to suppress immune defence i.e. immuno surveillance by dendritic cells (DCs), T cell activation and macrophage polarisation and they promote tumor vascularisation as well. [55, 19] They create so-called

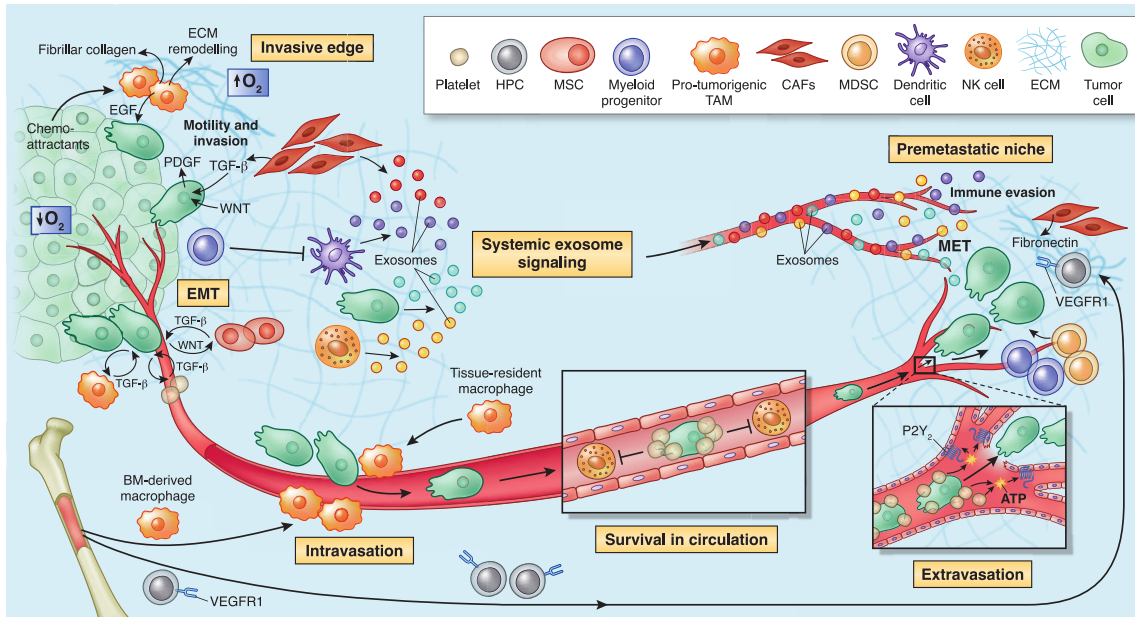


Figure 1.2: The microenvironment supports metastatic dissemination and colonization at secondary sites. Different tumor sites can communicate through exosomes realized by tumor cells and also immune and stromal cells such as NK cells, CAFs and DCs. Reprinted by permission from Springer Nature [46] © 2013 Nature America, Inc. All rights reserved.

niches that facilitates tumor colonization. Tregs and myeloid-derived suppressor cells can negatively impact natural immune defence and by these means allow growth and invasion of tumor cells [56]. Another cell type, a part of ECM, fibroblast, or more precisely Cancer Associated Fibroblasts (CAFs) have proven pro-tumor functions in breast cancer where they enhance metastasis [16]. The blood and lymphatic vessels maintain tumor growth providing necessary nutritive compound to malignant cells.

According to [26] immune and stroma cells participate in almost all of Cancer Hallmarks [25, 26] : Most of the hallmarks of cancer are enabled and sustained to varying degrees through contributions from repertoires of stromal cell types and distinctive subcell types.

1.1.2.3 Two-faced nature of immune cells

In the 1960s, the immune surveillance theory hypothesized “the ability to identify and destroy nascent tumors as a central asset of the immune system” [51, 7], but it was highly criticized in consequence of no increase in tumor incidence in athymic nude mice [53?]. Later it was shown, that this mice model was not adequate [8]. Over the years, it was shown that the immune surveillance theory was not wrong, but was not completely right neither.

Recent studies unveil ambivalent nature of immune cells of TME. While some as cytotoxic T cells, B cells and macrophages can manage to eliminate tumor cells. Treg cells role is to regulate expansion and activation of T and B cells. Depending on cancer type, they can be either pro- or anti-tumor. For example as it has been shown for Tregs, they can be also associated with improved survival (i.e. in colorectal cancer [18]). For innate immunity, there are widely accepted M1 (anti-tumor) and M2 (pro-tumor) extreme macrophages phenotypes in TME [45]. Most of the statements seem to be context dependent and not valid universally across all cancer types. We already mentioned Macrophages phenotypic plasticity as well as different behaviour of EMC depending on tumor stage.

From more general point of view, it has been observed that immunodeficiency can correlate with high cancer incidence. Results of analysis based on observations of 25,914 female immunosuppressed organ transplant recipients, the tumor incidence was higher than predicted for multiple cancers. However, the number of breast cancer cases decreased which can be really disturbing if we need to decide on the role of immune defence in tumor progression [52]. This trend was confirmed through a study on individuals with AIDS and other studies. This indicates that immune microenvironment can be cancer stimulating or inhibiting depending on the type of cancer.

1.1.2.4 Immune cell (sub)types in TME

Here will be a definition of what is immune cell type, how different phenotypes are can be associated with subtypes and why researches do it

Necessary for the chapter Heterogeneity of immune cell types

1.1.3 Cancer immune phenotypes

Since 20. century physicians decided on common nomenclature that classify tumors into distinct groups that are relatively homogenous or that share common characteristic important for treatment and prognosis. Tumor typing should help to better assess predicting prognosis, to adapt a therapy to the clinical situation, to enable therapeutic studies which are essential in proving any therapeutic progress.

Most of the classifications are based on clinical data. Most common factors taken into account are: the degree of local invasion, the degree of remote invasion, histological types of cancer with specific grading for each type of cancer, possibly various tumour markers, general status of the patient.

With a progress of molecular biology also gene markers or proteomic abnormalities can be part of classification panel.

Since the increase of importance of the immunotherapies, researches proposed several ways to classify tumors based on their microenvironment. Given different parameters describing TME, cancers can be sorted into groups that show similar characteristics. We will discuss most common frameworks that allow to phenotype cancers based on the TME.

The localisation of the immune cells can be an indicator of the state and response to the therapy [5].

The most standard approach is to convey an analysis of histopathological cuts to asses the number of infiltrating lymphocytes (TILs). Two typical patterns are usually identified: "hot" - immune inflamed and "cold" - no active immune response [3].

Chen and Mellman [10] describes classification into inflamed and non-inflamed tumors, where non-inflamed phenotypes: can be further split into the immune-desert phenotype and the immune-excluded phenotype (Fig. 1.3). The inflamed phenotype is characterised by rich presence of immune cells : T cells, myeloid cells, monocytes in tumor margin. Along with the immune cells, due to their communication, a high expression of cytokines is characteristic for this phenotype. According to Chen2017, this is a mark of anti-tumor response that was arrested by tumor. The inflamed phenotype has shown to be most responsive to immunotherapies. In the immune-excluded phenotype, the immune cells are present as well but located in the stroma [27], sometimes penetrating inside tumor. However, when exposed to check point immuotherapy, T cells does not gain the ability to infiltrate the tumor, therefore the treatment is inefficient. The immune-desert main features is little or no presence of immune cells, especially T cells. Surprisingly, this tumors have been to proven to rarely respond to the checkpoint therapy [27]. In non-inflamed tumours cytokines associated with immune suppression or tolerance are expressed.

The immunogenicity of the tumors can be explained by tumor-intrinsic factors and tumor-extrinsic factors [20]. Tumor-intrinsic factors are, the neoantigen load and frequency, the mutational load, the expression of immunoinhibitors and immunostimulators (e.i. PD-L1), and alteration of HLA class I molecules. Tumor-extrinsic factors include chemokines regulating T cell trafficking, infiltration of effector TILs and immunosuppressive TILs, and soluble immunomodulatory factors (cytokines).

A plethora of different computational methods have been developed in order to further characterize tumor samples using different factors. We mention here mainstream methods that cover different approaches of scoring the TME-cancer phenotype.

1.1.3.1 Immunoscore

Image-based tumors classification

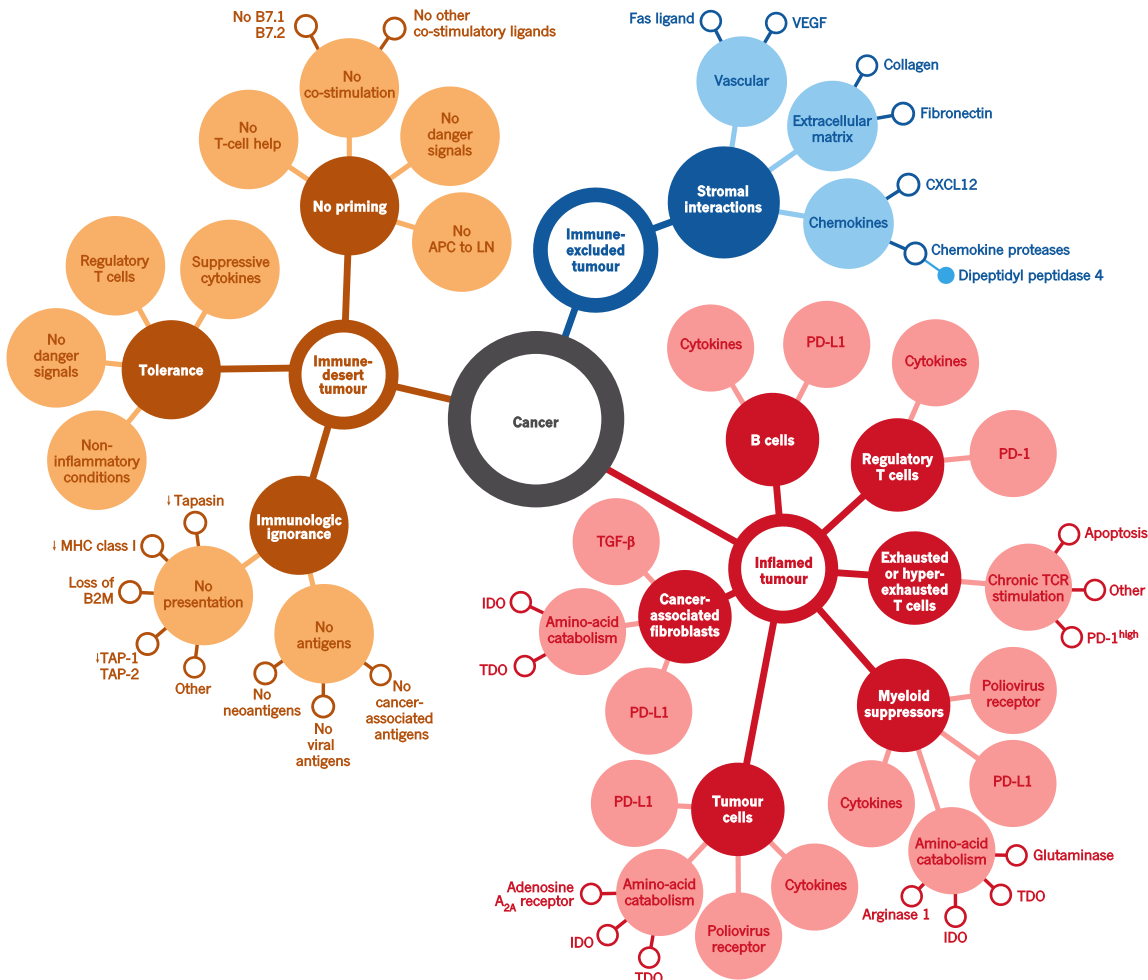


Figure 1.3: Cancer-immune phenotypes: the immune-desert phenotype (brown), the immune-excluded phenotype (blue) and the inflamed phenotype (red). The immune-desert phenotype is characterised by paucity of immune cells and cytokines. In the immune-excluded phenotypes the T cells are often present but trapped in stroma, enabled to migrate to the tumor site. The immune-inflamed phenotype is rich in immune cells and the most responsive to the immune check point therapies. Reprinted by permission from Springer Nature [10] © 2017 Macmillian Publishers Limited, part of Springer Nature. All rights reserved.

<http://www.haliodx.com/clinical-research-services/immunoscorer/>

Galon et al. [21]

1.1.3.2 Immunophenoscore

Different approaches are based on gene expression patterns. Most commonly, machine learning supervised algorithms are trained to match known phenotype (established with microscopy or with clinical features) to genetic patterns or an unsupervised clustering is used to discover new classification.

An example of well-formulated classification framework is Immunophenoscore [9], based on publication of Angelova et al. [1], where methylome, transcriptome and mutation of TCGA CRC dataset ($n = 598$) was used to describe *immunophenotypes*. Later on, it was reduced to gene expression indicator and summarised in a form of a score. In This scoring scheme is based on the data of 20 solid tumors, using expression of marker genes selected by a Machine Learning algorithm (random forest) for best prediction in each cancer. These indicators can be grouped into four categories:

- MHC molecules (MHC)
- Immunomodulators (CP)
- Effector cells (EC)
- Suppressor cells (SC)

The immunophenscore (IPS) is calculated on a 0-10 scale based on the expression of genes in each category. Stimulatory factors (cell types) impact the score positively and inhibitory factors (cell types) negatively. Z-scores ≥ 3 were designated as IPS10 and z-scores ≤ 0 are designated as IPS0. A similar conceptual framework called *cancer immunogram* was proposed by Blank et al. [6] included seven parameters: tumor foreignness (Mutational load), general immune status (Lymphocyte count), immune cell infiltration (Intratumoral T cells), absence of checkpoints (PD-L1), absence of soluble inhibitors (IL-6, CRP), absence of inhibitory tumor metabolism (LDH, glucose utilisation), tumor sensitivity to immune effectors (MHC expression, IFN- α sensitivity). Nonetheless, the details of *cancer immunogram* use in practice remain unclear and result could be sensitive to patients' and data heterogeneity as no standardisation was proposed.

Charoentong et al. [9] claim that the immunophenoscore can predict response to CTLA-4 and anti-PD-1.

1.1.3.3 Immune maps

Description on how immune portraits (NAVIcell) can be used to characterise tumor immune environment.

1.1.3.4 Summary

Despite those facts, the gene expression based classifications are not yet used in clinics. The measured multi-panel mRNA expression, that can be included into category of In Vitro Diagnostic Multivariate Index Assay (IVDMIA) [24, 49], may be a future of TME-based cancer classification, diagnosis and treatment recommendation [23]. For this best tools need to be used to properly evaluate the state of TME and tumor-stroma-immune cells communication.

1.1.4 Immune signatures - biological perspective

- definition of signature: marker genes, list of genes, weighted list, metagenes
- the general immune signature of signature of immune infiltration and stroma vs immune signature of a specific cell type or functional subpopulation
- purpose of signatures
- availability of immune signatures
- the problem of not consistency of immune signatures
- origin of signatures

"the gene expression profiles of tumour-associated immune cells differ considerably from those of blood derived immune cells" [50]

Immune signatures will be also discussed as a part of deconvolution pipeline in the Chapter 2 under the section about *basis matrix*.

1.2 Immunotherapies

This section outlines progress in cancer therapies with a focus on immune therapies. It will link the ongoing research on TME with therapeutical potential.

1.2.1 Cancer therapies

Cancer is a complex disease. Up to date, no uniform and fully effective treatment was proposed and usually different strategies are tested to kill tumor cells. **Surgery** is one of the oldest methods. The cancer is removed from the patient body. There are different ways, more or less invasive, that it can be performed. It is usually applied for solid tumor contained in a small area. **Radiation Therapy** uses high doses of radiation to eliminate tumor cells and shrink tumor mass. It can be applied externally or internally. **Chemotherapy** uses a drug (or a combination of drugs) that kill cancer cells, usually altering cell proliferation and growth. The drawback of radiotherapy and chemotherapy are strong side effects. **Hormone therapy** modulates hormone levels in the body in order to inhibit tumor growth in breast and prostate cancers. In leukemia and lymphoma, can be applied **stem cell transplants** that restore blood-forming stem cells destroyed by the very high doses of chemotherapy or radiation therapy that are used to treat certain cancers.

Alternatively, **targeted therapies** represent more focused strategy that aims to be more effective and cause less side effects than systematic therapies. Two main types of targeted therapies are small-molecule drugs and monoclonal antibodies. Targeted therapies usually aim to stimulate/inhibit a selected molecular function. A special type of targeted therapies are **Immunotherapies**. Through activation/inhibition of immune regulatory pathways, it stimulates immune system to destroy malignant cells. A continuation of targeted therapies is **precision medicine approach**. It is based on genetic information to specify patient's profile and find adapted treatment. A number of innovative treatments targeting a specific change in tumor ecosystem are being tested presently in precision medicine clinical trials [28].

1.2.2 Recent progress in immuno-therapies

The immunotherapies, in contrast with other types of cancer therapies discussed in the previous chapter, aim to trigger or restart the immune system to defend the organism and attack the malignant cells. All this, however without provoking persisting inflammation state [44]

The idea of stimulating immune system to fight malignant cell was not born recently. Since a long time a possibility of development of an anti-cancer vaccine has been investigated. Unfortunately, this idea faced two important limitations 1) lack of knowledge of antigens that should be used in vaccine to successfully stimulate cytotoxic T cells 2) the ability of cancer to block the immune response also called *immunostat*. Despite those impediments works on anti-tumor vaccines do not cease [39]. A very recent promising an in-situ anti-tumor vaccine was proposed by Sagiv-Barfi et al. [?]. The therapy tested in mice, would be based on local injections of the combination of "unmethylated CG-

enriched oligodeoxynucleotide (Cp-G) - a Toll-like receptor 9 (TLR9) ligand and anti-OX40 antibody. Low doses of CpG injected into a tumor induce the expression of OX40 on CD4+ T cells in the microenvironment in mouse or human tumors. An agonistic anti-OX40 antibody can then trigger a T cell immune response, which is specific to the antigens of the injected tumor". Sagiv-Barfi et al. claim this therapy could be applied to all tumor types, as long as they are leucocyte-infiltrated. As a local therapy, *in situ* vaccination should have less side-effects than systematic administration. It is now undergoing clinical trials to test its efficiency in human patients.

Another idea involving using immune system as a weapon to fight cancer, would be the use of genetically modified patient's T-cells, carrying CARs (chimeric antigen receptors) [29]. After a long period of small unsuccessful trials, recently in 2017, two CAR T-cell therapies were accepted, one to "treat adults with certain type of large B-cell lymphoma" [38], other to treat "children with acute lymphoblastic leukemia (ALL)" [37] , which are, at the same time, the first two gene therapies accepted by FDA.

However, the two most promising immuno-related strategies with proven clinical efficiency are based on blocking so called immune check point inhibitors: cytotoxic T-lymphocyte protein 4 (CTLA4) and programmed cell death protein 1 (PD-1). The anti-CLTA4 antibodies blocks repressive action of CLTA4 on T-cells and they become therefore activated. It was shown efficient in melanoma patients and accepted by FDA in 2015 as adjuvant therapy for stage III metastatic melanoma patients [34]. PD-1 is a cell surface receptor of T cells, that binds to PD-L1/PD-L2. After binding, an immunosuppressive pathway is activated and T cells activity is dampened. An action of an anti-PD-L1 antibody is to prevent this immune exhaustion [10]. A stepping stone for anti-PD-L1 therapies was approval of Tecentriq (atezolizumab) for Bladder cancer [35] and anit-PD1 Keytruda (pembrolizumab) initially accepted for NSCLC and further extended to head and neck cancer, Hodgkin's lymphoma, gastric cancer and microsatellite instability-high cancer [36]. Since other anti-PD-L1 or anti-PD1 antibodies were accepted or entered advanced stages of clinical trials [59]. A short history of immunotherapy FDA-accepted treatments can be found in Fig. 1.4

The main drawback of immunotherapies is a heterogeneity of response rate, which can vary i.e. from 10–40% in case of PD-L1blocking [60], suggesting that some patient can have more chances than others to respond to an immune therapy. So far, it has been shown that anti PD-L1 therapies works more effectively in T cell infiltrated tumors with exclusion of Tregs because of lack of difference in expression of FOXP3 in responding and non-responding group of patients [27]. Also some light has been shade by Rizvi et al. [47] who connected mutational rate of cancer cells to the chances of response to an immunotherapy.

Despite those fundings, the precise qualifications of patients that should be sensitive to an immunotherapy are not defined [42]. As most patients do not answer to immunother-

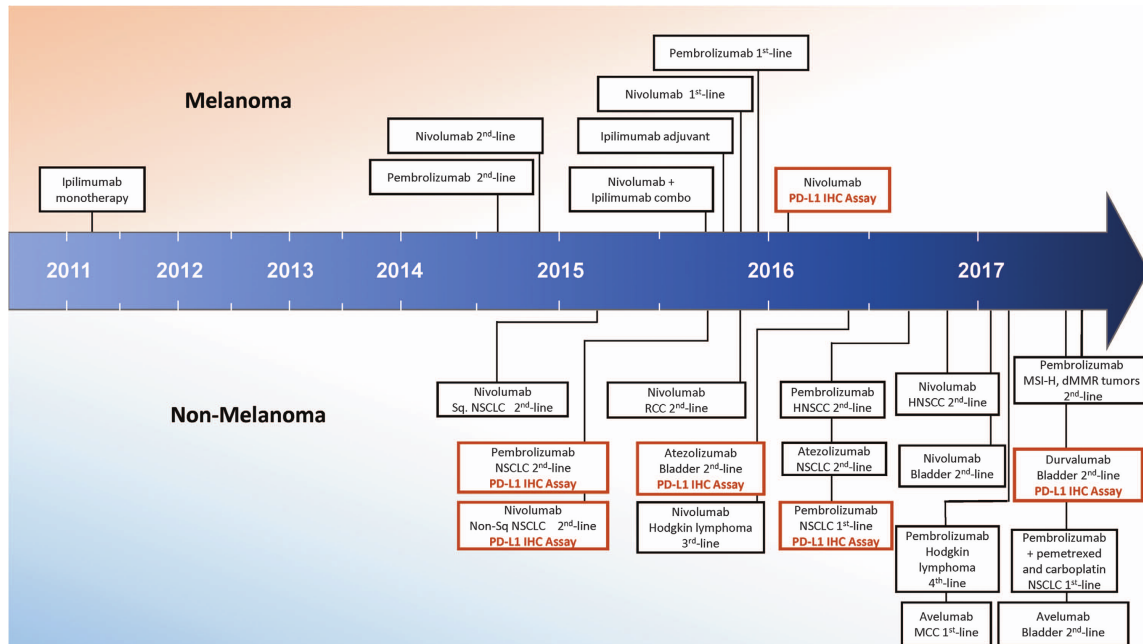


Figure 1.4: This timeline describes short history of FDA approval of checkpoint blocking immunotherapies up to 2017. Reprinted by permission from Springer Nature [56] Macmillan Publishers Limited, part of Springer Nature. All Rights Reserved.

opies, it stimulates researches to look for better biomarkers and patient stratifications, and pharmaceutical industries to discover new immune checkpoints based therapies.

1.3 Quantifying immune infiltration (data)

Nowadays, more and more biological data is produced. However, this proliferation of accessible resources is not proportional to generated insights and wisdom. In this thesis, we work mostly generate *Knowledge* and *Insights* and we hope to generate some *Wisdom* (Fig. 1.5). However, in this part, we will introduce the foundation of our analysis: different data types that will be further discussed in chapters that follow.

We will introduce most relevant data types that are used to study immune infiltration of tumors.

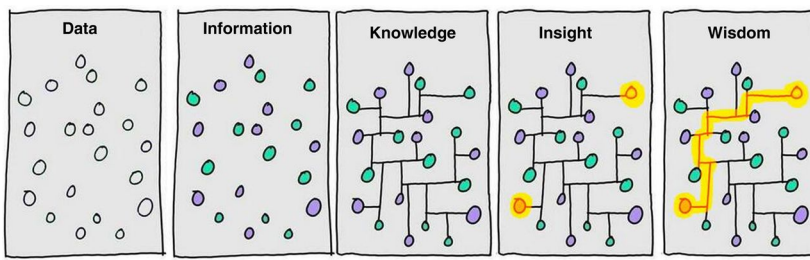


Figure 1.5: From Data to Wisdom. Illustration of different steps that it takes to go from *Data* to generating *Wisdom*. It highlights that generating data is not equal to understanding it and additional efforts are needed to generate value. Image authored by Clifford Stoll and Gary Schubert published by Portland Press Limited on behalf of the Biochemical Society and the Royal Society of Biology and distributed under the [Creative Commons Attribution License 4.0 \(CC-BY\)](#) in [43].

1.3.1 Cell sorting

1.3.1.1 Flow cytometry

Flow cytometry is a laser-based technology. It uses marker genes: cell surface proteins to sort cells in different compartments. Nowadays, it permits quantification of the abundance of up to 17 cell surface proteins using fluorescently labelled antibodies [40].

1.3.1.2 Mass cytometry

Mass cytometry (also known as CyTOF) allows for the quantification of cellular protein levels by using isotopes. It allows to quantify up to 40 proteins per cell [40].

1.3.2 Microscope Staining

Using microscope technics, histopathological cuts are analysed. The number of cells per a unit of area (i.e. mm²) is defined either manually by human or though diverse image analysis algorithms. Current pathology practice utilises chromogenic immunohistochemistry (IHC) [52]. Multiplexed approaches allow to identify multiple markers in the same histopathology cut. Modern techniques as imaging mass cytometry using FFPE tissue samples uses fluorescence and mass cytometry to identify and quantify marker proteins [22].

The main advantage of aforementioned technics the number of cells that can be analysed and the information about spatial distribution of the different cell types. The lim-

iting factor, as for cell sorting methods, is the number of markers (~10-100) and consequently number of cell types that can be identified [50].

The cell sorting methods and microscope staining are usually considered as a gold standard for multidimensional data techniques. The reason why they are not applied at large scale is the cost but also quite laborious and time consuming sample preparation demanding a fresh sample. In contrast, the -omics methods propose more scalable way to measure tumor micro environment.

1.3.3 omics

- Some kind of sequencing explanation needed for non-biologists

1.3.3.1 Transcriptome

Transcriptomics measures the number of counts of mRNA molecules using high-throughput techniques. mRNA is the part of genetic information that should be translated to proteins. It reflects the activity of cell ongoing processes. In contrast to DNA, mRNA is highly variant [58]. In addition, many genetic and epigenetic events can be either directly observed or indirectly inferred from transcriptomic data. Transcriptome can be measured with microarrays or RNA-seq NGS technology.

Bulk transcriptome data are quite accessible. They can be obtained from either flash-frozen or formalin-fixed, paraffin-embedded (FFPE) tissue samples, including both surgically resected material and core needle biopsies [50].

The main flaw of transcriptomic data is that the reproducibility between different platforms is limited. As a result, direct comparison between two datasets produced by different platforms is not advised.

Different strategies can be adapted to analyse bulk transcriptome.

Cieślik and Chinnaiyan [12] describes five groups of most popular approaches that can be applied to study transcriptome (Fig. 1.6). Despite a diversity of bioinformatic and statistical tools, the most popular differential approaches, mainly differential gene expression (DGE) based on difference between two experimental conditions.

RNA-seq data was proven to be a useful indicator for clinical applications [30, 33, 48]. Its utility for immune profiling was demonstrated in many studies through a use of transcriptomic signatures to predict immunotherapy response or survival [11].

In this work transcriptome data are analyzed to propose an alternative method to describe immune infiltration.

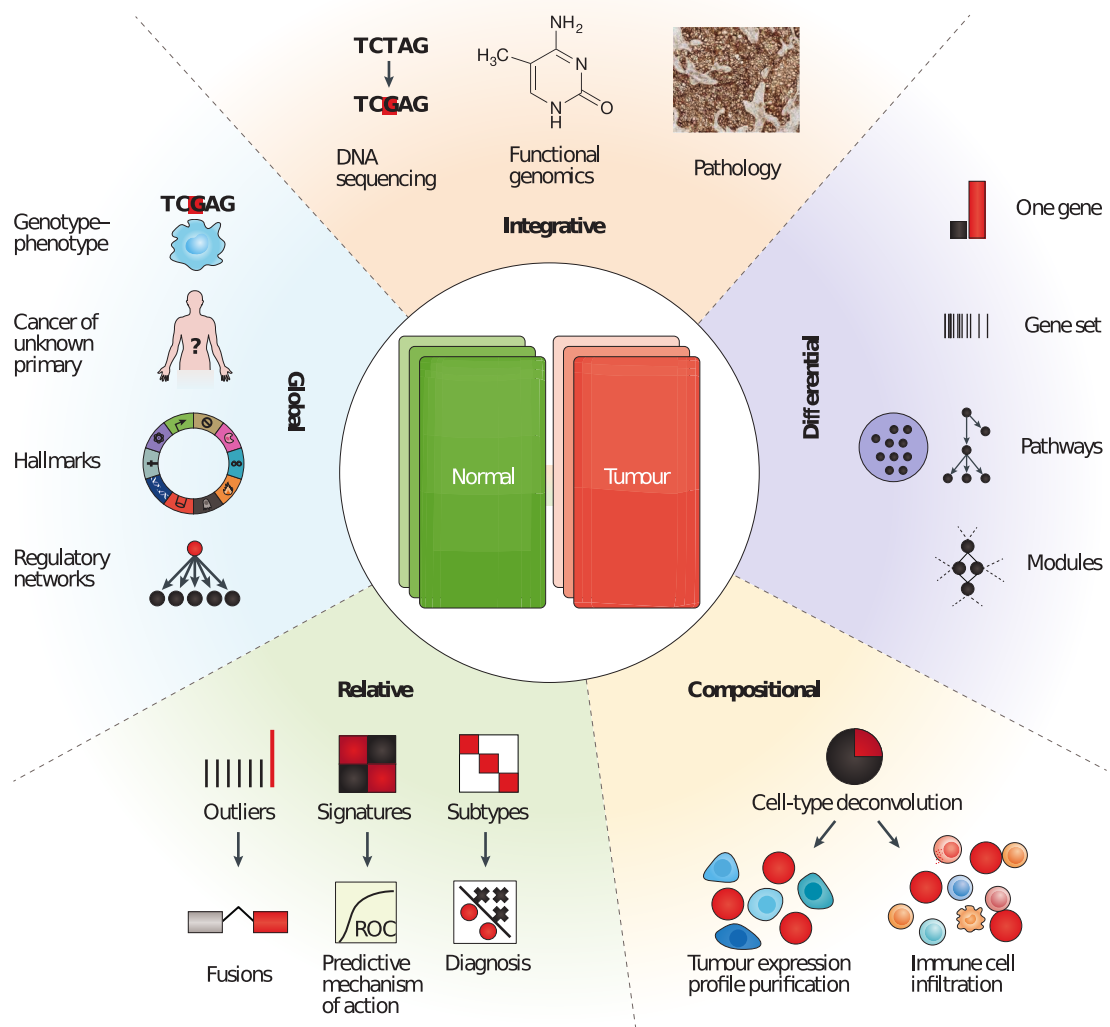


Figure 1.6: Five categories of RNA-seq data analysis. Differential analyses: comparing two (or more) conditions, Relative analyses: comparing to an internal reference (average, base level), Compositional analyses: inferring cell types or groups of cell types (i.e. tumor purity), Global analyses: pan-tissue and pan-cancer analyses and Integrative analyses: compiling heterogeneous data types. Reprinted by permission from Springer Nature [12] © 2018 Macmillan Publishers Limited, part of Springer Nature. All rights reserved.

1.3.3.2 Epigenome

An epigenome can be defined as a record of the chemical changes to the DNA and histone proteins of an organism. Changes to the epigenome can provoke changes to the structure of chromatin and changes to the function of the genome [4]. Epigenome data usually contains information about methylation CpG island changes. In cancer, global genomic hypomethylation, CpG island promoter hypermethylation of tumor suppressor genes, an altered histone code for critical genes, a global loss of monoacetylated and trimethylated histone H4 were observed. Methylome profiles can be also used as molecular signature [NMF and other ref]

1.3.3.3 Single cell RNA-seq

Described above methods of process DNA from hundreds of thousands of cells simultaneously and report averaged gene expression of all cells. In contrast, scRNA-seq technology allows getting results for each cell individually. This is tremendous step forward enhancement of our understanding of cell heterogeneity and opens new avenues of research questions.

Continuous discovery of new immune subtypes has proven that cell surface markers that are used for phenotyping by techniques like FACS and immunohistochemistry cannot capture the full complexity. ScRNA-seq methods allow to cluster known cell types in subpopulations based on their genetic features [40]. ScRNA-seq is also able to capture particularly rare cell types as it requires much less of RNA material (1 ng isolated from 100-1000 cells) compared to ‘bulk’ RNA-seq (~1 µg of total mRNA transcripts). It also allows to study cells at high resolution where the phenotypes can be re-defined in much more refined scale than previously [40]

This new data type also brings into the field new challenges related to data processing due to the volume, distribution, noise, and biases. Experts highlight as the most “batch effect”, “noise” and “dropout effect” [41]. So far, there are no official standards that can be applied which makes data comparison and post-processing even more challenging. Up to date, there are around 70 reported tools and resources for single cell data processing [15].

A limited number of single-cell datasets of tumors are made publicly available (@ TABLE ?).

One can ask why then developing computational deconvolution of transcriptome if we can learn relevant information from single-cell data. Today’s reality is that single cell data does not provide a straightforward answer to the estimation of cell proportions. The coverage is not full and sequenced single cells are not fully representative of the true pop-

ulation. For instance, neutrophiles are not found in scRNA-seq data because of they are “difficult to isolate, highly labile ex vivo and therefore difficult to preserve with current single-cell methods” [50]. In addition, a number of patients included in published studies of range <100 cannot be compared to thousand people cohorts sequenced with bulk transcriptome methods. This is mostly because single cell experiments are challenging to perform, especially in clinical setting as fresh samples are needed [50]. Today, single cell technology brings very interesting “zoom in” perspective, but it would be incautious to make fundings from a restricted group of individuals universal to the whole population. Major brake to the use of single cell technology more broadly might be as well the price that is neatly 10x higher for single cell sample compared to bulk [13].

Technology	Price
scRNA-seq	3000\$ / sample
RNA-seq	200 \$ / sample
FACS	0.05\$ / cell
CyTOF	35\$/cell

In this work, we are using single cell data in two ways. Firstly, in Comparative... chapter we compare immune cell profiles defined by scRNA-seq, blood and blind deconvolution (problem introduced in Immune signatures section). Secondly, in Heterogeneity of immune... we use single cell data of Metastatic melanoma generated by Tirosh et al. [57] to demonstrate subpopulations of Macrophages and NK cells.

1.4 Biological dimension of the thesis

Explaining the biological dimension of the project

- help to better understand tumor immunophenotypes (cell types present and their biology, interactions)
- propose predictive biomarkers - precision medicine
- better explore available data
- integrate the data (transcriptome & methylome, validate transcriptome with FACS etc.)

Chapter 2

Mathematical foundation of cell-type deconvolution of biological data

In this chapter, we will discuss how mathematical models can be used to extract information about specific cell-types from ‘bulk’ data or how to unmix mixed sources. It will introduce you to basic concepts of data analysis as well as most popular advanced solutions adapted for estimating presence and proportion of immune cells within cancer biopsies.

Note: Parts of this chapter with benchmark data might be a part of a future review

Explain the principle

2.1 Introduction to supervised and unsupervised learning

- Explaining difference between supervised and non-supervised learning technically and in our context

2.2 Blind source separation

(ICA, NMF, CAM)

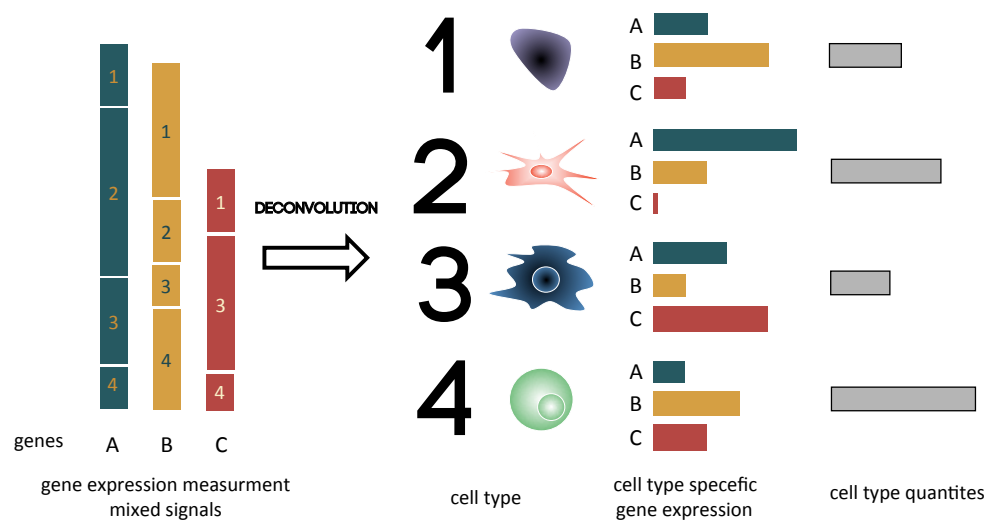


Figure 2.1: Principle of the deconvolution applied to transcriptome Graphical illustration of the deconvolution of mixed samples. Starting from the left, gene expression of genes A B C is a sum of expression of cell types 1, 2, 3, 4. After deconvolution, cell types are separated and gene expression of each cell type is estimated taking into account cell type proportions.

2.3 Finding optimal number of components and over-decomposition of transcriptopmes

- Explain why this problem is important
- Explain shortly my role in the paper

[?]

RESEARCH ARTICLE

Open Access



Determining the optimal number of independent components for reproducible transcriptomic data analysis

Ulykbek Kairov^{2†}, Laura Cantini^{1†}, Alessandro Greco¹, Askhat Molkenov², Urszula Czerwinska¹, Emmanuel Barillot¹ and Andrei Zinovyev^{1*+ID}

Abstract

Background: Independent Component Analysis (ICA) is a method that models gene expression data as an action of a set of statistically independent hidden factors. The output of ICA depends on a fundamental parameter: the number of components (factors) to compute. The optimal choice of this parameter, related to determining the effective data dimension, remains an open question in the application of blind source separation techniques to transcriptomic data.

Results: Here we address the question of optimizing the number of statistically independent components in the analysis of transcriptomic data for reproducibility of the components in multiple runs of ICA (within the same or within varying effective dimensions) and in multiple independent datasets. To this end, we introduce ranking of independent components based on their stability in multiple ICA computation runs and define a distinguished number of components (Most Stable Transcriptome Dimension, MSTD) corresponding to the point of the qualitative change of the stability profile. Based on a large body of data, we demonstrate that a sufficient number of dimensions is required for biological interpretability of the ICA decomposition and that the most stable components with ranks below MSTD have more chances to be reproduced in independent studies compared to the less stable ones. At the same time, we show that a transcriptomics dataset can be reduced to a relatively high number of dimensions without losing the interpretability of ICA, even though higher dimensions give rise to components driven by small gene sets.

Conclusions: We suggest a protocol of ICA application to transcriptomics data with a possibility of prioritizing components with respect to their reproducibility that strengthens the biological interpretation. Computing too few components (much less than MSTD) is not optimal for interpretability of the results. The components ranked within MSTD range have more chances to be reproduced in independent studies.

Keywords: Transcriptome, Independent component analysis, Reproducibility, Cancer

Background

Independent Component Analysis (ICA) is a matrix factorization method for data dimension reduction [1]. ICA defines a new coordinate system in the multi-dimensional space such that the distributions of the data point projections on the new axes become as mutually independent as possible. To achieve this, the standard approach is maximizing the non-gaussianity of the data

point projection distributions [1]. ICA has been widely applied for the analysis of transcriptomic data for blind separation of biological, environmental and technical factors affecting gene expression [2–6].

The interpretation of the results of any matrix factorization-based method applied to transcriptomics data is done by the analysis of the resulting pairs of metagenes and metasamples, associated to each component and represented by sets of weights for all genes and all samples, respectively [6, 7]. Standard statistical tests applied to these vectors can then relate a component to a reference gene set (e.g., cell cycle genes), or to clinical

* Correspondence: Andrei.Zinovyev@curie.fr

†Equal contributors

¹Institut Curie, PSL Research University, INSERM U900, Mines ParisTech, Paris, France

Full list of author information is available at the end of the article

annotations accompanying the transcriptomic study (e.g., tumor grade). The application of ICA to multiple expression datasets has been shown to uncover insightful knowledge about cancer biology [3, 8]. In [3] a large multi-cancer ICA-based metaanalysis of transcriptomic data defined a set of metagenes associated with factors that are universal for many cancer types. Metagenes associated with cell cycle, inflammation, mitochondria function, GC-content, gender, basal-like cancer types reflected the intrinsic cancer cell properties. ICA was also able to unravel the organization of tumor microenvironment such as the presence of lymphocytes B and T, myofibroblasts, adipose tissue, smooth muscle cells and interferon signaling. This analysis shed light on the principles underlying bladder cancer molecular subtyping [3].

It has been demonstrated that ICA has advantages over the classical Principal Component Analysis (PCA) with respect to interpretability of the resulting components. The ICA components might reflect both biological factors (such as proliferation or presence of different cell types in the tumoral microenvironment) or technical factors (such as batch effects or GC-content) affecting gene expression [3, 5]. However, unlike principal components, the independent components are only defined as local minima of a non-quadratic optimization function. Therefore, computing ICA from different initial approximations can result in different problem solutions. Moreover, in contrast to PCA, the components of ICA cannot be naturally ordered.

To improve these aspects, several ideas have been employed. For example, an *icasso* method has been developed to improve the stability of the independent components by: (1) applying multiple runs of ICA with different initializations; (2) clustering the resulting components; (3) defining the final result as cluster centroids; and (4) estimating the compactness of the clusters [9]. The resulting components can be then naturally ordered from the most stable to the least stable ones. This ranking is usually different from more commonly used independent component rankings based on the value of the used non-gaussianity measure (such as kurtosis) or the variance explained by the components.

The fundamental question is the determination of the number of independent components to produce. This problem can be split into two parts: a) what dimension should be selected for reducing the transcriptomic data before applying ICA (determining the effective data dimension); and b) which is the most informative number of components to use in the downstream analysis?

Determining the optimal effective data dimension for application of signal deconvolution was a subject of research in various fields. For example, ICA appeared to be a powerful method for analyzing the fMRI (functional magnetic resonance) data [9–12]. In this field, it was

shown that choosing a too small effective data dimension might generate “fused components,” not reflecting the heterogeneity of the data, leading to a loss of interesting sources (under-decomposition). At the same time, choosing the effective dimension too high might lead to signal-to-noise ratio deterioration, overfitting and splitting of the meaningful components (over-decomposition) [10–12]. The influence of the effective dimension choice on the ICA performance has not been well studied in the context of transcriptomic data analysis. For example, in [3] each dataset was decomposed into a number of components in an ad hoc manner ($n = 20$).

Several theoretical approaches for estimating effective data dimension exist. The simplest ones, developed for PCA analysis, are represented by the Kaiser rule aimed at keeping a certain percentage of explained variance and the broken stick model of resource distribution [13]. More sophisticated approaches employ the information theory (e.g., Akaike’s information or Minimal Description Length criteria) [13] or investigate the local-to-global data structure organization [14]. Also, computational approaches based on cross-validation have been suggested in the literature [15]. Specifically for ICA analysis, few methods have been proposed to optimize the effective dimension. For example, the Bayesian Information Criterion (BIC) can be applied to the Bayesian formulation of ICA for selecting the optimal number of components [16].

Although many of the above theoretical methods are “parameter-free,” selecting the best method for choosing an effective dimension for transcriptomic data can be challenging in the absence of a clearly defined validation strategy. One possible approach to overcome this limitation is to apply the same computational method to multiple transcriptomic datasets derived from the same tissue and disease. In this situation, it is reasonable to expect that a matrix factorization method should detect similar signals in all datasets. By taking advantage of the rich collection of public data such as The Cancer Genomic Atlas (TCGA) [17] and Gene Expression Omnibus [18], it is possible to compare and contrast the parameters of different gene expression analysis methods such as ICA.

In this study, we used TCGA pan-cancer (32 different cancer types) transcriptomic datasets and a set of six independent breast cancer transcriptomic datasets to evaluate the effect of the number of computed independent components on reproducibility and biological interpretability of the obtained results. We evaluated the reproducibility of ICA on three aspects: First, we analyzed the stability of the computed components with respect to multiple runs of ICA; second, we analyse the conservation of the computed components by varying the choice of the reduced data dimension; and third, we consider the reproducibility of the resulting set of ICA

metagenes across multiple independent datasets. Our reproducibility analysis thus explores 13,027 transcriptomic profiles in 37 transcriptomic datasets, for which more than 100,000 ICA decompositions have been computed.

We finally defined a novel criterion adapted for choosing the effective data dimension for ICA analysis of gene expression, which takes into account the global properties of transcriptomic multivariate data. The Maximally Stable Transcriptome Dimension (MSTD) is defined as the maximal dimension where ICA does not yet produce a large proportion of highly unstable signals. By numerical experiments, we showed that components ranked by stability within the MSTD range tend to be more reproducible and easier to interpret than higher-order components.

Results

Definition of component reproducibility measures used in this study

Stability of an independent component, in terms of varying the initial starts of the ICA algorithm, is a measure of internal compactness of a cluster of matched independent components produced in multiple ICA runs *for the same dataset and with the same parameter set but with random initialization*. The exact index used for quantifying the clustering is documented in the Methods section. Conservation of an independent component in terms of choosing various orders of ICA decomposition is a correlation between matched components computed in two ICA decompositions of different orders (reduced data dimensions) *for the same dataset*. Reproducibility of an independent component is an (average) correlation between the components that can be matched after applying the ICA method using the same parameter set but *for different datasets*. For example, if a component is reproduced between the datasets of the same cancer type, then it can be considered a reliable signal less affected by technical dataset peculiarities. If the component is reproduced in datasets from many cancer types, then it can be assumed to represent a universal carcinogenesis mechanism, such as cell cycle or infiltration by immune cells. The details on computing correlations between components from different datasets are described in Methods.

Maximally stable Transcriptome dimension (MSTD), a novel criterion for choosing the optimal number of ICs in transcriptomic data analysis

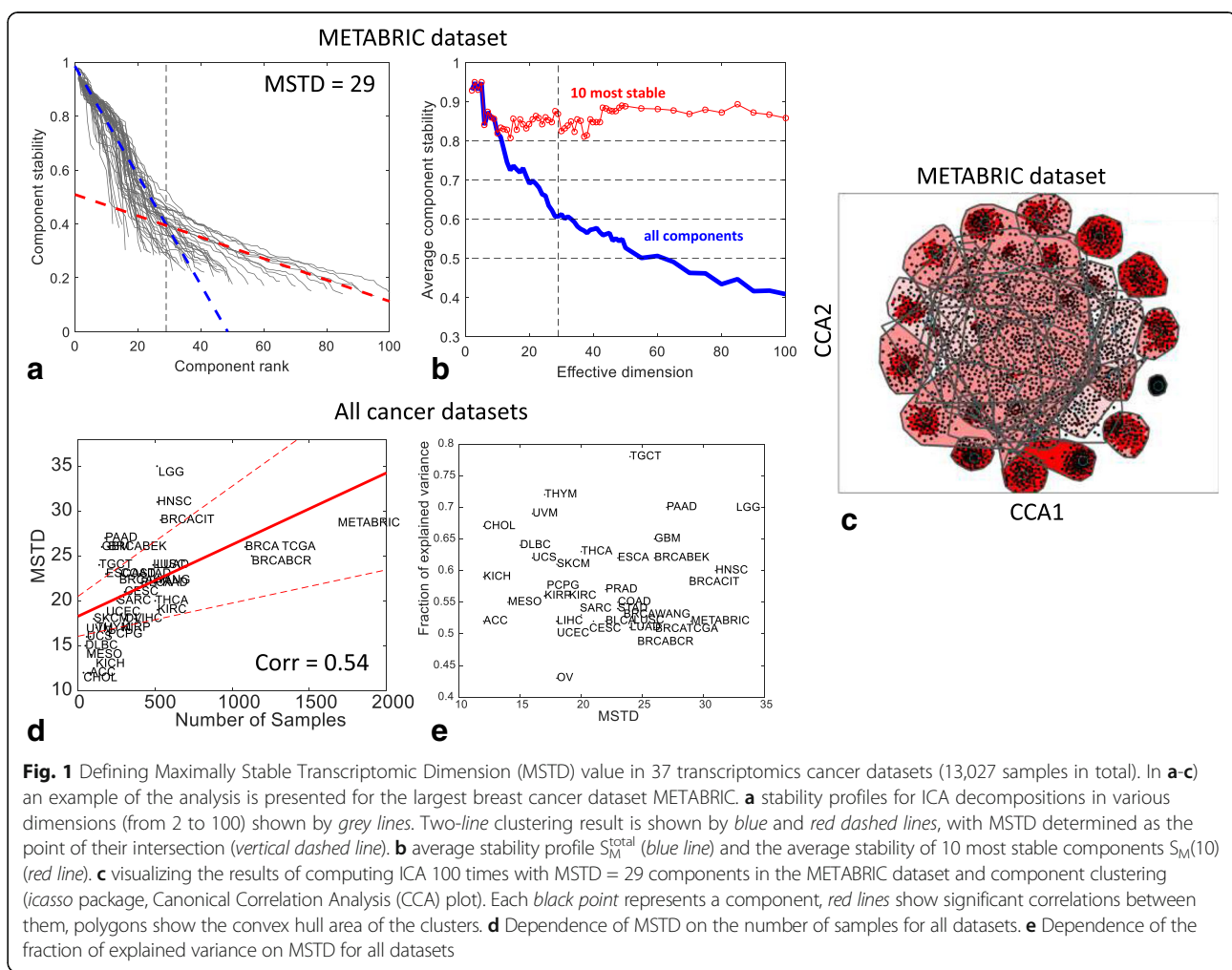
We used 37 transcriptomic datasets to analyze the stability and reproducibility of the ICA results conditional on the chosen number of components. ICA has been applied separately to 37 cancer transcriptomic datasets

following the ICA application protocols as described in Methods.

The proposed protocol depends on a fundamental parameter M (effective dimension of the data and, at the same time, the number of computed independent components) whose effect on the stability of the ICs is investigated. For each transcriptomic dataset, the range of M values 2–100 has been considered. For each value of M , the data dimension is reduced to M by PCA and then data whitening is applied. Subsequently, the actual signal decomposition is applied in the whitened space by defining M new axes, each maximizing the non-gaussianity of data point projections distribution.

For transcriptomic data, ICA decomposition provides: (a) M metagenes ranked accordingly to their stability in multiple runs ($n = 100$) of ICA; and (b) a profile of stability of the components (set of M numbers in [0,1] range in descending order). Considering the largest dataset METABRIC as an example, the behavior of the stability profile as a function of M is reported in Fig. 1a. The results for stability analysis for other breast cancer datasets are similar (See Additional file 1: Figure SF2). To recapitulate the behaviour of many stability profiles, the average stability of the first k top-ranked components $S_M(k)$ is used (See Fig. 1b). For $k = M$, the average stability of all computed components is denoted as S_M^{total} . Three major conclusions can be made from Fig. 1. First, the average stability of the computed components S_M^{total} decreases with the increase of M , while the average stability of the first few top ranked components, e.g., $S_M(10)$, weakly depends on M (Fig. 1b). Moreover, S_M^{total} is characterized by the presence of local maxima, defining certain distinguished values of M that correspond to the (locally) maximally stable set of components (Fig. 1b). Third, the stability profiles for various values of M can be classified into those for which the stability values are distributed approximately uniformly and those (usually, in higher dimensions) forming a large proportion of the components with low stability (I_q between 0.2 and 0.4) (Fig. 1a).

Considering these observations, we hypothesized that the optimal number of independent components – large enough to avoid fusing meaningful components and yet small enough to avoid producing an excessive amount of highly unstable components – should correspond to the inflection point in the distribution of the stability profiles (Fig. 1a). To find this point, the stability measures have been clustered along two lines, which is analogous of 2-means clustering but with lines as centroids. In this clustering, the line with a steeper slope (Fig. 1a, blue line) grouped the stability profiles with uniform distribution, while another line (Fig. 1a, red line) matched the mode of low stability components. The intersection of these lines provided a consistent estimate of the effective



number of independent components. We call this estimate Maximally Stable Transcriptome Dimension (MSTD) and in the following we investigated its properties. We note that, as in various information theory-based criteria (BIC, AIC), this estimate is free of parameters (thresholds), and it only exploits the property of the qualitative change in the character of the stability profile in higher data dimensions for transcriptomic data.

In most of the cancer transcriptomics datasets used in our analysis, MSTD was found to correspond roughly to the average stability profile $S_M^{\text{total}} \approx 0.6$ (Additional file 1: Figure SF2). In Fig. 1d, the dependence of MSTD on the number of samples contained in the transcriptomic dataset is investigated for all the 37 transcriptomic datasets. As shown in Additional file 2: Figure SF1, MSTD increased with the number of samples; however, this trend was weaker than other estimates of an effective dimension such as Kaiser rule and broken stick distribution-based data dimension estimates. Finally, the fraction of variance explained by the linear subspace spanned by MSTD number of components was evaluated (Fig. 1e),

and it was observed that the fraction of variance explained varied from 0.45 to 0.75 with a median of 0.56.

Underestimating the effective dimension ($M < \text{MSTD}$) leads to a poor detection of known biological signals

Previous large-scale ICA-based meta-analyses [3] have shown that some of the ICs derived from the decomposition of a cancer transcriptomic data were clearly and uniquely associated with known biological signals. For example, one of these signals was the one connected to proliferative status of tumors. Another example was given by the signals related to the infiltration of immune cells that were also strongly heterogeneous across cancer patients.

We have checked the reproducibility of several metagenes obtained in previous meta-analyses [3] for all ICA decompositions as a function of M . For this analysis, we employed the METABRIC breast cancer dataset, which was not included in the input data of the previous publication [3] and thus it had not been used to derive the metagenes of that work. In addition, we checked how

the significance of intersections between the genes defining the components and several reference gene sets (produced independently of the ICA analyses) behaved as a function of M.

We applied the previously developed correlation-based approach to match previously identified metagenes with the ones computed for a new METABRIC dataset (see Methods section). The components were oriented accordingly to the direction of the heaviest tail of the projection distribution. When matching an oriented component to the previously defined set of metagenes, we verified that the resulting maximal correlation should be positive, i.e. large positive weights in one metagene should correspond to large positive weights in another metagene.

One of the most important case studies is reproducibility of the “proliferative” metagene in different data dimensions. It is investigated in Fig. 2a-c. For this metagene, we computed correlations with M newly identified independent components. As an example, the profile of correlations for M = 100 is shown in Fig. 2b. It can be seen that one of the components (ranked #7 by stability analysis) is much better correlated to the proliferative metagene than any other component. Therefore, component #7 is called “best matched” in this case, for M = 100, and “well separable.” Repeating this analysis for all M and reporting the observed maximal correlation coefficient and the corresponding stability value gives a plot shown in Fig. 2a. Separability of the best matched component from the other components is visualized in Fig. 2c.

As it can be seen from Fig. 1a, the biologically expected signals (i.e., cell cycle) can be poorly detected for $M < \text{MSTD}$; however, once the best matching component with significant correlation was found, it remained unique and was detected robustly even for very large values of $M > \text{MSTD}$. For example, even when 100 components (M) were computed, the correlation between the previously defined proliferative metagene and the best matched independent component did not diminish (Fig. 2a). Moreover, the separability of the best matched component from the rest of the components was not ruined (Fig. 2c). In this example, the identification of cell cycle component remained clear (large and well-separated correlation coefficient) for $M > \text{MSTD}$. This result was consistent and complementary when compared with the previously observed weak dependence of $S_M(10)$ on M. Indeed, the “proliferative” best matched component had stability rank k in the range [6, 11]. That is, it remained stable in ICA decompositions in all dimensions. Moreover, the intersection of a recently established proliferation gene signature [19] with the set of top contributing genes of the best matched component improved with increasing M and saturated (Fig. 2d). This proves that the detection of the proliferation-associated signal with

ICA does not depend on the ICA-based definition of the proliferative metagene.

Together with the proliferative signal, other metagenes from the previously cited ICA-based meta-analysis [3] were robustly identified in our analysis. In Fig. 2e-h, we showed the correlation with the best matching component for the metagenes associated with the presence of myofibroblasts, inflammation, interferon signaling and immune system, as a function of M. These plots illustrated different scenarios that can result from such analysis. The myofibroblast-associated metagene was robustly detected for all values of $M > 7$ (Fig. 2f). However, the stability of the best matching component was deteriorated in higher-order ICA decompositions ($M > 45$). For the inflammation-associated metagene, an ICA decomposition with $M > 38$ was needed to robustly detect a component that correlates with the metagene (Fig. 2e).

Interestingly, the immune-associated metagene was found robustly matched starting from $M = 4$. However, in higher-order decompositions (starting from $M = 30$) it could be matched to several components that can be associated with specific immune system-related signals (Fig. 2h-i). Hypergeometric tests applied to the sets of top-contributing genes (weights larger than 5.0) allowed us to reliably interpret these components as being associated with the presence of three types of immune-related cells: T cells (corrected enrichment p -value = 10^{-39} with “alpha beta T cells” signature [20], other immune signatures are much less significant), B cells (p -value = 10^{-7} with “B cells, preB.FrD.BM” signature) and myeloid cells (p -value = 10^{-78} with “Myeloid Cells, DC.11cloSer.Salm3.SI” signature).

Overestimating the number of components ($M > \text{MSTD}$) produces multiple ICs driven by small gene sets

We observed that the higher-order ICA decompositions ($M > \text{MSTD}$) produced a larger number of components driven by small gene sets (frequently, one gene), such that the projections of the genes in this “outlier” set is separated by a relatively large gap with the rest of the projections. We thus designed a simple algorithm to distinguish such components driven by a small gene set from all the others. The names of the genes composing these small sets were used for annotating the corresponding components (Fig. 3a, right part).

It was observed that the presence of such “small gene set-driven” components is a characteristic of higher-order ICA decompositions ($M > \text{MSTD}$), much less present in ICA decompositions with $M \leq \text{MSTD}$ (compare Fig. 3a and Additional file 1: Figure SF2).

To check the biological significance of the outlier genes, we considered as a case study the higher-order ($M = 100$) ICA decomposition of the METABRIC breast cancer dataset. We collected all those genes found to be

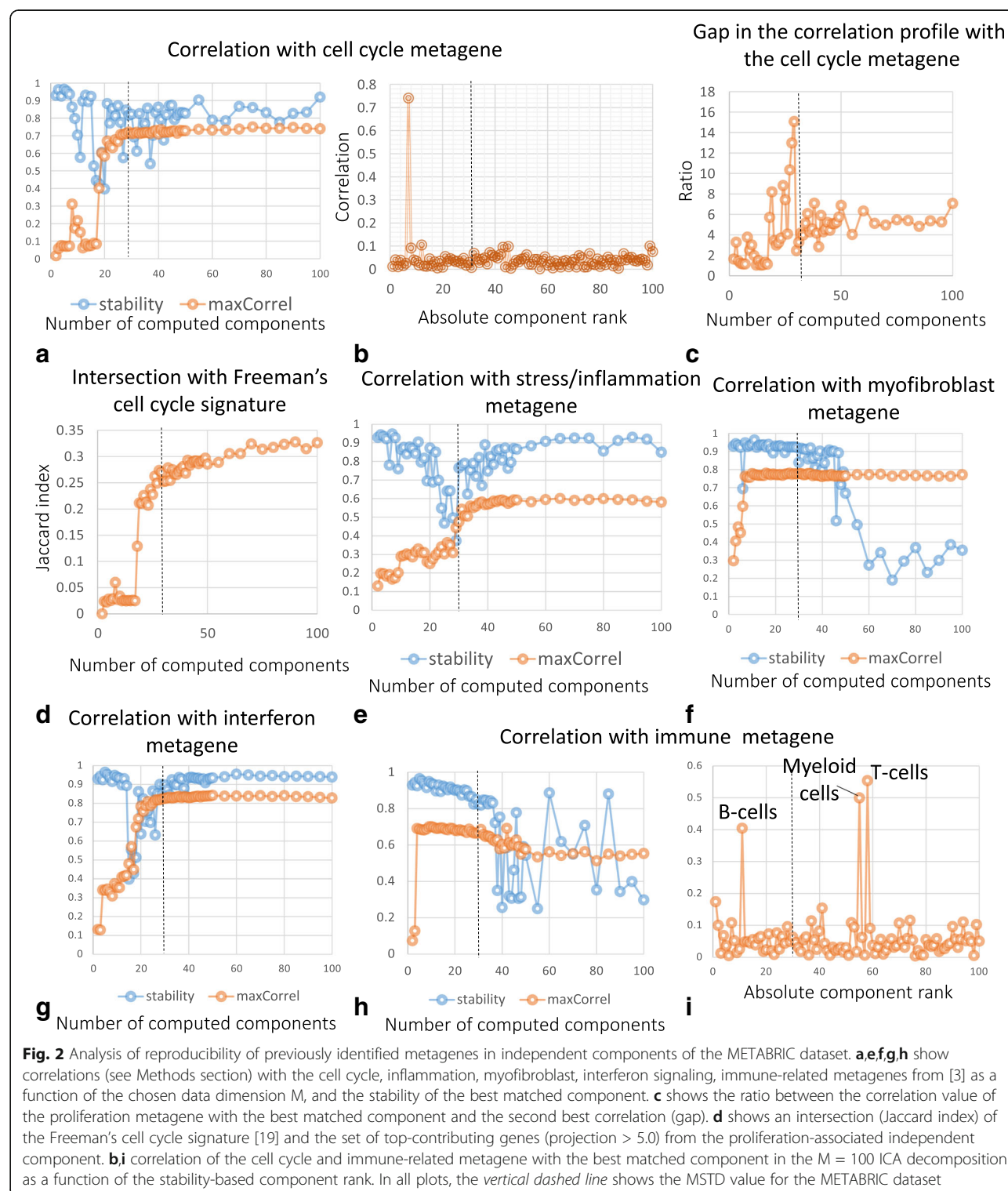
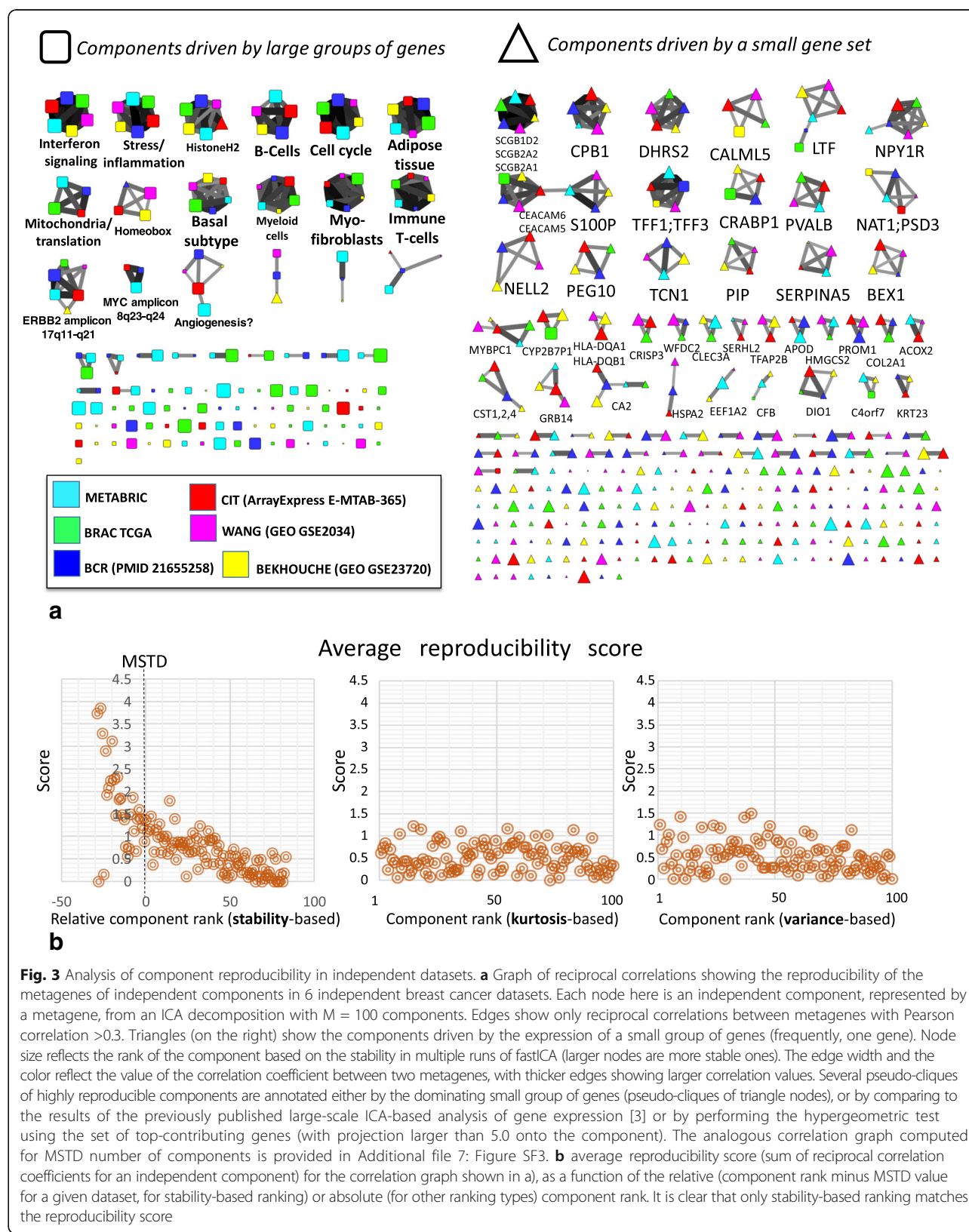


Fig. 2 Analysis of reproducibility of previously identified metagenes in independent components of the METABRIC dataset. **a,e,f,g,h** show correlations (see Methods section) with the cell cycle, inflammation, myofibroblast, interferon signaling, immune-related metagenes from [3] as a function of the chosen data dimension M, and the stability of the best matched component. **c** shows the ratio between the correlation value of the proliferation metagene with the best matched component and the second best correlation (gap). **d** shows an intersection (Jaccard index) of the Freeman's cell cycle signature [19] and the set of top-contributing genes (projection > 5.0) from the proliferation-associated independent component. **b,i** correlation of the cell cycle and immune-related metagene with the best matched component in the $M = 100$ ICA decomposition as a function of the stability-based component rank. In all plots, the vertical dashed line shows the MSTD value for the METABRIC dataset

drivers of at least one “small gene set-driven” component. We obtained in this way a set of 98 genes listed in Additional file 3: Table ST2. This list appeared to be strongly enriched ($p\text{-value} = 10^{-12}$ after correction for multiple testing) in the genes of the signature

DOANE_BREAST_CANCER_ESR1_UP “Genes up-regulated in breast cancer samples positive for ESR1 compared to the ESR1 negative tumors” from Molecular Signature Database [21] and several other specific to breast cancer gene signatures. This analysis thus



suggested that at least some of the identified “small gene set-driven” components are not the artifacts of the ICA decomposition, but they can be biologically meaningful and reproducible in independent datasets (Fig. 3a, right part).

Most stable components with stability rank \leq MSTD have more chances to be reproduced across independent datasets for the same cancer type

It would be reasonable to expect that the main biological signals characteristic for a given cancer type should be the same when one studies molecular profiles of different independent cohorts of patients. Therefore, we expect that for multiple datasets related to the same cancer type, ICA decompositions should be somewhat similar; hence, reciprocally matching each other. We called this expected behavior “reproducibility,” and here we studied this by applying ICA to six relatively large breast cancer transcriptomic datasets. Of note, these datasets were produced using various technologies of transcriptomic profiling (Additional file 4: Table ST1).

To identify the reproducible components, we applied the same methodology as in the previously published ICA-based gene expression meta-analysis [3]. We decomposed the six datasets separately and then constructed a graph of reciprocal correlations between the obtained metagenes. Correlation between two sets of components is called reciprocal when a component from one set is the best match (maximally correlated) to a component from another set, and vice versa (see Methods for a strict definition).

Pseudo-cliques in this graph, consisting of several nodes, correspond to reproducible signals detected by ICA. As shown in Fig. 3, multiple reproducible signals were identified in the analysis. Some of them correspond to signals already identified in [3] (e.g., cell cycle, interferon signaling, microenvironment-related signals), and some correspond to newly discovered biological signals (e.g., ERBB2 amplicon-associated). Some other pseudo-cliques are associated with “small gene set-driven” components (frequently, one gene-driven), such as TFF1–3-associated or SCGB2A1–2-associated components.

The genes driver of reproducible and “small gene set-driven” components (S100P, TFF1, TFF3, SCGB2A1, SCGB1D2, SCGB2A2, LTF, CEACAM6, CEACAM5 being most remarkable examples) have been investigated in detail, to further check their biological interest. They were found to be the genes known to be associated with breast cancer progression [22]. For example, seven of the nine previously mentioned genes form a part of a gene set known to be up-regulated in the bone relapses of breast cancer (M3238 gene set from MSigDB).

To quantify the reproducibility of the components, we computed a reproducibility score. It is a sum of

correlation coefficients between the component and all reciprocally correlated components from other datasets. By construction, the maximum value of the score is 5, which meant that a component with such a score would be perfectly correlated with the reciprocally related components from five other datasets. We studied the dependence of this score as a function of the relative to MSTD component stability-based rank (Fig. 3b). From this study, it follows that even for the high-order ICA decompositions, the components ranked by their stability within MSTD range, have an increased likelihood of being reproduced in independent datasets collected for the same cancer type.

To show that the stability-based ranking of genes is more informative compared with the standard rankings of independent components, we performed a computational analysis in which we compared the stability-based ranking with the rankings based on non-gaussianity (kurtosis) and explained variance. These two measures are frequently used to rank the independent components [6]. From Fig. 3b it is clear that the stability-based ranking of independent components corresponds well to the reproducibility score, while two other simpler measures do not.

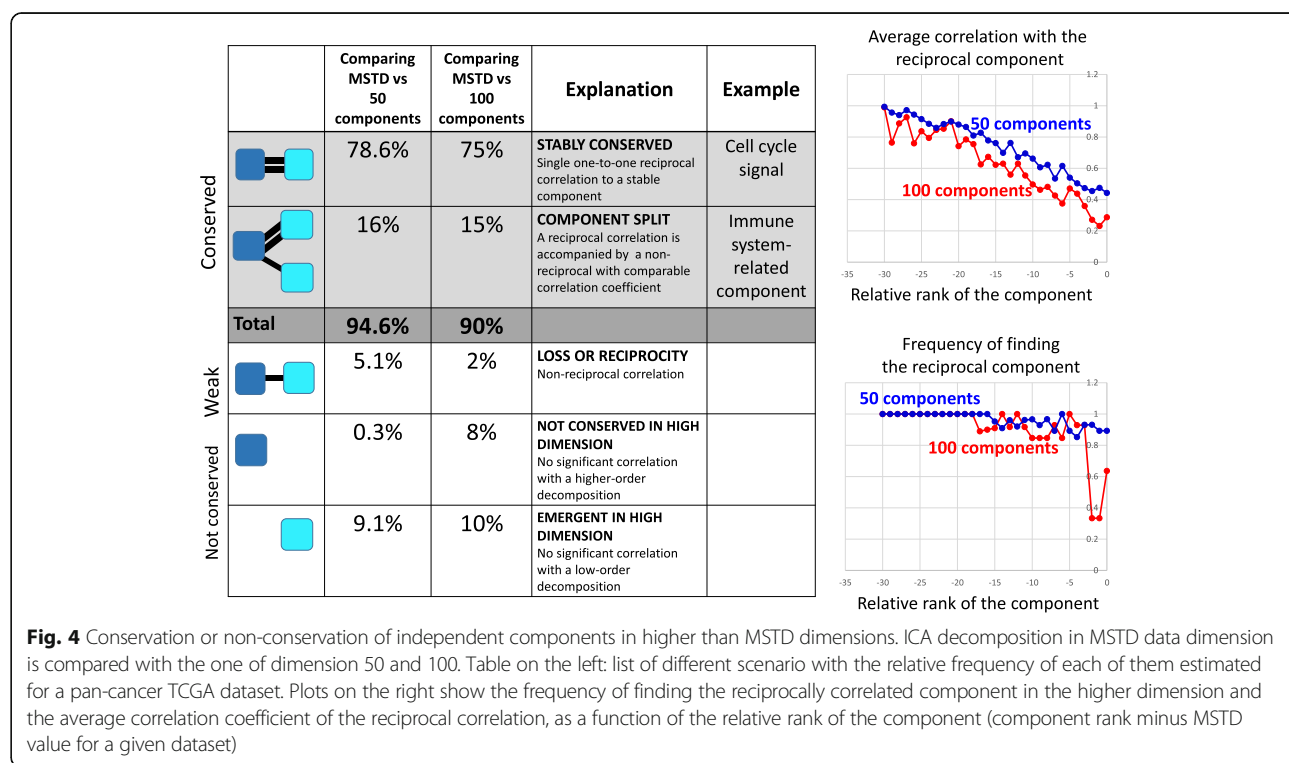
It can also be shown that the total number of reciprocal correlations with relatively large correlation coefficients ($|r| > 0.3$) between ICA-based metagenes computed for several independent datasets is significantly bigger when the component stabilization approach is applied (Additional file 5: Figure SF4). This proves the utility of the applied stabilization-based protocol of ICA application to transcriptomic data.

Computing large number of components ($M > MSTD$) does not strongly affect the most stable ones

We lastly used ICA decompositions of 37 transcriptomic datasets to compare the ICA decompositions corresponding to $M = MSTD$ with the higher-order decompositions, $M = 50$ or $M = 100$.

It was found that the components calculated in lower data dimensions can be relatively well matched to the components from higher-order ICA decompositions (Fig. 4). More precisely, 90% of the components defined for $M = MSTD$ had a reciprocal best matched component in the $M = 100$ ICA decomposition. Most stable components had a clear tendency to be reproduced with high correlation coefficient ($r > 0.8$). Only 10% of the components had only non-reciprocal or too small correlations between two decompositions (in other words, *not conserved* in higher-order ICA decompositions).

Approximately 15% of the components in $M = MSTD$ ICA decomposition together with reciprocal maximal correlation also had a non-reciprocal correlation to one of the components in $M = 100$ ICA decomposition (Fig. 4). This case can be described as splitting a component into



two or more components in the higher-order ICA decompositions. At least one such split had a clear biological meaning, namely the splitting of the component representing the generic “immune infiltrate.” The resulting “split” components more specifically represented the role of T cells, B cells and myeloid cells in the tumoral micro-environment (see the “*Underestimating the effective dimension...*” Results section).

Discussion

Our results shed light on the organization of the multivariate distribution of gene expression in the high-dimensional space. It appears that the organization contained two relatively well separated parts: *the dense one* of a relatively small effective dimension and *the sparse one*. The former contained the genes from within co-regulated modules that contained from few tens to few hundreds of genes. The latter was spanned by the genes with unique regulatory programs (perhaps tissue-specific) weakly shared by the other genes. Here the sparsity was understood in the sense of low local multivariate distribution density.

Independent Component Analysis can capture both these parts of the multivariate distribution. However, while the dense part defined independent components with approximately uniformly distributed stabilities, starting from highly stable to less stable, the sparse part was spanned by the components characterized mostly by small stability values.

This organization of the gene expression space is captured in the distribution of ICA stability profiles for varying M , which allowed us to define the Maximally Stable Transcriptome Dimension (MSTD) value, roughly reflecting the dimension of the dense part of the gene expression distribution. In one hand, when underdecomposing (compressing too much by dimension reduction, $M < \text{MSTD}$) a transcriptomic dataset, the resulting independent components are hard to interpret. In the other hand, overdecomposing transcriptomes (choosing the effective dimension much bigger than MSTD) is not dramatically detrimental: one can choose to explore a relatively multi-dimensional subspace of a transcriptomic dataset, taking into account that applying matrix factorization methods in higher dimensions becomes computationally challenging and prone to bad algorithm convergence. Nevertheless, higher-order decompositions might allow capturing the behavior of some tissue-specific or cancer type-specific biomarker genes from the sparse part of the distribution, which can be found reproducible in other independent studies.

In our computational experiments, we selected 100 as the maximum order of ICA decomposition (M) to test. However it is possible to examine even higher orders of ICA decompositions, reducing the data to more than 100 dimensions, but not more than the total number of samples, of course. In practice, computing ICA in such high dimension leads to significant deterioration of the fastICA algorithm convergence, so exploring $M > 100$

might be too expensive in terms of computational time. Moreover, our study suggests that the most interesting for interpretation components are usually positioned within the first few ten top ranks: therefore, 100 seems to be a reasonable limit for dimension reduction when applying ICA to transcriptomic data.

Our proposed approach can be used for comparing intrinsic reproducibility, at different levels, of various matrix factorization methods. For example, it would be of interest to compare the widely used Non-negative matrix factorization (NMF) method [6, 7] with ICA to assess reproducibility of extracted metagenes in independent datasets of the same nature.

More generally, systematic reproducibility analysis can be a useful approach for establishing the best practices of application of the bioinformatics methods.

Conclusion

By using a large body of data and comparing 0.1 million decompositions of transcriptomic datasets into the sets of independent components, we have checked systematically the resulting metagenes for their reproducibility in several runs of ICA computation (measuring *stability*), for their reproducibility between a lower order and higher-order ICA decompositions (*conservation*), and between metagene sets computed for several independent datasets, profiling tumoral samples of the same cancer type (*reproducibility*).

From the first of such analyses, we formulated a minimally advised number of dimensions to which a transcriptomic dataset should be reduced called Maximally Stable Transcriptome Dimension (MSTD). Reducing a transcriptomic dataset to a dimension below MSTD is not optimal in terms of the interpretability of the resulting ICA components. We showed that for relatively large transcriptomic datasets, MSTD could vary from 15 to 30 and that the number of samples matters relatively weakly.

From the second analysis, we concluded that the suggested protocol of ICA application to transcriptomic data is conservative, i.e., the components identified in a higher dimension (for example, in one hundred dimensional space) can be robustly matched with those components obtained in the dimensions comparable with MSTD. Moreover, we described an effect of interpretable component splitting in higher dimensions, leading to detection of finer-grained signals (e.g., related to the decomposition of the immune infiltrate in the tumor microenvironment). At the same time, the application of ICA in high dimensions resulted in a greater proportion of unstable components, many of them were driven by expression of small (one to three members) gene sets. Yet, some of these small gene set-driven components were highly reproducible and biologically meaningful.

From the third analysis, we established that the used protocol of ICA application, with ranking the independent components based on their stability, prioritized those components having more chances to be reproduced in independent transcriptomic datasets. Moreover, when ICA was applied in higher dimensions, the components within the MSTD range still have more chances to be reproduced.

In sum, our results confirmed advantageous features of ICA applied to gene expression data from different platforms, leading to interpretable and quantifiably reproducible results. Comparing ICA analyses performed in various dimensions and multiple independent datasets for the same cancer types allow prioritizing of the most reliable and reproducible components which can be quantitatively recapitulated in the form of metagenes or the sets of top contributing genes. We expect that ICA will demonstrate similar properties in other large-scale transcriptomic data collections such as scRNA-seq data.

Methods

Transcriptomics cancer data used in the analysis

Expression data derived for 32 solid cancer types (ACC, BLCA, BRCA, CESC, CHOL, COAD, DLBC, ESCA, GBM, HNSC, KICH, KIRC, KIRP, LGG, LIHC, LUAD, LUSC, MESO, OV, PAAD, PCPG, PRAD, READ, SARC, SKCM, STAD, TGCT, THCA, THYM, UCEC, UCS, UVM) were downloaded from the TCGA web-site and internally normalized. Normalized breast cancer datasets from CIT, BCR, WANG, BEKHOUCHE were re-used from the previous study [3]. Normalized METABRIC breast cancer expression dataset was downloaded from cBioPortal at this link http://www.cbioportal.org/study?id=brca_metabric. When it was not already the case, the data values were converted into logarithmic scale.

The list of breast cancer transcriptomic datasets used for reproducibility study is available in Additional file 4: Table ST1.

ICA decompositions computation

We applied the same protocol of application of ICA decomposition as in [3]. In the ICA decomposition $X \approx AS$, X is the gene expression (sample vs gene) matrix, A is the (sample vs. component) matrix describing the loadings of the independent components, and S is the (component vs. gene matrix) describing the weights (projections) of the genes in the components. To compute ICA, we used the *fastICA* algorithm [1] accompanied by the *icasso* package [23] to improve the components estimation and to rank the components based on their stability. ICA was applied to each transcriptomic dataset separately.

For each analysed transcriptomic dataset, we computed M independent components (ICs), using *pow3* nonlinearity and *symmetrical* approach to the decomposition, where $M = [2\dots 50, 55, 60, 65, 70, 75, 80, 85, 90, 95, 100]$. In those

cases, when M exceeded the total number of samples, the maximum M was chosen equal to 0.9 multiplied by the number of samples (moderate dimension reduction improves convergence). We found that the MATLAB implementations of *fastICA* performs superior to other implementations (such as those provided in *R* [24]). The computational time required for performing all the 0.1 million ICA decompositions used in this study is estimated in ~1500 single processor hours using MATLAB while other implementations would not make this analysis feasible at all. In our analysis, we used Docker with packaged compiled MATLAB code for *fastICA* together with MATLAB Runtime environment, which can be readily used in other applications and does not require MATLAB installed [25]. An example of computational time needed for the analysis of two transcriptomic datasets of typical size (full transcriptome, from 200 to 1000 samples) is provided in Additional file 6: Figure SF5. As a rough estimate, it takes 3 h to analyze a transcriptomic dataset with 200 samples and 7 h to analyze a dataset with 1000 samples, using an ordinary laptop. In each such analysis, more than 2000 ICA decompositions of different orders have been made.

The algorithm for determining the most stable Transcriptome dimension (MSTD)

- 1) Define two numbers $[M_{min}, M_{max}]$ as the minimal and maximal possible numbers of the computed components.
- 2) Define the number K of ICA runs for estimating the components stability. In all our examples, we used $K = 100$.
- 3) For each M between M_{min} and M_{max} (or, with some step) do
 - 3.1) Compute K times the decomposition of the studied dataset into M independent components using the *fastICA* algorithm. This results in computation of $M \times K$ components.
 - 3.2) Cluster $M \times K$ components into M clusters using agglomerative hierarchical clustering algorithm with the measure of dissimilarity equal to $1 - |r_{ij}|$, where r_{ij} is the Pearson correlation coefficient computed between components.
 - 3.3) For each cluster C_k out of M clusters (C_1, C_2, \dots, C_N) compute the stability index using the following formula

$$I_q(C_k) = \frac{1}{|C_k|^2} \sum_{i,j \in C_k} |r_{ij}| - \frac{1}{|C_k| \sum_{l \neq k} |C_l|} \sum_{i \in C_k} \sum_{j \in C_k} |r_{ij}|$$

where $|C_k|$ denotes the size of the k th cluster.

3.4) Compute the average stability index for M clusters:

$$S(M) = \frac{1}{M} \sum_k I_q(C_k)$$

- 4) Select the MSTD as the point of intersection of the two lines approximating the distribution of stability profiles (Fig. 1a). The lines are computed using a simple k-lines clustering algorithm [26] for $k = 2$, implemented by the authors in MATLAB, with the initial approximations of the lines matching the abscissa and the ordinate axes of the plot. The index used in 3.3 is a widely used index of clustering quality defined as a difference between the average intra-cluster similarity and the average inter-cluster similarity. In [9] this index was introduced to estimate the quality of clustering of independent components after multiple runs with random initial conditions, and tested in application to fMRI data. In the case of clustering independent components, $I_q = 1$ corresponds to the case of perfect clustering of components such that all the components in one cluster are correlated with each other with $|r| = 1$, and that all components in the same cluster are orthogonal to any other component (in the reduced and whitened space).

Comparing metagenes computed for different datasets and in different analyses

Following the methodology developed previously in [3], the metagenes computed in two independent datasets were compared by computing a Pearson correlation coefficient between their corresponding gene weights. Since each dataset can contain a different set of genes, the correlation is computed on the genes which are common for a pair of datasets. Note that this common set of genes can be different for different pairs of datasets. The same correlation-based comparison was done with previously defined and annotated metagenes. We computed the correlation only between those genes having projection value more than 3 standard deviations in the identified component.

When comparing two sets of metagenes $\mathbf{A} = \{A_1, \dots, A_M\}$ and $\mathbf{B} = \{B_1, \dots, B_N\}$, in order to do component matching, we focused on the maximal correlation of a metagene from one set with all components from another set. If $B_i = \arg \max(\text{corr}(A_j, \mathbf{B}))$ then B_i is called *best matched*, for A_j , metagene from the set \mathbf{B} . If $B_i = \arg \max(\text{corr}(A_j, \mathbf{B}))$ and $A_j = \arg \max(\text{corr}(B_i, \mathbf{A}))$, then the correlation between B_i and A_j is called *reciprocal*.

In all correlation-based comparisons, the absolute value of the correlation coefficient was used.

The orientation of independent components was chosen such that the longest tail of the data projection

distribution would be on the positive side. Then, for quantifying an intersection between a metagene and a reference set of genes (e.g., cell cycle genes), simple Jaccard index was computed between the reference gene set and the set of top-contributing genes to the component, with positive weights >5.0.

Determining if a small gene set is driving an independent component

To distinguish whether an independent component is driven by a small gene set, the distribution of gene weights W_i from the component was analyzed. For each tail of the distribution (positive and negative), the tail weight was determined as the total absolute sum of weights of the genes exceeding certain threshold W^{top} . The heaviest tail of the distribution was identified as the tail with the maximum weight. For the heaviest tail and for the set of genes P with absolute weights exceeding W^{top} , sorted in descending order by absolute value, we studied the gap distribution of values $G_i = W_i/W_{i+1}$, $i \in P$. If there was a single value of G_i exceeding a threshold G^{\max} , then the component was classified as being driven by a small set of genes corresponding to the indices $\{i; i \leq \max(k; G_k \leq G^{\max})\}$. The values $W^{\text{top}} = 3.0$, $G^{\max} = 1.5$ collected the maximal gene set size = 3 in all ICA decompositions. These are few genes with atypically high weights separated by a significant gap from the rest of the distribution (note that these genes cannot always be considered outliers since they and the resulting independent components can be reproducible in independent datasets).

Additional files

Additional file 1: Figure SF2. Estimating MSTD dimension for six breast cancer datasets. The notations are the same as in Fig. 1. (PDF 479 kb)

Additional file 2: Figure SF1. Standard estimations of intrinsic dimensionality (by Keiser rule or by broken stick distribution) of cancer datasets. (PDF 288 kb)

Additional file 3: Table ST2. Genes associated with ICA components of the METABRIC dataset, in the case when a component is driven by a small group of genes (frequently, one gene). Gene names marked in bold also drive independent components in several other breast cancer datasets and the corresponding components are reciprocally reproducible in terms of the correlation of the whole ICA-based metagenes. (XLSX 10 kb)

Additional file 4: Table ST1. Breast cancer transcriptomic datasets used for the analysis of component reproducibility in independent datasets. (XLSX 13 kb)

Additional file 5: Figure SF4. The histograms of the total number of reciprocal correlations in the correlation graph such as the one shown in Fig. 3, with and without applying the component stabilization approach. (PDF 164 kb)

Additional file 6: Figure SF5. Computational time for ICA decomposition of different orders from 2 to 100 with step 5, using compiled MATLAB fastICA implementation and stability analysis by re-computing fastICA from 100 various initial conditions. The computation is made using an ordinary laptop with Intel Core i7 processor and 16Gb of memory, in a single thread. The BRCA BEK dataset (from [27]) contains 10,000 genes in 197 samples, and the

BRCA TCGA dataset (from [28]) contains 20,503 genes in 1095 samples. The overall timing for computing all ICA decomposition with their stability analysis is 3.0 h for BRCA BEK dataset, and 6.5 h for BRCA TCGA dataset. These computations can be repeated using BIODICA software [29] (<https://github.com/LabBandSB/BIODICA>), by launching ICA computation in scanning mode. (PDF 361 kb)

Additional file 7: Figure SF3. Graph of reciprocal correlations between components computed with MSTD choice for the reduced dimension and the number of components. The size of the points reflects their stability (larger points corresponds to more stable components). The color and the width of the edges reflect the Pearson correlation coefficient. Propositions of annotations of the pseudo-cliques in the graph are made based on the comparison with previously annotated metagenes [3] and the analysis of the top contributing genes using hypergeometric test and the *toppgene* web tool [30]. (PDF 315 kb)

Abbreviations

IC: Independent Component; ICA: Independent Component Analysis

Acknowledgements

We thank Dr. Anne Biton for sharing the normalized public transcriptomics data for four breast cancer datasets. We also thank Prof. Joseph H. Lee (Columbia University) for critical reading and improving the manuscript text.

Funding

This study is supported by "Analysis of cancer transcriptome data using Independent Component Analysis" project from the budget program "Creation and development of genomic medicine in Kazakhstan" (0115RK01931) from the Ministry of Education and Science of the Republic of Kazakhstan. This work was partly supported by ITMO Cancer within the framework of the Plan Cancer 2014–2019 and convention Biologie des Systèmes N°BIO2015–01 (M5 project) and MOSAIC project.

Availability of data and materials

The results shown in this paper are in part based upon publicly available data generated by the TCGA Research Network: <http://cancergenome.nih.gov/>. The provenance of the public data used in this study is indicated in the Method section and Additional file 4: Table ST1.

Authors' contribution

UK LC EB AZ designed the study and developed the methodology, UK LC AG AM UC AZ performed the computational experiments, UK LC UC AZ wrote the manuscript, all authors read, approved and edited the manuscript.

Ethics approval and consent to participate

Not applicable.

Consent for publication

Not applicable.

Competing interests

Not applicable.

Publisher's Note

Springer Nature remains neutral with regard to jurisdictional claims in published maps and institutional affiliations.

Author details

¹Institut Curie, PSL Research University, INSERM U900, Mines ParisTech, Paris, France. ²Laboratory of bioinformatics and computational systems biology, Center for Life Sciences, National Laboratory Astana, Nazarbayev University, Astana, Kazakhstan.

Received: 16 April 2017 Accepted: 4 September 2017

Published online: 11 September 2017

References

- Hyvärinen A, Oja E. Independent component analysis: algorithms and applications. *Neural Netw.* 2000;13(4-5):411–30.

2. Teschendorff AE, Journée M, Absil P a, Sepulchre R, Caldas C. Elucidating the altered transcriptional programs in breast cancer using independent component analysis. *PLoS Comput Biol.* 2007;3(8):e161.
3. Biton A, Bernard-Pierrot I, Lou Y, Krucker C, Chapeaublanc E, Rubio-Pérez C, et al. Independent component analysis uncovers the landscape of the bladder tumor Transcriptome and reveals insights into luminal and basal subtypes. *Cell Rep.* 2014;9(4):1235–45.
4. Gorban A, Kegl B, Wunch D, Zinovyev A. Principal Manifolds for Data Visualisation and Dimension Reduction. *Lect notes Comput Sci Eng.* 2008;58:340p.
5. Saidi SA, Holland CM, Kreil DP, MacKay DJ, Charnock-Jones DS, Print CG, et al. Independent component analysis of microarray data in the study of endometrial cancer. *Oncogene.* 2004;23(39):6677–83.
6. Zinovyev A, Kairov U, Karpenyuk T, Ramanculov E. Blind source separation methods for deconvolution of complex signals in cancer biology. *Biochem Biophys Res Commun.* 2013;430(3):1182–7.
7. Brunet JP, Tamayo P, Golub TR, Mesirov JP. Metagenes and molecular pattern discovery using matrix factorization. *Proc Natl Acad Sci U S A.* 2004;101(12):4164–9.
8. Bang-Bertelsen CH, Pedersen L, Fløyel T, Hagedorn PH, Gylvin T, Pociot F. Independent component and pathway-based analysis of miRNA-regulated gene expression in a model of type 1 diabetes. *BMC Genomics.* 2011;12:97.
9. Himberg J, Hyvärinen A, Esposito F. Validating the independent components of neuroimaging time-series via clustering and visualization. *NeuroImage.* 2004;22(3):1214–22.
10. Li Y-O, Adali T, Calhoun VD. Estimating the number of independent components for functional magnetic resonance imaging data. *Hum Brain Mapp.* 2007;28(11):1251–66.
11. Hui M, Li R, Chen K, Jin Z, Yao L, Long Z. Improved estimation of the number of independent components for functional magnetic resonance data by a whitening filter. *IEEE J Biomed Heal Informatics.* 2013;17(3):629–41.
12. Majeed W, Avison MJ. Robust data driven model order estimation for independent component analysis of fMRI data with low contrast to noise. *PLoS One.* 2014;9(4):e94943.
13. Cangelosi R, Goriely A. Component retention in principal component analysis with application to cDNA microarray data. *Biol Direct.* 2007;2:
14. Kégl B. Intrinsic dimension estimation using packing numbers. *Symp. A Q. J. Mod Foreign Lit.* 2003;15:681–8.
15. Bro R, Kjeldahl K, Smilde AK, Kiers HA. Cross-validation of component models: a critical look at current methods. *Anal Bioanal Chem.* 2008;390(5):1241–51.
16. Krumsieck J, Suhre K, Illig T, Adamski J, Theis FJ. Bayesian independent component analysis recovers pathway signatures from blood metabolomics data. *J Proteome Res.* 2012;11:4120–31.
17. Cancer Genome Atlas Research Network. The Cancer Genome Atlas Pan-Cancer analysis project. *Nat Genet.* 2013;45(10):1113–20.
18. Edgar R, Domrachev M, Lash AE. Gene Expression Omnibus: NCBI gene expression and hybridization array data repository. *Nucleic Acids Res.* 2002;30(1):207–10.
19. Giotto B, Joshi A, Freeman TC. Meta-analysis reveals conserved cell cycle transcriptional network across multiple human cell types. *BMC Genomics.* 2017;18(1):30.
20. Heng TSP, Painter MW, Consortium IGP. The immunological genome project: networks of gene expression in immune cells. *Nat Immunol.* 2008;9(10):1091–4.
21. Subramanian A, Tamayo P, Mootha VK, Mukherjee S, Ebert BL, Gillette MA, et al. Gene set enrichment analysis: a knowledge-based approach for interpreting genome-wide expression profiles. *Proc Natl Acad Sci U S A.* 2005;102(43):15545–50.
22. Dhivya P, Harris L. Circulating Tumor Markers for Breast Cancer Management. *Mol. Pathol. Breast Cancer.* Springer International Publishing; 2016. p. 207–18.
23. Himberg J, Hyvärinen A. ICASSO: Software for investigating the reliability of ICA estimates by clustering and visualization. *Neural Networks Signal Process. - Proc. IEEE Work.* 2003. p. 259–68.
24. R Core Team. R: A language and environment for statistical computing. R Foundation for Statistical Computing. Vienna, Austria; 2017. <https://www.R-project.org/>.
25. BIODICA docker web-page [Internet]. 2017. Available from: <https://hub.docker.com/r/auranic/biodica/>
26. Agarwal S, Lim J, Zelnik-Manor L, Perona P, Kriegman D, Belongie S. Beyond pairwise clustering. *Proc. IEEE Comput. Soc. Conf. Comput. Vis. Pattern Recognit.* 2005. p. 838–45.
27. Bekhouche I, Finetti P, Adelaïde J, Ferrari A, Tarpin C, Charafe-Jauffret E, et al. High-resolution comparative genomic hybridization of inflammatory breast cancer and identification of candidate genes. *PLoS One.* 2011;6(2):e16950.
28. Koboldt DC, Fulton RS, McLellan MD, Schmidt H, Kalicki-Veizer J, McMichael JF, et al. Comprehensive molecular portraits of human breast tumours. *Nature.* 2012;490(7418):61–70.
29. Kairov U, Zinovyev A, Kalykhbergenov Y, Molkenov A. BIODICA GitHub page [Internet]. 2017. Available from: <https://github.com/LabBandSB/BIODICA/>.
30. Chen J, Bardes EE, Aronow BJ, Jegga AG. ToppGene suite for gene list enrichment analysis and candidate gene prioritization. *Nucleic Acids Res.* 2009;37:W305–11.

Submit your next manuscript to BioMed Central and we will help you at every step:

- We accept pre-submission inquiries
- Our selector tool helps you to find the most relevant journal
- We provide round the clock customer support
- Convenient online submission
- Thorough peer review
- Inclusion in PubMed and all major indexing services
- Maximum visibility for your research

Submit your manuscript at
www.biomedcentral.com/submit



2.4 Cell-type deconvolution models

(families of approaches/strategies)

2.4.1 basis matrix

- define what basis matrix is vs signatures vs marker genes
- explain the differences between basis matrices in published algorithms

2.4.2 regression algorithm

- explain what it is for
- explain how it works
- explain the different approaches

2.4.3 Others

- explain possible normalisation
- explain additional possible features

2.5 Short review of most popular cell-type deconvolution tools

Tools will already be mentioned in the section above. However a comment on other than mentioned aspects are needed.

Explain the success of CIBEROSRT

Explain originality of each tool

2.6 Methodological dimension of the thesis

- expose state of art and compare existing tools
- adjustment of existing methodology
- develop a new user-friendly tool

- discuss limitations of computational approaches in biology

Chapter 3

Study of sensitivity and reproducibility of known methods

3.1 Reproducibility of NMF versus ICA (vs CAM?)

NMF and ICA are both algorithms often applied to solve blind source deconvolution problem. NMF gained a popularity as a tool of transcriptomic analysis mainly thanks to the publications [publicaiton_list]. However, the non-negativity constraint, an attractive concept in the case of non-negative transcriptome counts, may be a reason why the reuslts of NMF decomposition are not the best candidate for our deconvolution task. We observed that NMF-based metagenes are less reproducible between different transcriptomic datasets than ICA-based metagenes.

3.1.1 Comparing metagenes obtained with NMF vs ICA.

We compared the reproducibility of NMF and ICA through decomposition of four breast cancer datasets (BRCATCGA, METABRIC, BEK, WAN)[ref]. Those datasets were selected because of their size (number of samples > 50) and because they were available in not centred format necessary for NMF.

For NMF the procedure was following:

- data was transformed into log2
- zero rows were removed
- the algorithm assesing cophentic index was applied to chose optimal number of components

- datasets were decomposed with matlab NMF implementation from Brunet et al. [?] into (i) number of components suggested by cophenetic coefficient (ii) MSTD dimension (iii) 50 components (approaching overdecomposition)
- the obtained metagenes were decorrelated from the mean using a linear regression model

For ICA, the procedure was following:

- data were transformed into log2
- transformed data were mean-centered by gene
- our implementation of MSTD (most stable transcriptomic dimension) from [?] was used to evaluate most stable dimension
- datasets were demposed into (i) MSTD dimension and (ii) 50 components (approaching overdecomposition) with matlab implementantion of fastICA with icasso stabilisation

We did not decompose ICA into low number of components as we consider it as strong underdecomposition and we suspect signals would not be the most reproducible. We limited the over decomposition higher than 50 with NMF as for our biggest dataset (METABRIC) NMF decomposition into 50 took 30245 minutes (3 weeks).

Then separately for NMF and ICA, we correlated all obtained metagens with each other and with known Biton et al. metagenes (obtain from previous ICA decompostion applied pan-cancer). We represented the results in a form of a correlation graph where nodes are metagenes from different datasets and decompostion levels and edge width corresponds pearson correaltion coefficients (Fig 3.1).

We hoped to observe a subset of components from different datasets (no matter the decomposition level) correlate with each strongly and much less with other components in order to confirm that the signal is reproducible (can be found in several dataset) and specific. We used the Biton et al. componemts here to help with eventual identification of signals (labelling). What we observe from ICA-decomposition that indeed, without applying any threshold some emerging clusters can be remarked and after application of >0.4 threshold on the correlation coeffcient pseudo-cliques emerge. While metagenes from NMF-decpmpostion are more tightly connected globally and when the threshold is applied, remaing metagenes do not form clear clusters but group by data set. In NMF decomposition if it hard to define different signals as the datasets seem to be all related to each other. We can see from (Fig 3.1D) that the IMMUNE signal is correlated >0.4 with a high number of NMF components that are also linked to some other components. In ICA (Fig 3.1C) components related to the IMMUNE metagens form a pseudo-clique that is related with one link to INTERFERON metagene.

This simple analysis illustrates that NMF applied to cancer transcriptomes decomposes them to metagenes that are not highly reproducible between datasets. In practice, it

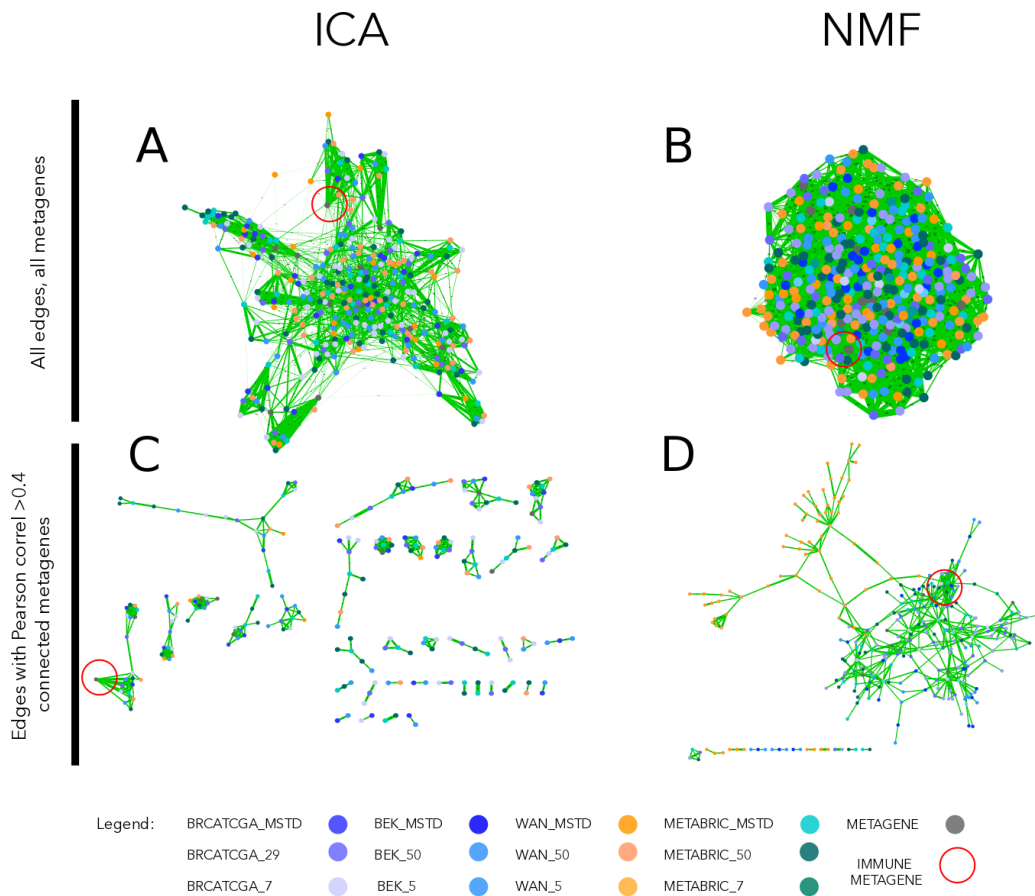


Figure 3.1: Correlation graph of ICA and NMF multiple decompositions. In the upper part of the figure (A,B) we observe the correlation graph of all metagenes (ICA or NMF-based) disposed using edge-weighted bio layout. In the lower part of the figure (C,D) we applied >0.4 thereshold in order to filter the edges. In the case of ICA (C), remaining nodes form pseudo-cliques, immune-related pseudo-clique is highlighted. In the case of NMF (D), components cluster by dataset. Edges' width coressponds to Pearson correlation coefficient. Node colors correspond to dataset from which a metagene was obtained (see legend).

will not always be possible to work with big cohorts and the same processing methods. Using ICA for decomposition gives more credit that it will be possible to use the obtained metagenes as reference in which new data of similar type could be projected.

to do:

- quantify: with clustering coefficient?
- Explain why ICA is more reproducible

3.2 Impact of modification of signatures list on result for signature-based deconvolution methods

Carry on a “sensitivity study”:

- remove some % of genes from basis matrix or marker gene list
- evaluate how it changes results

Chapter 4

Deconvolution of transcriptomes and methylomes

We describe our methods in this chapter. The pre-eliminary pipeline and simple results are described in the manuscript submitted to Springer-Verlag's Lecture Notes in Computer Science ([LNCS](#)) entitled **Application of Independent Component Analysis to Tumor Transcriptomes Reveals Specific And Reproducible Immune-related Signals** that is placed at the end of this chapter. In the final thesis final pipeline will be split into following structure

4.1 From blind deconvolution to cell-type quantification: general overview

Few lines describing our idea

Figure?

4.1.1 The ICA-based deconvolution of Transcriptomes

- remind shortly ICA
- describe stabilisation procedure *icasso*
- explain IC-metagene concept

If completed add related section about two other ways of getting metagenes

- attractor metagenes

- k-lines

4.1.2 Interpretation of Independent components

4.1.2.1 Correlation based identification of confounding factors

4.1.2.2 Identification of immune cell types with enrichment test / other

4.1.3 Transforming metagenes into signature matrix

4.1.4 Regression-based estimation of cell-type proportions : solving system of equations

4.2 DeconICA R package for ICA-based deconvolution

This part of the chapter will be adapted from package vignettes

It will contain

- technical package description
- user guide
- examples

4.2.1 Demo

The package needs to installed and then imported.

```
#import package
library(deconica)
```

Then we can perform our pipeline on sample data available in the package

```
#import sample data
data(BRCA)
#decompose data
fastica.res <- run_fastica (
  BRCA,
  optimal = TRUE,
  row.center = TRUE,
```

```

with.names = TRUE,
gene.names = NULL,
alg.typ = "parallel",
method = "C",
n.comp = 100,
isLog = TRUE,
R = TRUE
)
#correlate obtained metagenes with Biton et al.
#metagenes (by default)
correlate.res <-
  correlate_metagenes(fastica.res$S, fastica.res$names)
#assign reciprocal components
assign.res <- assign_metagenes(correlate.res$r)
#identify components that are >0.1 correlated with
#immune and are not assigned to any other component
identify.immune <-
  identify_immune_ic(correlate.res$r[, "M8_IMMUNE"], assign.res[, 2])
#test enrichment with fisher test in
#Immgen signatures (by default)
enrichment.res <- gene.enrichment.test(
  fastica.res$S,
  fastica.res$names,
  names(identify.immune),
  gmt = ImmgenHUGO,
  alternative = "greater",
  p.adjust.method = "BH",
  p.value.threshold = 0.05
)

```

The present state of the package is described in Fig 4.1.

Next step will be:

- adding the metagenes selection and transformation into basis matrix for deconvolution
- identifying confounding factors
- estimating purity with an existing tool
- running an equations solver (based on least squares or other type of regression) including basis matrix, confounding factors, purity
- including regularisation factors
- adding graphics

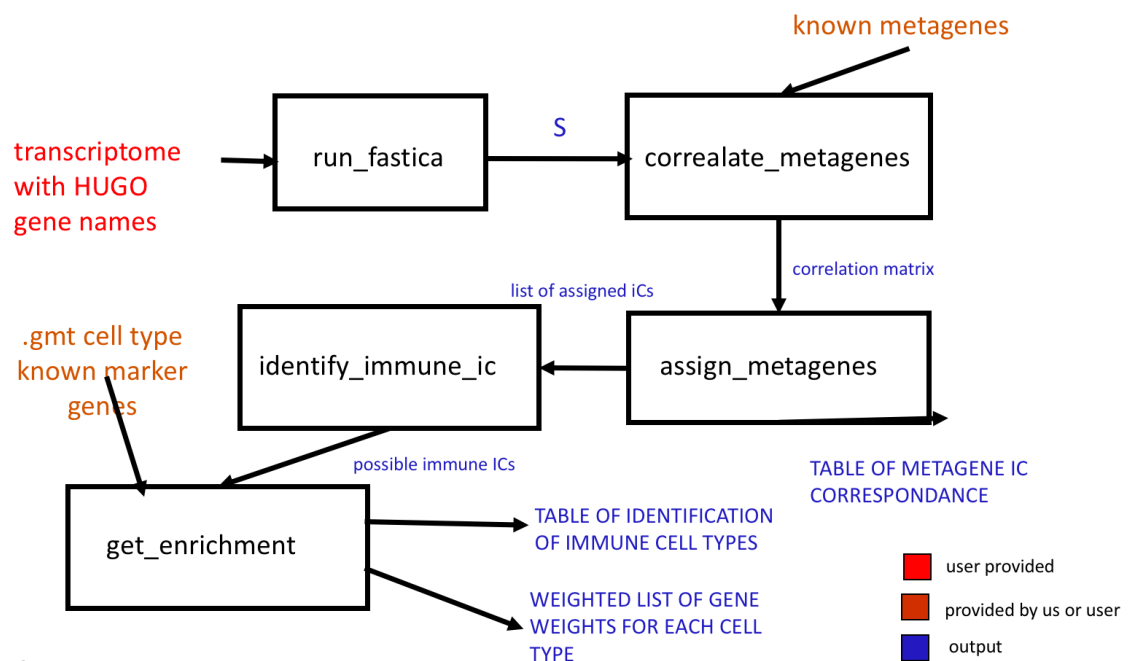


Figure 4.1: State of the deconICA package in January 2018. The flow chart illustrates existing functions in the R package DeconICA. Squares represent functions, red are user-provided inputs, brown are inputs we provide but that can be replaced easily by user and in blu we marked outputs.

- adding user interface
- writing a demo (best interactive)

Application of Independent Component Analysis to Tumor Transcriptomes Reveals Specific And Reproducible Immune-related Signals

Urszula Czerwinska¹[0000-0002-5244-0708], Laura Cantini¹[0000-0001-6360-4440], Ulykbek Kairov²[0000-0001-8511-8064], Emmanuel Barillot¹[0000-0003-2724-2002], and Andrei Zinov'yev¹[000-0002-9517-7284]

¹ Institut Curie, INSERM U900, PSL Research University, Mines ParisTech
26 rue d'Ulm, Paris, France
urszula.czerwinska@curie.fr,
web page: <https://sysbio.curie.fr/>

² Laboratory of bioinformatics and computational systems biology
Center for Life Sciences, National Laboratory Astana, Nazarbayev University
Astana, Kazakhstan

Abstract. Independent Component Analysis (ICA) can be used to model gene expression data as an action of a set of statistically independent hidden factors. The ICA analysis with a downstream component analysis was successfully applied to transcriptomic data previously in order to decompose bulk transcriptomic data into interpretable hidden factors. Some of these factors reflect the presence of an immune infiltrate in the tumor environment. However, no foremost studies focused on reproducibility of the ICA-based immune-related signal in the tumor transcriptome. In this work, we use ICA to detect immune signals in six independent transcriptomic datasets. We observe several strongly reproducible immune-related signals when ICA is applied in sufficiently high-dimensional space (close to one hundred). Interestingly, we can interpret these signals as cell-type specific signals reflecting a presence of T-cells, B-cells and myeloid cells, which are of high interest in the field of oncoimmunology. Further quantification of these signals in tumoral transcriptomes has a therapeutic potential.

Keywords: blind deconvolution, unsupervised learning, genomic data analysis, cancer, immunology

1 Introduction

In many fields of science (biology, technology, sociology) observations on a studied system represent complex mixtures of signals of various origins. It is known that tumors are engulfed in a complex microenvironment (TME) that critically impacts progression and response to therapy. In the light of recent findings [1], many cancer biologists believe that the state of tumor microenvironment (in particular, la composition of immune system-related cells) defines the long-term effect of the cancer treatment.

Given the way transcriptomic data is collected, in the resulting dataset, for each observation or sample, the measured transcripts' expression level is affected by a mixture of signals coming from various sources. Thus, we adopt a hypothesis that a transcriptome is a mixture of different signals (that can be biological or technical), including cell-type specific signals.

Recent works [2; 3; 4] showed that expression data from complex tissues (such as tumor microenvironment) can be used to estimate the cell-specific expression profiles of the main cellular components present in a tumor sample. This methodology is based on a linear model of a mixture of signals and their interaction and termed deconvolution. The mentioned methods take advantage of the prior knowledge (and, at the same time, heavily depend) on the signatures of transcriptome components; therefore, they fall into supervised learning category.

A methodology using an unsupervised data decomposition was applied, so far, in the context of tumor clonality deconvolution by Roman et al. [5]. Some attempts were done to apply Non-negative Matrix factorization to transcriptomic data as well. However, they were either applied in very simplified context of *in vitro* cell mixtures [6] or without a specific focus on the immune signals [7].

In our work, we propose to apply an unsupervised method that will decompose mixture into independent sources based uniquely on data structure and without any prior knowledge. For this purpose, we are applying Independent Component Analysis (ICA) [8] that solves blind source separation problem. ICA defines a new coordinate system in the multi-dimensional space such that the distributions of the data point projections on the new axes become as mutually independent as possible. To achieve this, the standard approach is maximizing the non-gaussianity of the data point projection distributions.

As a result of ICA, deconvolution data matrix X can be approximated: $X \approx AS$, where X is a matrix of data of size $m \times n$, and A is a $m \times k$ matrix, $k \ll m$. The rows of the A matrix can be named components (m -dimensional vectors), and the columns of the S matrix projections of data vectors onto the components (a k -dimensional vector for each of n data points) [9].

ICA has been widely applied for the analysis of transcriptomic data for blind separation of biological, environmental and technical factors affecting gene expression [9; 10; 11; 12; 13].

The interpretation of the results of any matrix factorization-based method applied to transcriptomics data is done by the analysis of the resulting pairs of metagenes and metasamples, associated to each component and represented by sets of weights for all genes and all samples, respectively [7; 9]. Standard statistical tests applied to these vectors can then relate a component to a reference gene set (e.g., cell cycle genes), or to clinical annotations accompanying the transcriptomic study (e.g., tumor grade). The application of ICA to multiple expression datasets has been shown to uncover insightful knowledge about cancer biology [11; 14]. In [11] a large multi-cancer ICA-based metaanalysis of transcriptomic data defined a set of metagenes associated with factors that are universal for many cancer types. Metagenes associated with cell cycle, inflammation, mi-

tochondria function, GC-content, gender, basal-like cancer types reflected the intrinsic cancer cell properties.

In our previous work, we introduced a ranking of independent components based on their stability in multiple independent components computation runs and define a distinguished number of components (Most Stable Transcriptome Dimension, MSTD) corresponding to the point of the qualitative change of the stability profile [15].

However, an interesting observation can be made employing a number of components going far beyond the MSTD ($M \gg \text{MSTD}$), that we call here *overdecomposition*. Applying this approach, one can discover more specific components that remain reproducible between independent datasets. In this work, we present results of overdecomposition with focus on the fine decomposition of the immune signal into cell-type specific signals.

In this analysis, we used a set of six independent breast cancer transcriptomic datasets (BRCAATCGA [16], METABRIC [17], BRCACIT [18], BRCABEK [19], BRCAWAN [20] and BRCABCR [21]) to evaluate a detectability and a reproducibility of the immune cell-type related signal.

Through this publication we employ terms: *stability*, *conservation* and *reproducibility* that we define as follows. Stability of an independent component, in terms of varying the initial starts of the ICA algorithm, is a measure of internal compactness of a cluster of matched independent components produced in multiple ICA runs for the same dataset and with the same parameter set but with random initialization. Conservation of an independent component in terms of choosing various orders of the ICA decomposition is a correlation between matched components computed in two ICA decompositions of different orders (reduced data dimensions) for the same dataset. Reproducibility of an independent component is an (average) correlation between the components that can be matched after applying the ICA method using the same parameter set but for different datasets. We claim that if a component is reproduced between the datasets of the same cancer type, then it can be considered a reliable signal less affected by technical dataset peculiarities. If the component is reproduced in datasets from many cancer types, then it can be assumed to represent a universal cancerogenesis mechanism, such as cell cycle or infiltration by immune cells.

2 Methods

2.1 ICA overdecomposition procedure

The pipeline of our deconvolution procedure can be described as follows. Started with six public transcriptomic data of breast cancer, we apply the fastICA algorithm [8] accompanied by the icasso package [22] to improve the components estimation and to rank the components based on their stability. ICA was applied to each transcriptomic dataset separately. For each analyzed transcriptomic dataset, we computed M independent components (ICs), using *pow3* nonlinearity and symmetrical approach to the decomposition. The number of dimensions

was set to 100 ($M=100$) as it is significantly greater than MSTD for these datasets (that is in the order of $M=30$). As a result, S matrix is *metagene matrix* with dimensions $number_{genes} \times number_{ICs}$. Then each component was oriented in the direction of its heavy tail, being defined as the tail with the maximum weight, so that it has always the positive sign.

2.2 Interpretation of components

In order to confirm that we can recover expected known signals performing the overdecomposition procedure, we correlate previously described in Biton et al. [11] metagenes with the S matrix. Correlations are performed on common genes for each component and metagene. The result was graphically represented using R package *ggplot2* [23]. An interpretation is assigned to a component only if its assignment is reciprocal. In our analysis reciprocity is defined as follows. Given a correlations between the set of metagenes $A = \{A_1, \dots, A_m\}$ and S matrix $S = \{IC_1, \dots, IC_N\}$, if $S_i = argmax(corr(A_j, S))$ and $A_j = argmax(corr(S_i, A))$. In this way, the breast cancer metagenes were matched against the following set of previously defined metagenes: MYOFIBROBLASTS, BLCAPATHWAYS, STRESS, GC CONTENT, SMOOTH MUSCLE, MITOCHONDRIAL TRANSLATION, INTERFERON, BASALLIKE, CELLCYCLE, UROTHERIALDIFF. Details about these metagenes construction and interpretation can be found in Biton et al. The correlation plot was visualized in Cytoscape 2.8 [24].

2.3 Selecting immune-related components

In order to preselect immune-related signals, we focused on all Independent Components (ICs) with Pearson correlation > 0.1 between IMMUNE metagene and ICs (columns of the S matrix). The interpretation was given using Fisher exact test on 100 top-ranked genes of each of the preselected components and Immgen [25] signatures containing in total 6467 genes of six immune cell types: $\alpha\beta$ T-cells, $\gamma\delta$ T-cells, B-cells, CD+, Myeloid cells, NK cells and four non-immune cell types: Fetal-Liver, Stem cells, Stromal cells and Pasmocytoid, 241241 signatures in total, each of 480 genes in average.

2.4 Comparing independent components from different datasets

Following the methodology developed previously in [11], the metagenes computed in two independent datasets were compared by computing a Pearson correlation coefficient between their corresponding gene weights. Since each dataset can contain a different set of genes, the correlation is computed on the genes which are common for a pair of datasets. Note that this common set of genes can be different for different pairs of datasets. The same correlation-based comparison was done with previously defined and annotated metagenes. In all correlation-based comparisons, the absolute value of the correlation coefficient was used.

3 Results

3.1 Most of known metagenes can be found in overdecomposed datasets

In all six overdecomposed datasets of breast cancer, we could find major metagenes of Biton et al. As an example, we present results for METABRIC dataset [17] (Fig. 1) where we can observe correlations between metagenes and all 100 ICs. For some metagenes (MYOFIBROBLASTS, INTERFERON, MITOCHONDRIAL TRANSLATION, CELL CYCLE), there is only one reciprocal and strongly (> 0.3) correlated component, which can be understood as a good signal conservation. Some other as STRESS, BASALLIKE and SMOOTH MUSCLE can have two similarly correlated components. This is probably due to component split in higher-order decomposition. Of note, the Biton et al. metagenes were defined in significantly lower dimensional space ($M = 25$) and as a result of high-dimensional decomposition, these signals are decomposed to more specific sources that can still be interpreted in biological terms. For few, no strong correlations were found (UROTHELIALDIFFERENTIATION and BLCPATHWAYS). These metagenes are more specific to Bladder cancer and we can consider them as negative control here. Also, GC Content and IMMUNE metagenes have several corresponding components. The IMMUNE metagene is considered here as a special case as we can find several components correlated to it and, in addition, their interpretation can be interesting for biological applications. We investigate more about the immune-related components in the subsection *Three pseudo-cliques related to three immune cell types*.

3.2 Reproducibility of the signals in breast cancer datasets

It would be reasonable to expect that the main biological signals are characteristic for a given cancer type. Thus, they should be the same when one studies molecular profiles of different independent cohorts of patients. For this reason, we expect that for multiple datasets related to the same cancer type, the ICA decompositions should be somewhat similar; hence, reciprocally matching each other.

We correlated the ICA overdecompositions of all six datasets with each other and with the forementioned metagenes [11]. One can notice from the correlation graph (Fig. 2A), that some pseudo-cliques characterized with strong correlation coefficient (thick edges) and reciprocal (green) edges are present in the mass of low correlation coefficients edges. If the edges with correlation coefficient < 0.4 are filtered out, we can better visualize a collection of pseudo-cliques (Fig. 2B). Some of those pseudo-cliques are connected to a metagene and can be given an interpretation directly, some others would need a further investigation of the gene signature in order to attribute a meaning to them. We can see that in some pseudo-cliques not all datasets are represented. It may suggest that some signals, still reproducible, are not representative for all datasets. In order to explain,

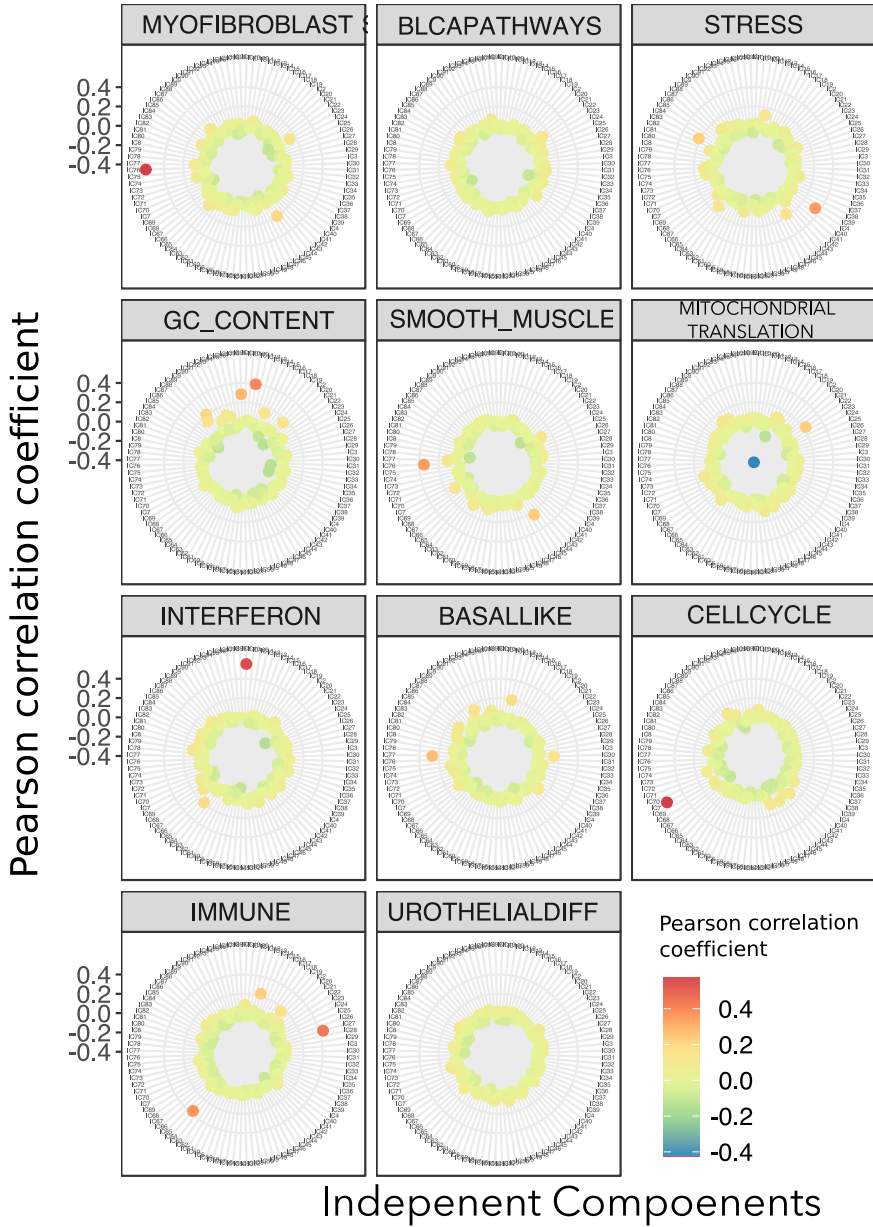


Fig. 1. Correlations between 11 metagenes [11] and 100 independent components of METABRIC dataset [17]. Each panel shows correlation coefficients between a given metagene and 100 ICs of METABRIC, the components are ordered in the same manner for all panels from 1 to 100 in a circle. For a high correlation coefficient, the point is red, for low, it is blue (see legend)

why a signal is missing, one should first interpret the signal, then try to understand the similarities or differences of samples based on provided metadata. From our previous analysis [11], the components that do not find reciprocity (absent from the pseudo-cliques) are either dataset specific or they correspond to unknown batch effects that cannot be guessed without an additional knowledge. It is remarkable that despite overdecomposition, the metagenes conceived in lower-dimensional space are highly conserved and reproducible, which suggests the overdecomposition does not diminish strong signals conceived in "optimal" dimensional space (i.e. MSTD). Of note, these datasets were produced using various technologies of transcriptomic profiling.

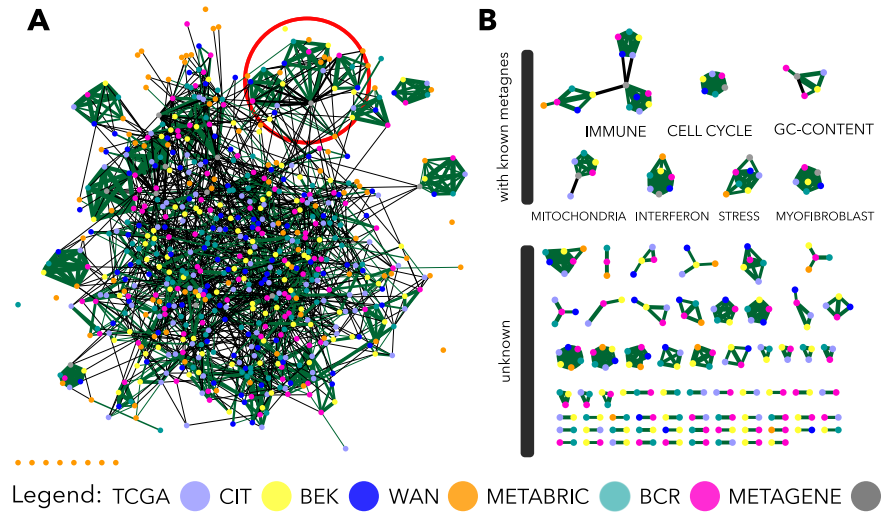


Fig. 2. Correlation plot of six tumor datasets and the metagenes [11] A- Correlation graph between decompositions into 100 ICs of the six transcriptomic datasets and the 11 known metagenes. The IMMUNE metagene and related ICs in encircled; B - collection of pseudo-cliques extracted from A through filtering edges of the < 0.4 . They were split in two groups, the ones that are directly interpretable via their correlation with a metagene and cliques that are not related to any known metagene; The thickness of edges is proportional to the Pearson correlation coefficients, green color indicates reciprocity of edges, colors of nodes indicate dataset (see legend)

3.3 Three pseudo-cliques related to three immune cell types

To better understand the reproducibility of the immune-related signal, we extracted only components correlated with $\text{IMMUNE} > 0.1$. Hence, we obtain three strongly connected cliques (Fig. 3) and some disconnected components. We interpreted each of the ICs with an enrichment test. The results of Fisher

exact test indicate mainly three cell types T-cell, B-cell and Myeloid cells with p-value < 0.05 or lower as indicated in the Fig. 3. While T-cell and Myeloid cell are indicated with very high certainty, the B-cell signal seems to be more complex. It can be said from higher p-values and presence of other cell types as T-cells and NK cells among significant results. This is not unexpected. Some studies report on functional and phenotypic similarities between NK and B cells [26]. Also, T cell and B cell as they are both lymphocytes, they share common features. It is worth highlighting that definition of cell type signature is a part of ongoing debate [27] and here we use them as an indicator of possible signal definitions. Also, some ICs belonging to one pseudo-clique are correlated (with lower coefficients) with ICs from another pseudo-clique (i.e. BRCABCR IC2). It may suggest an inclination of the signal towards the other phenotype. As far as the mentioned *free* components are concerned, through interpretation BRCACIT IC42 can be associated with B cells, METABRIC IC28 with Myeloid cells, BRCAWAN IC68 and BRCABEK IC27 with T-cells. Thus, the correlations of the disconnected, even though they are low, they are most probably not spurious. Some other components not included in the pseudo-cliques like BRCAWAN IC28 and BRCABCR IC19 seem to contain stroma elements. It would be worth understanding more deeply the nature of each signal and interpret in terms of biological functions or sub-phenotypes.

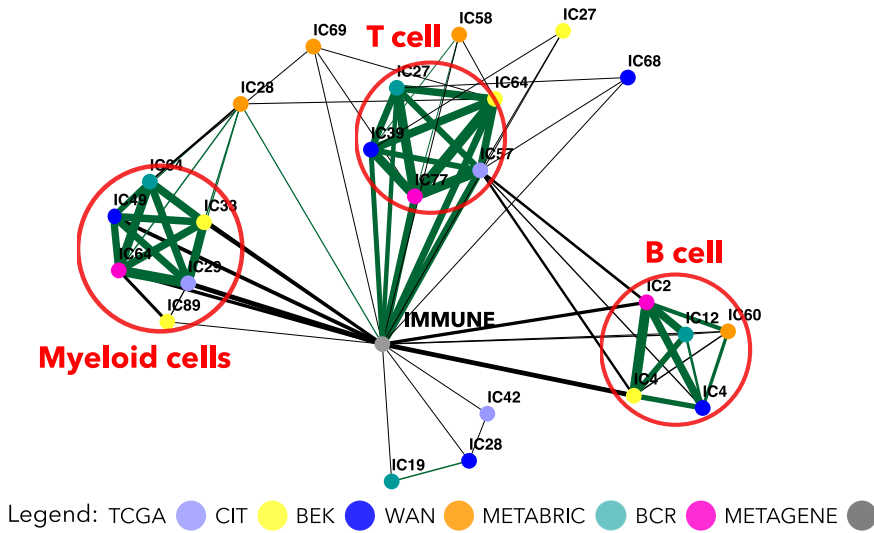


Fig. 3. Correlation graph of ICs correlated with IMMUNE metagene > 0.1 . Three pseudo-cliques are encircled and labeled according to the results of Fisher exact test. The thickness of edges is proportional to the Pearson correlation coefficients, green color indicates reciprocal edges, colors of nodes indicate dataset (see legend)

4 Discussion

The overdecomposition of six breast cancer datasets, where different normalization methods and different transcriptome profiling platforms were used, showed that even in high dimensions signal decomposition, the ICA-based analysis can be reproducible between datasets. Moreover, the most stable signals are conserved and not affected by the number of dimensions. Interestingly, for some signals we can observe a split into more specific signals that can still be interpreted in biological terms. In the case of the immune-related signals, it allows robust reproduction of three main signals that form pseudo-cliques on the correlations graph in the Fig. 3. This result let us believe that ICA allows to deconvolute cancer transcriptomes in an unsupervised manner and detect the most represented immune cell-types. We found highly interesting that technically non-stable signal is found reproducible and interpretable in the six breast cancer datasets.

More time should be dedicated to analyze those signatures in details, to report their similarities and differences. As well as, this analysis could be applied in a pan-cancer manner to observe the reproducibility of the signal among different tumor types. Such an analysis would possibly identify components and/or genes linked with patients' survival or response to treatment and eventually, use them to compose a predictive score for tumor immune therapy outcome.

5 Conclusions

We applied overcomposition into one hundred components of six transcriptomic datasets using Independent Components Analysis, a blind source deconvolution algorithm. We used a known collection of ranked ICA-derived genetic signatures (that we call Biton et al. metagenes) to conclude that most of the signals are conserved in the higher dimensions. We noticed that some of the components split into more specific signals. Our correlation analysis of the ICA overdecompositions of the transcriptomes stated that majority of components are reproducible between datasets. Our more focused investigation of immune-related ICs demonstrated that three cell types can be named: T-cell, B-cell and myeloid cells as a reproducible source signal in the breast cancer datasets. Further interpretation of those cell-type related genomic signatures can find application in immuno-oncology therapeutics as predictive biomarkers for immunotherapies.

References

- [1] Swartz, M.A., Iida, N., Roberts, E.W., Sangaletti, S., Wong, M.H., Yull, F.E., Coussens, L.M., DeClerck, Y.A.: Tumor microenvironment complexity: Emerging roles in cancer therapy. In: *Cancer Research*. (2012)
- [2] Becht, E., Giraldo, N.A., Lacroix, L., Buttard, B., Elarouci, N., Petitprez, F., Selvès, J., Laurent-Puig, P., Sautès-Fridman, C., Fridman, W.H., de Reyniès, A.: Estimating the population abundance of tissue-infiltrating immune and stromal cell populations using gene expression. *Genome Biology* **17**(1) (2016)
- [3] Newman, A.M., Liu, C.L., Green, M.R., Gentles, A.J., Feng, W., Xu, Y., Hoang, C.D., Diehn, M., Alizadeh, A.A.: Robust enumeration of cell subsets from tissue expression profiles. *Nature Methods* **12**(5) (2015) 453–457
- [4] Racle, J., de Jonge, K., Baumgaertner, P., Speiser, D.E., Gfeller, D.: Simultaneous enumeration of cancer and immune cell types from bulk tumor gene expression data. *eLife* **6**(0) (2017) e26476
- [5] Roman, T., Xie, L., Schwartz, R.: Automated deconvolution of structured mixtures from heterogeneous tumor genomic data. *PLoS Computational Biology* **13**(10) (2017)
- [6] Gaujoux, R., Seoighe, C.: Semi-supervised Nonnegative Matrix Factorization for gene expression deconvolution: A case study. *Infection, Genetics and Evolution* **12**(5) (2012) 913–921
- [7] Brunet, J.P., Tamayo, P., Golub, T.R., Mesirov, J.P.: Metagenes and molecular pattern discovery using matrix factorization. *Proceedings of the National Academy of Sciences* **101**(12) (2004) 4164–4169
- [8] Hyvärinen, A., Oja, E.: Independent Component Analysis: Algorithms and Applications. *Neural Networks* **13**(45) (2000) 411–430
- [9] Zinovyev, A., Kairov, U., Karpenyuk, T., Ramanculov, E.: Blind source separation methods for deconvolution of complex signals in cancer biology (2013)
- [10] Teschendorff, A.E., Journée, M., Absil, P.A., Sepulchre, R., Caldas, C.: Elucidating the altered transcriptional programs in breast cancer using independent component analysis. *PLoS Computational Biology* **3**(8) (2007) 1539–1554
- [11] Biton, A., Bernard-Pierrot, I., Lou, Y., Krucker, C., Chapeaublanc, E., Rubio-Pérez, C., López-Bigas, N., Kamoun, A., Neuzillet, Y., Gestraud, P., Grieco, L., Rebouissou, S., DeReyniès, A., Benhamou, S., Lebret, T., Southgate, J., Barillot, E., Allory, Y., Zinovyev, A., Radvanyi, F.: Independent Component Analysis Uncovers the Landscape of the Bladder Tumor Transcriptome and Reveals Insights into Luminal and Basal Subtypes. *Cell Reports* **9**(4) (2014) 1235–1245
- [12] Gorban, a., Kegl, B., Wunch, D., Zinovyev, A.: Principal Manifolds for Data Visualisation and Dimension Reduction. *Lecture notes in Computational Science and Engineering* (2008) 340

- [13] Saidi, S.A., Holland, C.M., Kreil, D.P., MacKay, D.J.C., Charnock-Jones, D.S., Print, C.G., Smith, S.K.: Independent component analysis of microarray data in the study of endometrial cancer. *Oncogene* **23**(39) (2004) 6677–6683
- [14] Bang-Berthelsen, C.H., Pedersen, L., Fløyel, T., Hagedorn, P.H., Gylvin, T., Pociot, F.: Independent component and pathway-based analysis of miRNA-regulated gene expression in a model of type 1 diabetes. *BMC Genomics* **12** (2011)
- [15] Kairov, U., Cantini, L., Greco, A., Molkenov, A., Czerwinska, U., Barillot, E., Zinovyev, A.: Determining the optimal number of independent components for reproducible transcriptomic data analysis. *BMC Genomics* **18**(1) (2017)
- [16] Cancer, T., Atlas, G.: Comprehensive molecular portraits of human breast tumours. *Nature* **490**(7418) (2012) 61–70
- [17] Curtis, C., Shah, S.P., Chin, S.F., Turashvili, G., Rueda, O.M., Dunning, M.J., Speed, D., Lynch, A.G., Samarajiwa, S., Yuan, Y., Gräf, S., Ha, G., Haffari, G., Bashashati, A., Russell, R., McKinney, S., Aparicio, S., Brenton, J.D., Ellis, I., Huntsman, D., Pinder, S., Murphy, L., Bardwell, H., Ding, Z., Jones, L., Liu, B., Papatheodorou, I., Sammut, S.J., Wishart, G., Chia, S., Gelmon, K., Speers, C., Watson, P., Blamey, R., Green, A., MacMillan, D., Rakha, E., Gillett, C., Grigoriadis, A., De Rinaldis, E., Tutt, A., Parisien, M., Troup, S., Chan, D., Fielding, C., Maia, A.T., McGuire, S., Osborne, M., Sayalero, S.M., Spiteri, I., Hadfield, J., Bell, L., Chow, K., Gale, N., Kovalik, M., Ng, Y., Prentice, L., Tavaré, S., Markowetz, F., Langerød, A., Provenzano, E., Purushotham, A., Børresen-Dale, A.L., Caldas, C.: The genomic and transcriptomic architecture of 2,000 breast tumours reveals novel subgroups. *Nature* **486**(7403) (2012) 346–352
- [18] Guedj, M., Marisa, L., De Reynies, A., Orsetti, B., Schiappa, R., Bibeau, F., MacGrogan, G., Lerebours, F., Finetti, P., Longy, M., Bertheau, P., Bertrand, F., Bonnet, F., Martin, A.L., Feugeas, J.P., Bièche, I., Lehmann-Che, J., Lidereau, R., Birnbaum, D., Bertucci, F., De Thé, H., Theillet, C.: A refined molecular taxonomy of breast cancer. *Oncogene* **31**(9) (2012) 1196–1206
- [19] Bekhouche, I., Finetti, P., Adelaïde, J., Ferrari, A., Tarpin, C., Charafe-Jauffret, E., Charpin, C., Houvenaeghel, G., Jacquemier, J., Bidaut, G., Birnbaum, D., Viens, P., Chaffanet, M., Bertucci, F.: High-resolution comparative genomic hybridization of Inflammatory breast cancer and identification of candidate genes. *PLoS ONE* **6**(2) (2011)
- [20] Wang, Y., Klijn, J.G., Zhang, Y., Sieuwerts, A.M., Look, M.P., Yang, F., Talantov, D., Timmermans, M., Meijer-Van Gelder, M.E., Yu, J., Jatkoe, T., Berns, E.M., Atkins, D., Foekens, J.A.: Gene-expression profiles to predict distant metastasis of lymph-node-negative primary breast cancer. *Lancet* **365**(9460) (2005) 671–679
- [21] Reyal, F., Rouzier, R., Depont-Hazelzet, B., Bollet, M.A., Pierga, J.Y., Alran, S., Salmon, R.J., Fourchet, V., Vincent-Salomon, A., Sastre-Garau, X., Antoine, M., Uzan, S., Sigal-Zafrani, B., de Rycke, Y.: The molecular

- subtype classification is a determinant of sentinel node positivity in early breast carcinoma. *PLoS ONE* **6**(5) (2011)
- [22] Himberg, J., Hyvärinen, A.: ICASSO: Software for investigating the reliability of ICA estimates by clustering and visualization. In: Neural Networks for Signal Processing - Proceedings of the IEEE Workshop. Volume 2003-Janua. (2003) 259–268
 - [23] Wickham, H.: ggplot2 Elegant Graphics for Data Analysis. Volume 35. (2009)
 - [24] Shannon, P., Markiel, A., Ozier, O., Baliga, N.S., Wang, J.T., Ramage, D., Amin, N., Schwikowski, B., Ideker, T.: Cytoscape: A software Environment for integrated models of biomolecular interaction networks. *Genome Research* **13**(11) (2003) 2498–2504
 - [25] Shay, T., Kang, J.: Immunological Genome Project and systems immunology (2013)
 - [26] Kerdiles, Y.M., Almeida, F.F., Thompson, T., Chopin, M., Vienne, M., Bruhns, P., Huntington, N.D., Raulet, D.H., Nutt, S.L., Belz, G.T., Vivier, E.: Natural-Killer-like B Cells Display the Phenotypic and Functional Characteristics of Conventional B Cells. *Immunity* **47**(2) (aug 2017) 199–200
 - [27] Schelker, M., Feau, S., Du, J., Ranu, N., Klipp, E., MacBeath, G., Schoeberl, B., Raue, A.: Estimation of immune cell content in tumour tissue using single-cell RNA-seq data. *Nature Communications* **8**(1) (dec 2017) 2032

Chapter 5

Comparative analysis of cancer immune infiltration

This chapter will include biological interpretation of Pan-cancer analysis with DeconICA

- application to Breast cancer
 - compare metagenes of the same cell type in different datasets
 - compare metagenes of the same cell type in the same dataset (happens sometimes)
 - compare A matrix (sample weights) with clinical metadata
 - compare patients with opposite extreme phenotypes (the gene expression) with DEG ou others
 - run enrichment with more specific list of genes ex. Th1/2/17 cells in T cels etc.
- application pan cancer
 - derivation of meta-metagenes for immune cell types
 - above points are true for pan cancer
- follow up of Biton paper ?
 - *Idea of Vassili from the lab meeting*, personally I am not sure if there is no conflict of interest with other members of the team

Chapter 6

Heterogeneity of immune cell types

We include here an extract of a *ready to submit* article of Kondratova et al. (**co-first authored by Urszula Czerwinska**) - the abstract and figures which are result of work on single cell heterogeneity.

Explication how deconvolution methodology can be used for analysis of heterogeneity of immune cells

- describe the context briefly
- describe more in details my part - data analysis of single cell data

To be defined:

- add CAFS (that will maybe appear in *JBM*)
- add unpublished analysis made for the *Nature Immunology* *Michea et al.* paper (to be defined)
- The single T-cell study (if done)

Signalling network map of innate immune response in cancer reveals signatures of cell heterogeneity and polarization in tumor microenvironment

SUMMARY (150 words) (now 190)

To describe the contribution of innate immune components to anti- and pro-tumor effect of tumor microenvironment (TME), we collected information on molecular mechanisms governing innate immune response in cancer and represented it in a form of network maps. The signalling maps of macrophages, dendritic cells, myeloid-derived suppressor cells, natural killers were constructed. These cell type-specific maps, integrated together and updated by intra-cellular interactions, gave rise to a seamless comprehensive meta-map of innate immune response in cancer. The meta-map depicts signalling of anti- and pro-tumor activities of innate immunity system as a whole. The cell type-specific maps and the meta-map were used for interpretation of single cell RNA-Seq data from natural killers and macrophages in metastatic melanoma. The analysis demonstrated existence of sub-populations within each cell type that possess different anti- and pro-tumor polarization status. In addition, we used the meta-map for interpretation of pan-cancer patient survival data to retrieve patient survival signature. The cell type-specific signalling maps together with the meta-map of innate immune response in cancer form an open source platform available online that can be applied by wide community for assessment of TME status in cancer and beyond.

Key words

Tumor immunology, tumor microenvironment, innate immunity signalling, cancer systems biology, comprehensive signalling network map, semantic zooming, single cell data analysis, bioinformatics, molecular pathways and networks, intercellular communication, cell reprogramming, polarization, heterogeneity

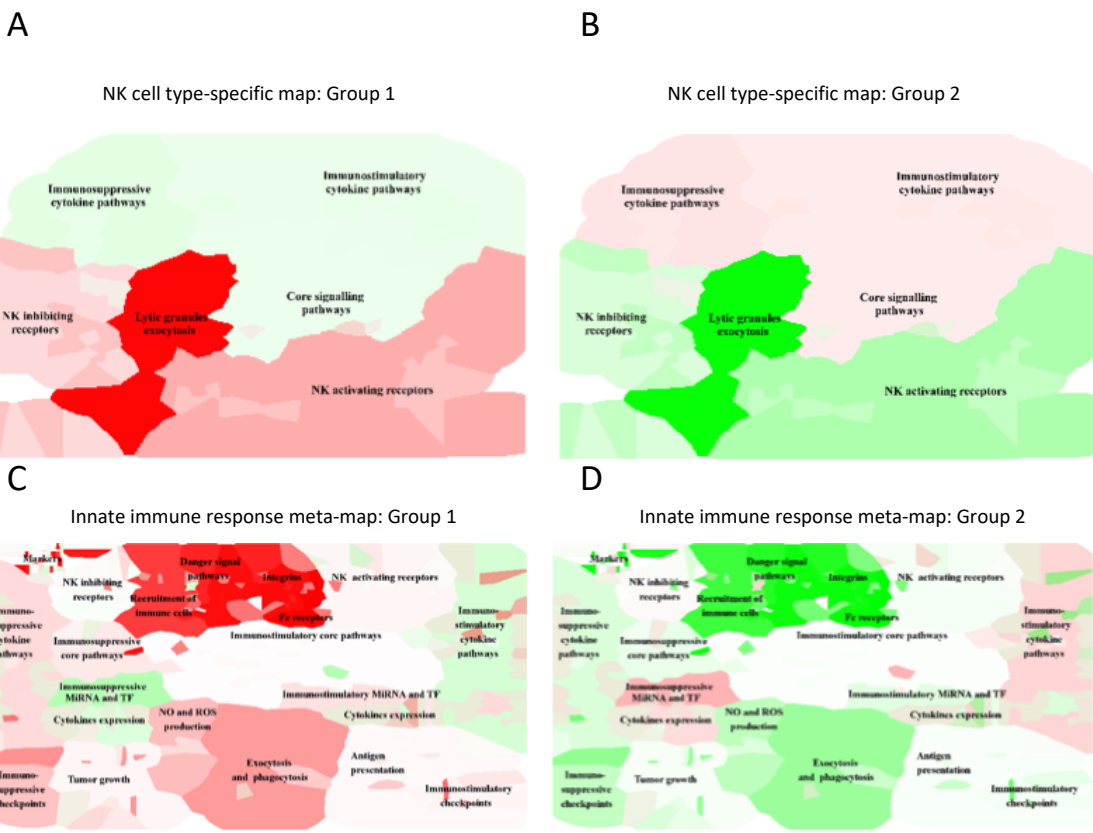


Figure 4. Visualization of modules activity scores using expression data from melanoma natural killers (NK) cells in the context of maps. Staining of the NK cell type-specific map with modules activity scores calculated from single cell RNAseq expression data for (A) NK Groups 1 and (B) NK Groups 2 cells. Staining of the innate immune response meta-map with modules activity scores for (C) NK Groups 1 and (D) NK Groups 2 cells. Red—upregulated, green—downregulated module activity.

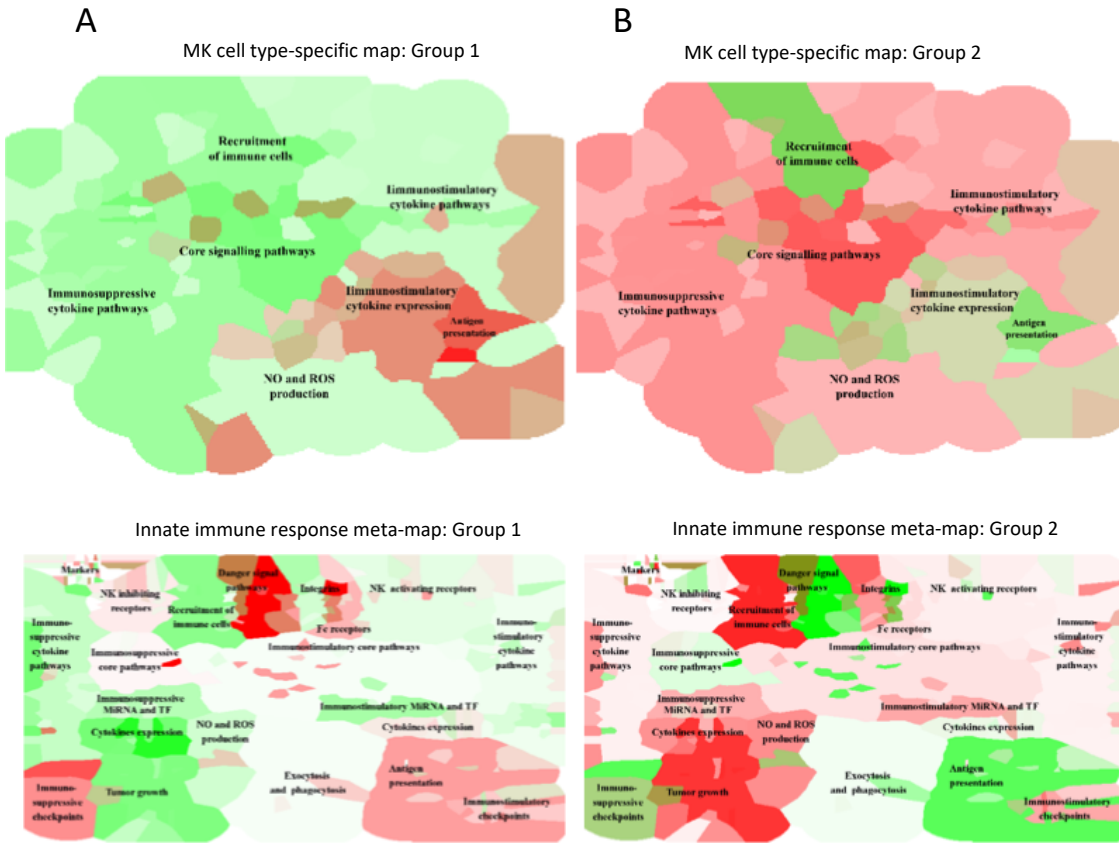
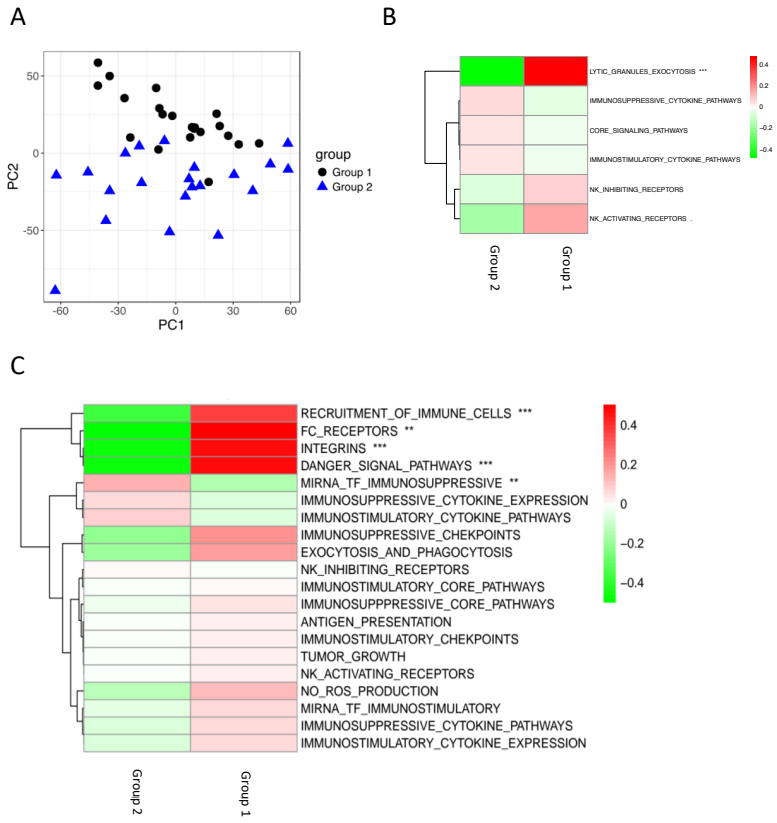
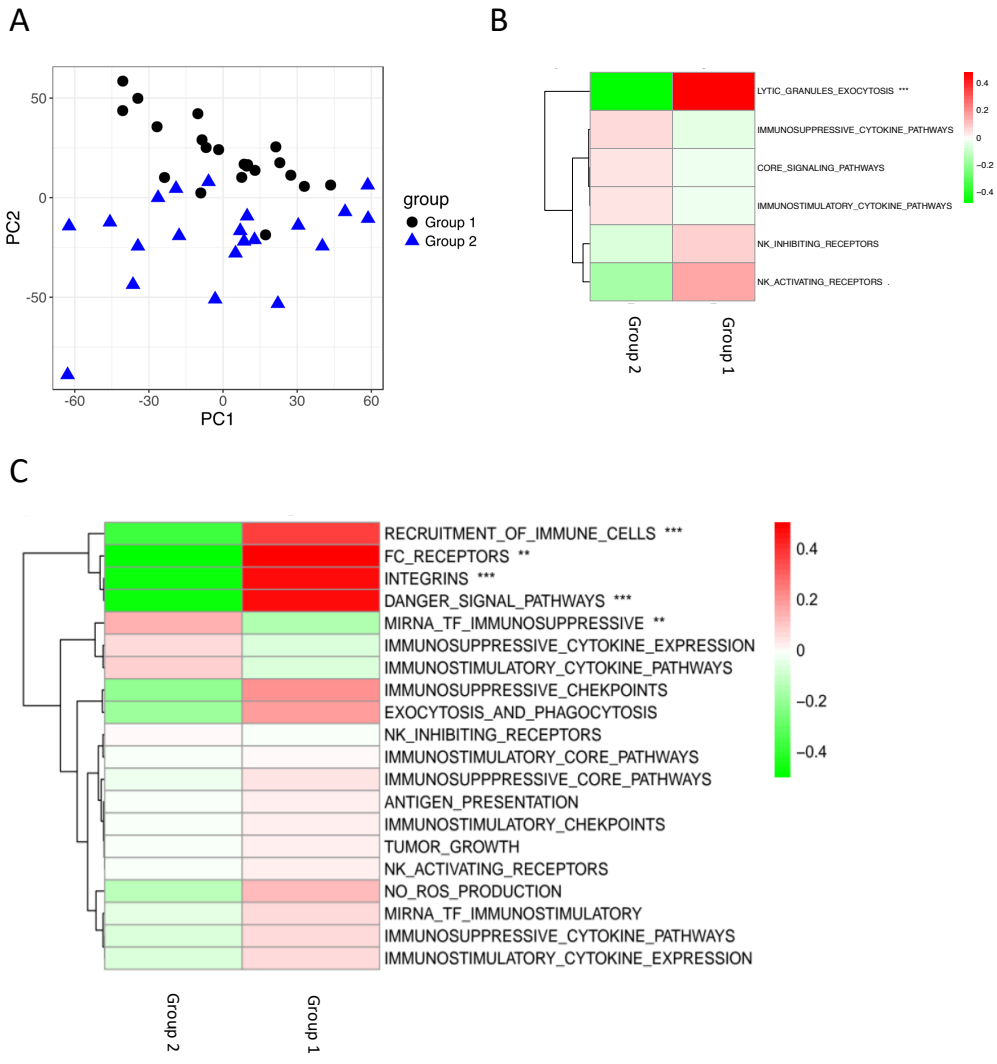


Figure 5. Visualization of modules activity scores using expression data from melanoma macrophages (Mph) cells in the context of maps. Staining of the Mph cell type-specific map with modules activity scores calculated from single cell RNAseq expression data for (A) Mph Groups 1 and (B) Mph Groups 2 cells. Staining of the innate immune response meta-map with modules activity scores for (C) Mph Groups 1 and (D) Mph Groups 2 cells. Red-upregulated, green-downregulated module activity.



Supplemental Figure 6. Sup-populations study and calculation of modules activity scores using expression data from melanoma natural killers (NK) cells. (A) NK single cells in PC1 and PC2 coordinates space. Two groups are colored distinctly in blue and black. Heatmap of mean values of 50% most variant genes divided by group of modules in (B) cell type-specific map and (C) meta-map. The p-value of the t-test between gene expression is reported following the code: *** < 0.001, ** < 0.01 , * < 0.05 , . < 0.1



Supplemental Figure 7. Sup-populations study and calculation of modules activity scores using expression data from melanoma macrophages (Mph) cells. (A) Mph single cells in PC1 and PC2 coordinates space. Two groups, the first and the fourth quartile of distribution along the IC1 axis, are colored distinctly in blue and black Heatmap of mean values of 50% most variant genes in groups in modules of (B) cell type-specific map and of(C) meta-map. The p-value of the t-test between gene expression is reported following the code: *** < 0.001, ** < 0.01 , * < 0.05 , . < 0.1

Chapter 7

Conclusions and perspectives

Here we will have some interesting and well-written conclusion that will validate the quality of this thesis.

Annexes

Note: *This annexe will not be a part of final manuscript*

PhD timeline for defence before the end of October 2018

In order to defend before 31 October, I need to follow the guidelines of the University.

- ~29 June - officially submitted the jury proposal and a draft of the thesis to the university
- ~end of July - send manuscript to reviewers
- 24 September - 31 October - defend

Thesis writing

This Report is written in [bookdown](#). I have chosen this form as it can easily compile to *LaTeX*, PDF, MS Word, ebook and html. Optimally, the final manuscript will be also published online in a form of an open source [gitBook](#) and an ebook including interactive figures and maybe even data demos. Another good reason for using [bookdown](#) is its simple syntax of markdown and natural integration of code snippets with .Rmd. It reduces formatting time and give multiple outputs.

The template of for this thesis manuscript was adapted from *LaTeX* template provided by University Paris Descartes.

Citations are stocked in Mendeley Desktop and exported to .bib files automatically.

[MendeleyBibFix](#) is used to cope with automatic export errors.

The format *thesis by publication* will be considered for parts of the thesis.

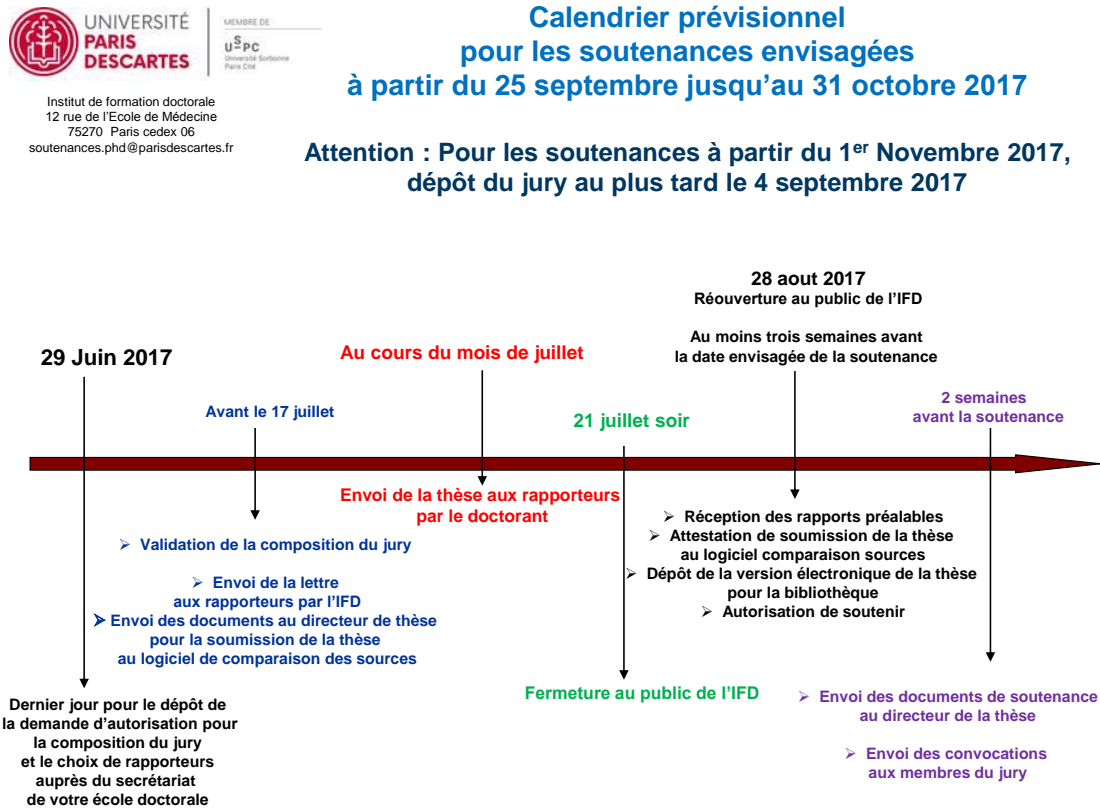


Figure 7.1: Timeline provided by University Paris Descartes for 2017

Activity Report 2017

This documents list main achievements of 2017 including conference, posters and publications list.

RAPPORT D'ACTIVITE 2017**ACTIVITY REPORT 2017**

LAST NAME : CZERWIŃSKA

FIRST NAME : URSZULA

TEAM : Computational Systems Biology for Cancer

0 – MISSION DESCRIPTION 2017:

PhD candidate. My doctoral project engages collaboration between Systems Biology (Emmanuel Barillot) and Immunology teams (Vassili Soumelis) at Institut Curie. In this project, we will develop and apply the *advanced methodology of signal deconvolution* to decipher sources of signals shaping *transcriptomes* (global quantitative profiling of mRNA molecules) of *tumor samples*, with a particular focus on *immune-related signals* in the context of the tumour environment.

1 – ACHIEVEMENTS 2017:**Projects:****1.1 PhD project: DECONVOLUTION OF CELL AND ENVIRONMENT SPECIFIC SIGNALS AND THEIR INTERACTIONS FROM COMPLEX MIXTURES IN BIOLOGICAL SAMPLES**

Supervisors: A. Zinovyev, V. Soumelis

Immuno-oncology remains a focal point of cancer research. Recently, there have been numerous publications related to the main topic of my PhD project: the immune infiltration of tumours. Our specific goal is to analyse transcriptome of tumour samples and infer composition of immune infiltration: deconvolute the mixed signals of different cell type in tumour microenvironment (TME).

In 2017, at first, I worked on simulated data that could be used as a “ground truth” data for our project. The issue turned out to be quite a complex one and is still under development. Secondly, I performed bibliographic study to formalise state of art of gene expression deconvolution in mathematical terms. The summary of this work will be a part of a chapter of my PhD thesis. Then mainly, we worked on standardized definition of pipeline of data treatment that will be published in a form of R package.

In April 2017, I successfully passed through thesis advisory committee. Perspectives and development of the project were assessed as highly satisfactory. The report and the assessment can be provided on the request.

In July 2017 I presented my work in a form of a poster at ISMB 2017 in Prague and subsequently at Data Science Summer School at l’Ecole Polytechnique in September 2017. The poster can be seen online: <https://drive.google.com/file/d/0BwbuCoLN00xpekloa31vdUxKOUE/view>.

I completed numerous hours of various training (compulsory and facultative). The FdV ED474 doctoral school officially validated the second year.

Paris Descartes attributed me ‘Mission d’enseignement’ of 64 hours at Faculté de Pharmacie de Paris Descartes in the department of Mathematics, Statistics and Informatics.

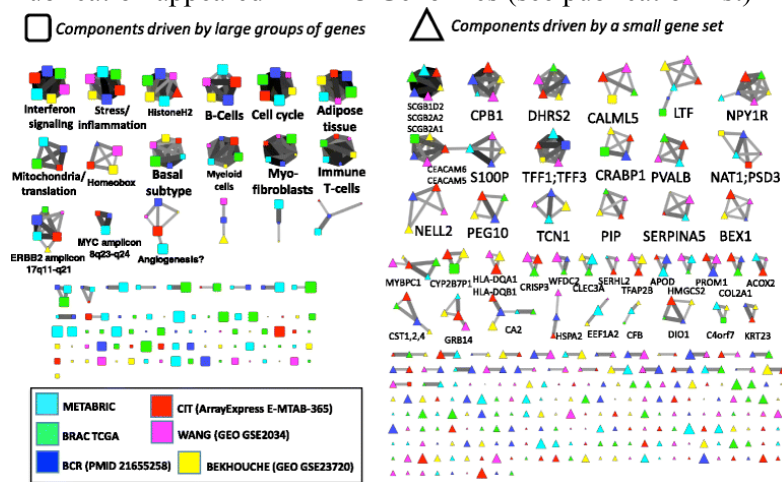
1.2 Determining the optimal number of independent components for reproducible transcriptomic data analysis

Collaborators : Ulykbek Kairov, Laura Cantini, Alessandro Greco, Askhat Molkenov, Emmanuel Barillot and Andrei Zinovyev

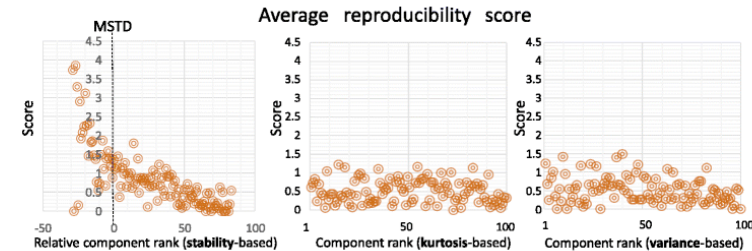
In this project the main goal was to define an optimal number of components for ICA that would be the most reproducible between different datasets.

My contribution was restricted to time benchmarking of ICA algorithm on R and MATLAB platforms, correction of the manuscript, checking reproducibility of obtained results through repeating established pipeline.

Publication appeared in BMC Genomics (see publication list)



a



b

Fig 3. Analysis of component reproducibility in independent datasets.
(from Kairov U & Cantini L et al. BMC Genomics. 2017)

1.3 Single cell data analysis for Immune Map

Collaborators : Maria Kondratova , Inna Kuperstein, Andrei Zinovyev

I explored Tirosh et al. publication of single-cell composition of metastatic melanoma, using their population of macrophages and natural killer cells. Using ICA and literature based gene-sets, we have discovered functional groups within the cell population, highlighting possible functional polarisation of immune cells.

In 2017 we refined results and added to the manuscript additional elements. Manuscript of this work is in preparation coordinated by Inna Kuperstein.

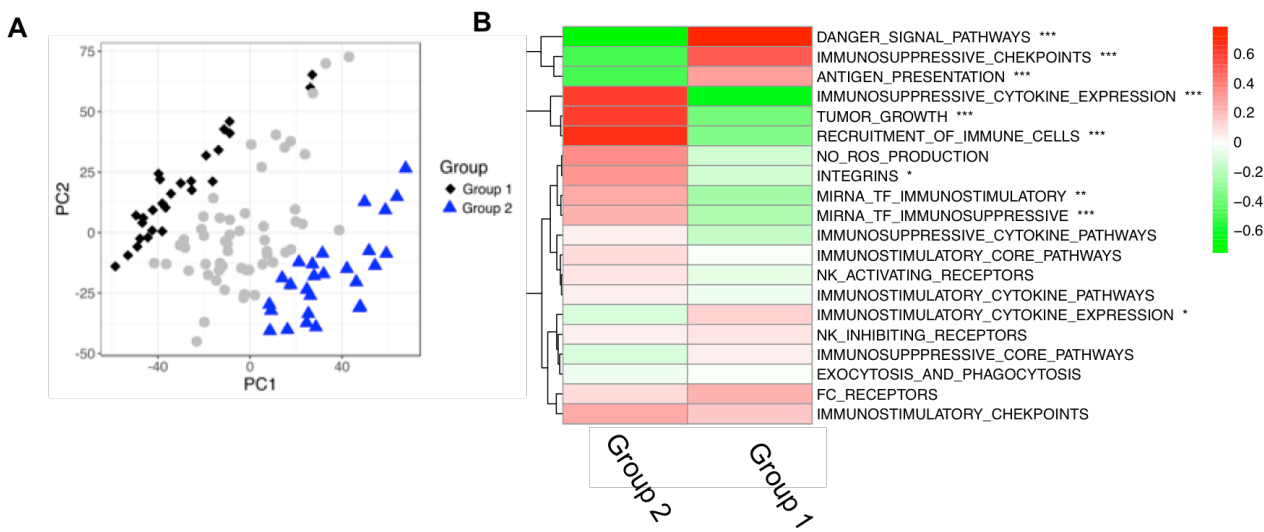


Fig. Enrichment of subgroups of macrophages in innate immune map (MK) A: Single cell data of macrophages (Tirosh et al.) was analysed with ICA and PCA algorithms. Extremes of two groups kept for further analysis. B: the mean value of expression of 50% of genes present in each module of the map was used to compute an average score for each group and each map module. T.test p.value were used to assess the significativity of the score difference between two groups.

1.4 DC cells heterogeneity

Collaborators : Vassili Soumelis, Paula Michta, Floriane Noel, Andrei Zinovyev

In 2016, I did supplementary analysis using ICA and ROMA module activity. I identified set of pathways that allow separation of DC subsets in an unsupervised manner. The manuscript of this work was initially accepted to Nature Immunology and then rejected because of reviewers' doubt concerning the experimental part of the work. I contributed to revision of the paper (before the rejection) and I will follow participate in the new submission.

1.5 Wikipedia protein-protein network

Collaborators : Andrei Zinovyev, Laura Cantini, Luca Albergante, José Lages, Dima Shepelyansky

Team of physicistes in Toulouse established an efficient way to compute reduced Google Matrix. In collaboration with them we obtained reduced Google matrix for Wikipedia pages of protein entries.

The project is in its initial phase. So far we focused on comparison of computed Wikipedia network with different properties and a protein-protein interaction database (SIGNOR)

Quality and reproducible research:

- Evernote posts of daily activity – I document for myself and my supervisor my everyday progress;
- writing readable code with comments/ .Rmd files – I put a lot of effort documenting my scripts and putting in an online repository, for some projects (like 1.5) we work on code that is stored in git system (BitBucket);
- writing R package – I am writing an R package that will allow anyone reproduce my analysis and apply to his/her needs

2 – PERSPECTIVES 2018:

1.1 In 2018 I will write the thesis and defend it. I will finish writing the package and related publication.

1.3 I will contribute in submission and revision of the publication

1.4 I will contribute in submission and revision of the publication

1.5 We will infer interesting characteristics of the “Wikipedia protein network”. We will write a publication on the topic.

3 – ELEMENTS STATISTIQUES / STATISTICS:

3.1 – TRAINING AND COURSES DELIVERED 2017:

Titre / Title : Mission d'enseignement : UFR Pharmacie, Statistique Informatique

Date : 1/09/2017-30/06/2018 (64h)

Lieu / Location : Faculté de Pharmacie de Paris de l'Université Paris Descartes, 4 av de l'observatoire, 75006 Paris.

Organizers : Chantal Guienneuc, Chantal.guienneuc@parisdescartes.fr

Audience : Pharmacy Students

3.2 – TRAINING RECEIVED 2017:

Titre / Title : HackinScience Python course

Date : 16-20 January 2017

Lieu / Location : CRI Montparnasse

Organizers : Hackinscience (Antoine Angot, Julien Palard)

Titre / Title : "Construire et activer son réseau dans le cadre de sa recherche d'emploi"

Date : 13 January 2017

Lieu / Location : Paris Diderot

Organizers : CFDiP (teacher: Barbara Filler)

Titre / Title : "Comment décrocher votre futur emploi "

Date : 12 January 2017

Lieu / Location : Paris Diderot

Organizers : CFDiP (Adoc Talent Management)

Titre / Title : " Big dive "

Date : 19 June – 21 July 2017

Lieu / Location : Turin, Italy

Organizers : TOP-IX

3.3 – PUBLICATIONS (Format Pubmed) 2017:

Type : article, abstract, book chapter

Status : published / in press / revised / submitted / in preparation

3.3.1 – ARTICLES 2017:

Type : article

Status : published

[The inconvenience of data of convenience: computational research beyond post-mortem analyses.](#)

Azencott, C. A., Aittokallio, T., Roy, S., Norman, T., Friend, S., Stolovitzky, G., ... & DREAM Idea Challenge Consortium.

[Nat Methods.](#) 2017 Sep 29;14(10):937-938. doi: 10.1038/nmeth.4457.
(among collaborators)

[Determining the optimal number of independent components for reproducible transcriptomic data analysis.](#)

Kairov U, Cantini L, Greco A, Molkenov A, **Czerwinska** U, Barillot E, Zinovyev A.
BMC Genomics. 2017 Sep 11;18(1):712. doi: 10.1186/s12864-017-4112-9.

[Reconstruction and signal propagation analysis of the Syk signaling network in breast cancer cells.](#)

Naldi A, Larive RM, **Czerwinska** U, Urbach S, Montcourier P, Roy C, Solassol J, Freiss G, Coopman PJ, Radulescu O.
PLoS Comput Biol. 2017 Mar 17;13(3):e1005432. doi: 10.1371/journal.pcbi.1005432. eCollection 2017 Mar.

Type : article

Status : submitted

A blood biomarker detecting severe disease in young dengue patients at hospital arrival.

Nikolayeva, I., Bost, P., Casademont I., Duong V., Koeth F., Prot M., **Czerwinska** U., & ... Schwikowski B. (2017)

3.3.2 – BOOK CHAPTERS 2017: not applicable

3.3.3 – TICK BOX I HAVE UPDATED THE U900 WIKI WITH MY PUBLICATIONS:

yes

3.4 – PARTICIPATION TO CONFERENCES 2017:

3.4.1 – TICK BOX I HAVE UPDATED THE U900 WIKI WITH MY CONFERENCES:

yes

Young Researchers in Life Science conference

15-17/05/17, Paris, France

Czerwinska U., Barillot E., Vassili S., Zinovyev A. DECONVOLUTION OF CELL AND ENVIRONMENT SPECIFIC SIGNALS AND THEIR INTERACTIONS FROM COMPLEX MIXTURES IN BIOLOGICAL SAMPLES

Talk

FdV PhD school retreat

8-11 June 2017, Porquerolles, France

Czerwinska U., Kairov U., cantini L., Greco A., Barillot E., Vassili S., Zinovyev A. Computational deconvolution of mixed signals in tumor microenvironment using Independent Components Analysis

Poster

ISMB/ECCB conference

22-25/07/17, Prague Czech Republic

Czerwinska U., Kairov U., cantini L., Greco A., Barillot E., Vassili S., Zinovyev A. Computational deconvolution of mixed signals in tumor microenvironment using Independent Components Analysis

Poster

DS3: Data Science Summer School

28/08/17 – 01/09/2017 Ecole Polytechnique, Massy Palaisau, France

Czerwinska U., Kairov U., cantini L., Greco A., Barillot E., Vassili S., Zinovyev A. Computational deconvolution of mixed signals in tumor microenvironment using Independent Components Analysis

Poster

3.5 – INVITATION TO SEMINARS 2017:

not applicable

3.5.1 – TICK BOX I HAVE UPDATED THE U900 WIKI WITH MY SEMINARS: *not applicable*

3.6 – ORGANISATION OF EVENTS 2017:

3.6.1 – ORGANISATION OF CONFERENCES 2017

not applicable

3.6.2 – ORGANISATION OF SEMINARS 2017 :

3.7 – PUBLIC OUTREACH 2017:

Personal blog: <http://urszulaczerwinska.github.io/thoughts/> & urszulaczerwinska.github.io/works

3.8 – BOARD MEMBERSHIP:

conseil de laboratoire : PhD representative

3.9 – PRIZES AND NOMINATIONS 2017:

none

4.0 – GRANTS AND COLLABORATIONS 2017:

4.0.1 – NATIONAL, INTERNATIONAL INDUSTRIAL COLLABORATIONS 2017 :

Collaboration with Immunology team (Vassili Soumelis) at Institut Curie through doctoral project.

4.0.2 – GRANTS OBTAINED 2017 :

FdV 474 ED, travel grant of 1000 eur

Aviesan PhD grant for 3 year of PhD (till November 2018)

Bibliography

- [1] Mihaela Angelova, Pornpimol Charoentong, Hubert Hackl, Maria L Fischer, Rene Snajder, Anne M Krogsdam, Maximilian J Waldner, Gabriela Bindea, Bernhard Mlecnik, Jerome Galon, and Zlatko Trajanoski. Characterization of the immunophenotypes and antigenomes of colorectal cancers reveals distinct tumor escape mechanisms and novel targets for immunotherapy. *Genome Biology*, 16(1):64, dec 2015. ISSN 1465-6906. doi: 10.1186/s13059-015-0620-6. URL <http://genomebiology.com/2015/16/1/64>.
- [2] Fran Balkwill and Alberto Mantovani. Inflammation and cancer: Back to Virchow?, 2001. ISSN 01406736.
- [3] Anna Berghoff, Jakob Kather, and Dirk Jäger. Genetics and immunology: Tumor-specific genetic alterations as a target for immune modulating therapies. In Laurence Zitvogel and Guido Kroemer, editors, *Oncoimmunology: a practical guide for cancer immunotherapy*, chapter 13, pages 231–246. 01 2018. ISBN 978-3-319-62430-3.
- [4] Bradley E Bernstein, Alexander Meissner, and Eric S Lander. The mammalian epigenome. *Cell*, 128(4):669–81, feb 2007. ISSN 0092-8674. doi: 10.1016/j.cell.2007.01.033. URL <http://www.ncbi.nlm.nih.gov/pubmed/17320505>.
- [5] Gabriela Bindea, Bernhard Mlecnik, Marie Tosolini, Amos Kirilovsky, Maximilian Waldner, Anna C. Obenauf, Helen Angell, Tessa Fredriksen, Lucie Lafontaine, Anne Berger, Patrick Bruneval, Wolf Herman Fridman, Christoph Becker, Franck Pagès, Michael R. Speicher, Zlatko Trajanoski, and Jérôme Galon. Spatiotemporal Dynamics of Intratumoral Immune Cells Reveal the Immune Landscape in Human Cancer. *Immunity*, 39(4):782–795, oct 2013. ISSN 10747613. doi: 10.1016/j.immuni.2013.10.003. URL <http://www.ncbi.nlm.nih.gov/pubmed/24138885> <http://linkinghub.elsevier.com/retrieve/pii/S1074761313004378>.
- [6] Christian U Blank, John B Haanen, Antoni Ribas, and Ton N Schumacher. CANCER IMMUNOLOGY. The "cancer immunogram". *Science (New York, N.Y.)*, 352(6286):658–60, may 2016. ISSN 1095-9203. doi: 10.1126/science.aaf2834. URL <http://www.ncbi.nlm.nih.gov/pubmed/27151852>.

- [7] F M Burnet. The concept of immunological surveillance. *Progress in experimental tumor research*, 13:1–27, 1970. ISSN 0079-6263. URL <http://www.ncbi.nlm.nih.gov/pubmed/4921480>.
- [8] Federica Cavallo, Carla De Giovanni, Patrizia Nanni, Guido Forni, and Pier-Luigi Lollini. No Title. 60(3), mar 2011. doi: 10.1007/s00262-010-0968-0. URL <http://link.springer.com/10.1007/s00262-010-0968-0>.
- [9] Pornpimol Charoentong, Francesca Finotello, Mihaela Angelova, Clemens Mayer, Mirjana Efremova, Dietmar Rieder, Hubert Hackl, and Zlatko Trajanoski. Pan-cancer Immunogenomic Analyses Reveal Genotype-Immunophenotype Relationships and Predictors of Response to Checkpoint Blockade. *Cell reports*, 18(1):248–262, jan 2017. ISSN 2211-1247. doi: 10.1016/j.celrep.2016.12.019. URL <http://www.ncbi.nlm.nih.gov/pubmed/28052254>.
- [10] Daniel S. Chen and Ira Mellman. Elements of cancer immunity and the cancer-immune set point, 2017. ISSN 14764687.
- [11] Pei Ling Chen, Whijae Roh, Alexandre Reuben, Zachary A. Cooper, Christine N. Spencer, Peter A. Prieto, John P. Miller, Roland L. Bassett, Vancheswaran Gopalakrishnan, Khalida Wani, Mariana Petaccia De Macedo, Jacob L. Austin-Breneman, Hong Jiang, Qing Chang, Sangeetha M. Reddy, Wei Shen Chen, Michael T. Tetzlaff, Russell J. Broaddus, Michael A. Davies, Jeffrey E. Gershenwald, Lauren Haydu, Alexander J. Lazar, Sapna P. Patel, Patrick Hwu, Wen Jen Hwu, Adi Diab, Isabella C. Glitza, Scott E. Woodman, Luis M. Vence, Ignacio I. Wistuba, Rodabe N. Amaria, Lawrence N. Kwong, Victor Prieto, R. Eric Davis, Wencai Ma, Willem W. Overwijk, Arlene H. Sharpe, Jianhua Hu, P. Andrew Futreal, Jorge Blando, Padmanee Sharma, James P. Allison, Lynda Chin, and Jennifer A. Wargo. Analysis of immune signatures in longitudinal tumor samples yields insight into biomarkers of response and mechanisms of resistance to immune checkpoint blockade. *Cancer Discovery*, 6(8):827–837, 2016. ISSN 21598290. doi: 10.1158/2159-8290.CD-15-1545.
- [12] Marcin Cieślik and Arul M. Chinnaiyan. Cancer transcriptome profiling at the juncture of clinical translation. *Nature Reviews Genetics*, 19(2):93–109, dec 2017. ISSN 1471-0056. doi: 10.1038/nrg.2017.96. URL <http://www.nature.com/doifinder/10.1038/nrg.2017.96>.
- [13] Cedar-Sinai Genomics Core. Single cell genomics, 2016. URL https://www.cedars-sinai.edu/Research/Research-Cores/Genomics-Core/Documents/website_pricing_jan_2018_final.pdf.
- [14] Alexandru Dan Corlan. Medline trend: automated yearly statistics of pubmed results for any query, 2004. URL <http://dan.corlan.net/medline-trend.html>.

- [15] Sean Davis. Github: awesome-single-cell, 2016. URL <https://github.com/seandavi/awesome-single-cell>.
- [16] Nancy Dumont, Bob Liu, Rosa Anna DeFilippis, Hang Chang, Joseph T. Rabban, Anthony N. Karnezis, Judy A. Tjoe, James Marx, Bahram Parvin, and Thea D. Tlsty. Breast Fibroblasts Modulate Early Dissemination, Tumorigenesis, and Metastasis through Alteration of Extracellular Matrix Characteristics. *Neoplasia*, 15(3):249–IN7, 2013. ISSN 14765586. doi: 10.1593/neo.121950. URL <http://linkinghub.elsevier.com/retrieve/pii/S1476558613800553>.
- [17] International Agency for Research in Cancer. Globocan - facts sheets by cancer, 2018. URL http://globocan.iarc.fr/Pages/fact_sheets_cancer.aspx.
- [18] Daniel M. Frey, Raoul A. Droeser, Carsten T. Viehl, Inti Zlobec, Alessandro Lugli, Urs Zingg, Daniel Oertli, Christoph Kettelhack, Luigi Terracciano, and Luigi Tornillo. High frequency of tumor-infiltrating FOXP3+ regulatory T cells predicts improved survival in mismatch repair-proficient colorectal cancer patients. *International Journal of Cancer*, 126(11):2635–2643, 2010. ISSN 00207136. doi: 10.1002/ijc.24989.
- [19] Dmitry I. Gabrilovich, Suzanne Ostrand-Rosenberg, and Vincenzo Bronte. Coordinated regulation of myeloid cells by tumours, 2012. ISSN 14741733.
- [20] Thomas F. Gajewski, Yuru Meng, Christian Blank, Ian Brown, Aalok Kacha, Justin Kline, and Helena Harlin. Immune resistance orchestrated by the tumor microenvironment. *Immunological Reviews*, 213(1):131–145, oct 2006. ISSN 1600-065X. doi: 10.1111/j.1600-065X.2006.00442.X. URL <http://onlinelibrary.wiley.com/doi/10.1111/j.1600-065X.2006.00442.x/abstract>.
- [21] Jérôme Galon, Franck Pagès, Francesco M Marincola, Magdalena Thurin, Giorgio Trinchieri, Bernard A Fox, Thomas F Gajewski, and Paolo A Ascierto. The immune score as a new possible approach for the classification of cancer. *Journal of Translational Medicine*, 10(1):1, jan 2012. ISSN 1479-5876. doi: 10.1186/1479-5876-10-1. URL <http://translational-medicine.biomedcentral.com/articles/10.1186/1479-5876-10-1>.
- [22] Charlotte Giesen, Hao A O Wang, Denis Schapiro, Nevena Zivanovic, Andrea Jacobs, Bodo Hattendorf, Peter J Schüffler, Daniel Grolimund, Joachim M Buhmann, Simone Brandt, Zsuzsanna Varga, Peter J Wild, Detlef Günther, and Bernd Bodenmiller. Highly multiplexed imaging of tumor tissues with subcellular resolution by mass cytometry. *Nature Methods*, 11(4):417–422, apr 2014. ISSN 1548-7091. doi: 10.1038/nmeth.2869. URL <http://www.nature.com/articles/nmeth.2869>.
- [23] Sacha Gnjatic, Vincenzo Bronte, Laura Rosa Brunet, Marcus O Butler, Mary L Disis, Jérôme Galon, Leif G Hakansson, Brent A Hanks, Vaios Karanikas, Samir N

- Khleif, John M Kirkwood, Lance D Miller, Dolores J Schendel, Isabelle Tanneau, Jon M Wigginton, and Lisa H Butterfield. Identifying baseline immune-related biomarkers to predict clinical outcome of immunotherapy. *Journal for immunotherapy of cancer*, 5:44, 2017. ISSN 2051-1426. doi: 10.1186/s40425-017-0243-4. URL <http://www.ncbi.nlm.nih.gov/pubmed/28515944http://www.pubmedcentral.nih.gov/articlerender.fcgi?artid=PMC5432988>.
- [24] Balázs Győrffy, Christos Hatzis, Tara Sanft, Erin Hofstatter, Bilge Aktas, and Lajos Pusztai. Multigene prognostic tests in breast cancer: past, present, future. *Breast cancer research : BCR*, 17(1):11, jan 2015. ISSN 1465-542X. doi: 10.1186/s13058-015-0514-2. URL <http://www.ncbi.nlm.nih.gov/pubmed/25848861http://www.pubmedcentral.nih.gov/articlerender.fcgi?artid=PMC4307898>.
- [25] D Hanahan and R A Weinberg. The hallmarks of cancer. *Cell*, 100(1):57–70, jan 2000. ISSN 0092-8674. doi: 10.1016/S0092-8674(00)81683-9. URL <http://www.ncbi.nlm.nih.gov/pubmed/10647931>.
- [26] Douglas Hanahan and Lisa M. Coussens. Accessories to the Crime: Functions of Cells Recruited to the Tumor Microenvironment. *Cancer Cell*, 21(3):309–322, mar 2012. ISSN 15356108. doi: 10.1016/j.ccr.2012.02.022. URL <http://www.ncbi.nlm.nih.gov/pubmed/22439926http://linkinghub.elsevier.com/retrieve/pii/S1535610812000827>.
- [27] Roy S. Herbst, Jean-Charles Soria, Marcin Kowanetz, Gregg D. Fine, Omid Hamid, Michael S. Gordon, Jeffery A. Sosman, David F. McDermott, John D. Powderly, Scott N. Gettinger, Holbrook E. K. Kohrt, Leora Horn, Donald P. Lawrence, Sandra Rost, Maya Leabman, Yuanyuan Xiao, Ahmad Mokatrin, Hartmut Koeppen, Priti S. Hegde, Ira Mellman, Daniel S. Chen, and F. Stephen Hodi. Predictive correlates of response to the anti-PD-L1 antibody MPDL3280A in cancer patients. *Nature*, 515(7528):563–567, nov 2014. ISSN 0028-0836. doi: 10.1038/nature14011. URL <http://www.ncbi.nlm.nih.gov/pubmed/25428504http://www.pubmedcentral.nih.gov/articlerender.fcgi?artid=PMC4836193http://www.nature.com/articles/nature14011>.
- [28] National Cancer Institute. Types of cancer treatment, 2017. URL <https://www.cancer.gov/about-cancer/treatment/types>.
- [29] Hollie J. Jackson, Sarwish Rafiq, and Renier J. Brentjens. Driving CAR T-cells forward, 2016. ISSN 17594782.
- [30] Rajen J. Mody, Yi-Mi Wu, Robert J. Lonigro, Xuhong Cao, Sameek Roychowdhury, Pankaj Vats, Kevin M. Frank, John R. Prensner, Irfan Asangani, Nallasivam Palanisamy, Jonathan R. Dillman, Raja M. Rabah, Laxmi Priya Kunju, Jessica Everett, Victoria M. Raymond, Yu Ning, Fengyun Su, Rui Wang, Elena M. Stoffel, Jeffrey W. Innis, J. Scott Roberts, Patricia L. Robertson, Gregory Yanik, Aghiad Chamdin,

- James A. Connelly, Sung Choi, Andrew C. Harris, Carrie Kitko, Rama Jasty Rao, John E. Levine, Valerie P. Castle, Raymond J. Hutchinson, Moshe Talpaz, Dan R. Robinson, and Arul M. Chinnaiyan. Integrative Clinical Sequencing in the Management of Refractory or Relapsed Cancer in Youth. *JAMA*, 314(9):913, sep 2015. ISSN 0098-7484. doi: 10.1001/jama.2015.10080. URL <http://jama.jamanetwork.com/article.aspx?doi=10.1001/jama.2015.10080>.
- [31] NPR. Science Diction: The Origin Of The Word 'Cancer' : NPR, 2010. URL <https://www.npr.org/templates/story/story.php?storyId=130754101>.
- [32] NPR. Science Diction: The Origin Of The Word 'Cancer', 2010. URL <https://www.npr.org/templates/story/story.php?storyId=130754101>.
- [33] Jennifer A. Oberg, Julia L. Glade Bender, Maria Luisa Sulis, Danielle Pendrick, Anthony N. Sireci, Susan J. Hsiao, Andrew T. Turk, Filemon S. Dela Cruz, Hanina Hibshoosh, Helen Remotti, Rebecca J. Zylber, Jiuhong Pang, Daniel Diolaiti, Carrie Koval, Stuart J. Andrews, James H. Garvin, Darrell J. Yamashiro, Wendy K. Chung, Stephen G. Emerson, Peter L. Nagy, Mahesh M. Mansukhani, and Andrew L. Kung. Implementation of next generation sequencing into pediatric hematology-oncology practice: moving beyond actionable alterations. *Genome Medicine*, 8(1):133, dec 2016. ISSN 1756-994X. doi: 10.1186/s13073-016-0389-6. URL <http://genomemedicine.biomedcentral.com/articles/10.1186/s13073-016-0389-6>.
- [34] U.S. Department of Health and Human Services. Fda approves yervoy to reduce the risk of melanoma returning after surgery, 2015. URL <https://www.fda.gov/NewsEvents/Newsroom/PressAnnouncements/ucm469944.htm>.
- [35] U.S. Department of Health and Human Services. Fda approves new, targeted treatment for bladder cancer, 2016. URL <https://www.fda.gov/newsevents/newsroom/pressannouncements/ucm501762.htm>.
- [36] U.S. Department of Health and Human Services. Pembrolizumab (keytruda) checkpoint inhibitor, 2016. URL <https://www.fda.gov/drugs/informationondrugs/approveddrugs/ucm526430.htm>.
- [37] U.S. Department of Health and Human Services. Fda approval brings first gene therapy to the united states, 2017. URL <https://www.fda.gov/NewsEvents/Newsroom/PressAnnouncements/ucm574058.htm>.
- [38] U.S. Department of Health and Human Services. Fda approves car-t cell therapy to treat adults with certain types of large b-cell lymphoma, 2017. URL <https://www.fda.gov/newsevents/newsroom/pressannouncements/ucm581216.htm>.

- [39] Karolina Palucka and Jacques Banchereau. Dendritic-Cell-Based Therapeutic Cancer Vaccines, 2013. ISSN 10747613.
- [40] Efthymia Papalexis and Rahul Satija. Single-cell RNA sequencing to explore immune cell heterogeneity. *Nature Reviews Immunology*, 18(1):35–45, 2017. ISSN 1474-1733. doi: 10.1038/nri.2017.76. URL <http://www.nature.com/doifinder/10.1038/nri.2017.76>.
- [41] Jeffrey M. Perkel. Single-cell sequencing made simple. *Nature*, 547(7661):125–126, jul 2017. ISSN 0028-0836. doi: 10.1038/547125a. URL <http://www.nature.com/doifinder/10.1038/547125a>.
- [42] Jonathan M Pitt, Marie Vétizou, Romain Daillère, María Paula Roberti, Takahiro Yamazaki, Bertrand Routy, Patricia Lepage, Ivo Gomperts Boneca, Mathias Chamaillard, Guido Kroemer, and Laurence Zitvogel. Resistance Mechanisms to Immune-Checkpoint Blockade in Cancer: Tumor-Intrinsic and -Extrinsic Factors. *Immunity*, 44(6):1255–69, jun 2016. ISSN 1097-4180. doi: 10.1016/j.jimmuni.2016.06.001. URL <http://www.ncbi.nlm.nih.gov/pubmed/27332730>.
- [43] Chris P. Ponting. Big knowledge from big data in functional genomics. *Emerging Topics in Life Sciences*, 1(3):245–248, nov 2017. ISSN 2397-8554. doi: 10.1042/ETLS20170129. URL <http://www.emergtoplifesci.org/lookup/doi/10.1042/ETLS20170129>.
- [44] J. Predina, E. Eruslanov, B. Judy, V. Kapoor, G. Cheng, L.-C. Wang, J. Sun, E. K. Moon, Z. G. Fridlander, S. Albelda, and S. Singhal. Changes in the local tumor microenvironment in recurrent cancers may explain the failure of vaccines after surgery. *Proceedings of the National Academy of Sciences*, 110(5):E415–E424, 2013. ISSN 0027-8424. doi: 10.1073/pnas.1211850110. URL <http://www.pnas.org/cgi/doi/10.1073/pnas.1211850110>.
- [45] Bin Z. Qian and Jeffrey W. Pollard. Macrophage Diversity Enhances Tumor Progression and Metastasis, 2010. ISSN 00928674.
- [46] D F Quail and J A Joyce. Microenvironmental regulation of tumor progression and metastasis. *Nat Med*, 19(11):1423–1437, 2013. ISSN 1546-170X. doi: 10.1038/nm.3394. URL <http://www.ncbi.nlm.nih.gov/pubmed/24202395>.
- [47] Naiyer A. Rizvi, Matthew D. Hellmann, Alexandra Snyder, Pia Kvistborg, Vladimir Makarov, Jonathan J. Havel, William Lee, Jianda Yuan, Phillip Wong, Teresa S. Ho, Martin L. Miller, Natasha Rekhtman, Andre L. Moreira, Fawzia Ibrahim, Cameron Bruggeman, Billel Gasmi, Roberta Zappasodi, Yuka Maeda, Chris Sander, Edward B. Garon, Taha Merghoub, Jedd D. Wolchok, Ton N. Schumacher, and Timothy A. Chan. Mutational landscape determines sensitivity to PD-1 blockade in non-small cell

- lung cancer. *Science*, 348(6230):124–128, 2015. ISSN 10959203. doi: 10.1126/science.aaa1348.
- [48] Dan R. Robinson, Yi-Mi Wu, Robert J. Lonigro, Pankaj Vats, Erin Cobain, Jessica Everett, Xuhong Cao, Erica Rabban, Chandan Kumar-Sinha, Victoria Raymond, Scott Schuetze, Ajjai Alva, Javed Siddiqui, Rashmi Chugh, Francis Worden, Mark M. Zalupski, Jeffrey Innis, Rajen J. Mody, Scott A. Tomlins, David Lucas, Laurence H. Baker, Nithya Ramnath, Ann F. Schott, Daniel F. Hayes, Joseph Vijai, Kenneth Offit, Elena M. Stoffel, J. Scott Roberts, David C. Smith, Lakshmi P. Kunju, Moshe Talpaz, Marcin Cieślik, and Arul M. Chinnaiyan. Integrative clinical genomics of metastatic cancer. *Nature*, 548(7667):297–303, aug 2017. ISSN 0028-0836. doi: 10.1038/nature23306. URL <http://www.nature.com/doifinder/10.1038/nature23306>.
- [49] J. S. Ross, C. Hatzis, W. F. Symmans, L. Pusztai, and G. N. Hortobagyi. Commercialized Multigene Predictors of Clinical Outcome for Breast Cancer. *The Oncologist*, 13(5):477–493, may 2008. ISSN 1083-7159. doi: 10.1634/theoncologist.2007-0248. URL <http://www.ncbi.nlm.nih.gov/pubmed/18515733><http://theoncologist.alphamedpress.org/cgi/doi/10.1634/theoncologist.2007-0248>.
- [50] Max Schelker, Sonia Feau, Jinyan Du, Nav Ranu, Edda Klipp, Birgit Schoeberl, Gavin MacBeath, Andreas Raue, MacBeath Gavin, Birgit Schoeberl, Andreas Raue, Gavin MacBeath, and Andreas Raue. Estimation of immune cell content in tumour tissue using single-cell RNA-seq data. *Nature Communications*, 8(1):2032, dec 2017. ISSN 2041-1723. doi: 10.1038/s41467-017-02289-3. URL <http://www.nature.com/articles/s41467-017-02289-3><http://dx.doi.org/10.1038/s41467-017-02289-3>.
- [51] Thomas A Sebeok. DISCUSSION. *Annals of the New York Academy of Sciences*, 280 (1 Origins and E):481, oct 1976. ISSN 0077-8923. doi: 10.1111/j.1749-6632.1976.tb25511.x. URL <http://doi.wiley.com/10.1111/j.1749-6632.1976.tb25511.x>.
- [52] T. Stewart, S. CJ Tsai, H. Grayson, R. Henderson, and G. Opelz. Incidence of de-novo breast cancer in women chronically immunosuppressed after organ transplantation. *The Lancet*, 346(8978):796–798, 1995. ISSN 01406736. doi: 10.1016/S0140-6736(95)91618-0.
- [53] O Stutman. Tumor development after 3-methylcholanthrene in immunologically deficient athymic-nude mice. *Science (New York, N.Y.)*, 183(4124):534–6, feb 1974. ISSN 0036-8075. URL <http://www.ncbi.nlm.nih.gov/pubmed/4588620>.
- [54] Akulapalli Sudhakar. History of Cancer, Ancient and Modern Treatment Methods. *Journal of cancer science & therapy*, 1(2):1–4, dec 2009. ISSN 1948-5956. doi: 10.4172/1948-5956.100000e2. URL <http://www.ncbi.nlm.nih.gov/pubmed/20740081><http://www.pubmedcentral.nih.gov/articlerender.fcgi?artid=PMC2927383>.

- [55] J E Talmadge and D I Gabrilovich. History of myeloid-derived suppressor cells. *Nat Rev Cancer*, 13(10):739–752, 2013. ISSN 1474-1768. doi: 10.1038/nrc3581. URL <http://www.nature.com/nrc/journal/v13/n10/pdf/nrc3581.pdf>.
- [56] Janis M Taube, Jérôme Galon, Lynette M Sholl, Scott J Rodig, Tricia R Cottrell, Nicolas A Giraldo, Alexander S Baras, Sanjay S Patel, Robert A Anders, David L Rimm, and Ashley Cimino-Mathews. Implications of the tumor immune microenvironment for staging and therapeutics. *Modern Pathology*, 2017. ISSN 0893-3952. doi: 10.1038/modpathol.2017.156. URL <http://www.nature.com/doifinder/10.1038/modpathol.2017.156>.
- [57] Itay Tirosh, Benjamin Izar, Sanjay M. Prakadan, Marc H. Wadsworth, Daniel Treacy, John J. Trombetta, Asaf Rotem, Christopher Rodman, Christine Lian, George Murphy, Mohammad Fallahi-Sichani, Ken Dutton-Regester, Jia Ren Lin, Ofir Cohen, Parin Shah, Diana Lu, Alex S. Genshaft, Travis K. Hughes, Carly G.K. Ziegler, Samuel W. Kazer, Aleth Gaillard, Kellie E. Kolb, Alexandra Chloé Villani, Cory M. Johannessen, Aleksandr Y. Andreev, Eliezer M. Van Allen, Monica Bertagnolli, Peter K. Sorger, Ryan J. Sullivan, Keith T. Flaherty, Dennie T. Frederick, Judit Jané-Valbuena, Charles H. Yoon, Orit Rozenblatt-Rosen, Alex K. Shalek, Aviv Regev, and Levi A. Garraway. Dissecting the multicellular ecosystem of metastatic melanoma by single-cell RNA-seq. *Science*, 352(6282):189–196, 2016. ISSN 10959203. doi: 10.1126/science.aad0501.
- [58] V E Velculescu, L Zhang, W Zhou, J Vogelstein, M A Basrai, D E Bassett, P Hieter, B Vogelstein, and K W Kinzler. Characterization of the yeast transcriptome. *Cell*, 88(2):243–51, jan 1997. ISSN 0092-8674. URL <http://www.ncbi.nlm.nih.gov/pubmed/9008165>.
- [59] Jedd D. Wolchok. PD-1 Blockers, 2015. ISSN 10974172.
- [60] Weiping Zou, Jedd D. Wolchok, and Lieping Chen. PD-L1 (B7-H1) and PD-1 pathway blockade for cancer therapy: Mechanisms, response biomarkers, and combinations. *Science Translational Medicine*, 8(328), 2016. ISSN 19466242. doi: 10.1126/scitranslmed.aad7118.